Analysis of Passive Satellite Systems Operating in the Ultraviolet to Microwave Spectral Region for Measurements of Greenhouse Gases, Ozone, Pressure, and Temperature

Technical Report

- Passive systems analysis part of TN 210 -

Prepared for

ESA/ESTEC study

Requirements Definition for Future DIAL Instrument

Prepared by

Institute of Environmental Physics (IUP) / Institute of Remote Sensing (IFE)
University of Bremen, FB 1
D-28334 Bremen, Otto-Hahn-Allee 1, Germany
Fax: +49-(0)421-218-4555
http://www.iup.physik.uni-bremen.de

Authors:

Michael Buchwitz
Phone: +49-(0)421-218-4475
E-mail: Michael.Buchwitz@iup.physik.uni-bremen.de
Responsibilities: Lead author and solar spectral region (TN/WP 213)

Heinrich Bovensmann
Phone: +49-(0)421-218-4008
E-mail: Heinrich.Bovensmann@iup.physik.uni-bremen.de
Responsibility: Thermal infrared spectral region (TN/WP 212)

Rüdiger de Beek
Phone: +49-(0)421-218-4475
E-mail: Ruediger.de_Beek@iup.physik.uni-bremen.de
Responsibility: Microwave spectral region (TN/WP 211)

Institute of Environmental Physics (IUP) / Institute of Remote Sensing (IFE)
University of Bremen, FB 1
28334 Bremen, Otto-Hahn-Allee 1, Germany
Fax: +49-(0)421-218-4555
http://www.iup.physik.uni-bremen.de

1 Table of Contents

2 Executive Summary

The objective of the study "Requirements Definition for Future DIAL Instruments" is to provide the background for the definition of a future space-borne lidar system capable to monitore key atmospheric parameters relevant for climate change, atmospheric chemistry and/or meteorology. Target species are the three greenhouse gases carbon dioxide (CO_2), methane (CH_4), and nitrous oxide (N_2O) (main goal: to better constrain their surface fluxes), ozone (O_3) (main goal: to improve our understanding of atmospheric chemistry), and atmospheric pressure and temperature (main goal: improvement of numerical weather prediction (NWP)).

In order to identify the most important one or two of these parameters appropriate for a future lidar system, it is important to assess (e.g., by literature review) to what extent the observational requirements can be met already now with existing passive systems or are likely to be met with passive systems in the near future. These aspects are addressed in this technote.

In the following a summary of the performance of existing and near future passive satellite systems is given including a comparison with the observational requirements. The findings are shortly summarized in the following overview table ("no" means that no systems has been identified that meets the corresponding requirements; one requirement that is not meet is given in brackets (prec.=precision; vert.=vertical; horiz.=horizotal; res.=resolution)):

Summary table:

Parameter	Threshold requirement met ?	Target req. met ?
CO2 column	**SCIAMACHY, AIRS,** TES?, **IASI, OCO**	*no (prec.)*
CO2 range resolved	*no (vert.res.)* GOSAT?	*no (vert.res.)*
CH4 column	**SCIAMACHY,** AIRS?, **TES, IASI**	**SCIAMACHY,** AIRS?, **TES, IASI**
CH4 range resolved	*no (vert.res.)*	*no (vert.res.)*
N2O column	*no (prec.)*	*no (prec.)*
N2O range resolved	*no (vert.res.)*	*no (vert.res.)*
O3 troposphere	*no (vert.res.)*	*no (vert.res.)*
O3 UTLS	*no (vert.+horiz.res.)*	*no (vert.res.)*
O3 stratosphere	*no (vert.+horiz.res.)*	*no (vert.res.)*
Pressure @ surface	*no (prec.)*	*no (prec.)*
Pressure LT	*no (prec.)*	*no (prec.)*
Pressure UT	*no (prec.)*	*no (prec.)*
Pressure LS	*no (prec.)*	*no (prec.)*
Temperature LT	**AIRS/AMSU/HSB, IASI**	*no (prec.)*
Temperature UT	**AIRS/AMSU/HSB, IASI**	*no (prec.)*
Temperature LS	**AIRS/AMSU/HSB, IASI**	*no (prec.)*
Temperature US	**AIRS/AMSU/HSB, IASI**	*no (prec.)*

GREEN: Requirement met (demonstrated by comprehensive analysis of real data)
BLUE: Potential exists that requirement can be met (verified at least partially by simulation)
BLACK: Potential exists but detailed analysis not available
Note on p and T: Threshold req. is global NWP req.; Target req. is regional NWP req.

Carbon dioxide (CO_2)

For carbon dioxide columns the requirements are *[REQ-GHG-2004]*: target precision: 0.8 ppmv or 0.2% (1 day average for 50 km horizontal resolution), threshold precision: 3.5 ppmv or 1% (6 days average for 500 km resolution). The precisions are relaxed by about a factor of two for the range resolved measurements which are required to provide independent information on three regions (boundary layer, free troposphere, stratosphere).

According to the requirement update given in *[REQ-GHG-2004Update1]* the following target requirements for the columns of CO_2 should be used:

- Temporal resolution: 6 days (instead of 1 day)
- Horizontal resolution: 500 km (instead of 50 km)

According to the latest requirement update given in [REQ-GHG-2004Update2] the target and threshold requirements for the columns are:

- *target requirements for columns: precision now 1.0 ppm instead of 0.8 ppm; temporal resolution: one week; horizontal resolution: $2^o x 2^o$*
- *threshold requirements for columns: precision unchanged; temporal resolution: one month; horizontal resolution: $5^o x 5^o$*

The conclusions that can be drawn from this study are:

- *Chedin et al., 2003a,* analysed TOVS/NOAA-10 data to retrieve atmospheric CO_2 concentrations. They report that they have achieved ("rough estimate") a precision of 3.6 ppmv (~1%) for mid-tropospheric CO_2 concentrations in the tropics (20^oN – 20^oS). It is, however, unclear if the methode used by *Chedin et al., 2003a,* can be extended to extra tropical regions as the methode requires low variability of atmospheric temperature (the measurements are very sensitive to temperature and significantly less sensitive to CO_2 concentration changes).
- Simulations performed by *Chedin et al., 2003a,* indicate that ~2 ppmv (~0.5%) may be achievable with the new generation of high resolution thermal infrared (TIR) nadir sounders such as AIRS/AQUA. This is similar to what has been found in other studies for AIRS and IASI/METOP, e.g., 1-2 ppmv reported by *Engelen and Stephens, 2004*. These TIR nadir measurements have their maximum sensitivity in the middle troposphere. They are insensitive to the lower troposphere and contain only little information about the stratosphere (see, e.g., *Chedin et al., 2003b; Engelen et al., 2001)*. CO_2 total columns from AIRS are not an operational Level 2 core product of AIRS but a scientific data product under development by members of the AIRS science team (we are not aware of any published results using real AIRS data).
- The near-infrared (NIR) nadir measurements of SCIAMACHY are sensitive to CO_2 concentration changes at all altitudes including the boundary layer *[Buchwitz and Burrows, 2004; Buchwitz et al., 2004c].* So far only column measurements have been investigated. Preliminary analysis of SCIAMACHY data indicates that the precision of the column measurements is in the range 1-4% for single cloud free measurements over land *[Buchwitz et al., 2004c; Buchwitz et al., 2004d]*. Assuming that the precision improves with the square root of the number of measurements added the following precisions can be achieved (over land):
  - 0.2-0.7% to be compared with the target requirement of 0.2%
  - 0.2-0.7% to be compared with the threshold requirement of 1%
  - More analysis is needed to confirm these estimates. In addition, biases need to be considered.
- TES/AURA (launch: mid 2004): CO_2 is not a standard operational TES data product. We are not aware of any publications where (scientific) CO_2 retrieval from TES has been investigated and accuracy/precision values are given.

- Future systems:
  - IASI/METOP (launch 2005): The performance of the high resolution thermal infrared nadir sounder IASI is expected to be similar as the estimated performance of AIRS/AQUA (see above), i.e., ~1-2 ppmv [*Engelen and Stephens, 2004]. Chedin et al., 2003b,* also have conducted a study dedicated to IASI concluding that changes at the level of 1% or less for 500 x 500 km^2 and 2 weeks averages are expected to be possible for the total column carbon dioxide amount. CO_2 is not a standard operational IASI data product.
  - NASA/JPLs Orbiting Carbon Observatory (OCO) satellite missions *[Crisp et al., 2004]* due for launch in 2007 aims at achieving a precision of 1 ppmv (0.3%) in 16 day intervals with a spatial resolution corresponding to regional scales (4^o x 5^o). This is similar as the values given above for AIRS and IASI but OCO's near-infrared nadir measurements are sensitive also to the boundary layer where the signal variation due to CO_2 sources and sinks is largest.
  - The Japanese space agency also plans to build a satellite for CO_2 measurements accurate enough for source/sink quantification, namely GOSAT which is due for launch in 2007 *[Ogawa et al., 2004; Shimoda, 2003]*. GOSAT shall make high spectral resolution Fourier transform nadir measurements in the NIR and TIR spectral regions. These measurements shall allow a discrimination between boundary layer and free tropospheric CO_2 concentrations.

- *Main conclusion*: Currently no passive satellite systems exist for which it has been demonstrated that the requirements given in *[REQ-GHG-2004]* can be met. There are, however, satellite systems which have the potential to meet at least the threshold requirement for the column measurements in the near future (e.g., SCIAMACHY over land (requires more studies), the TIR nadir instruments AIRS, TES, and IASI, and the NIR nadir instrument OCO (launch in 2007)).

Impact of latest requirement update given in [REQ-GHG-2004Update2] (only impact on columns has been assessed relative to [REQ-GHG-2004Update1]):

Target requirement: the precision has been slightly relaxed by a factor of 1.25 (=1/0.8); temporal resolution relaxed by a factor of 1.2 (=7/6); horizontal resolution changed from 500 km x 500 km to 2^ox2^o (we assume that this is equivalent to 200 km x 200 km) resulting in a change by a factor of 0.16 (=40000/250000). As a result 5 (=1/(1.2x0.16)) times less satellite data can be averaged now corresponding to a change (reduction) of the precision of the averaged data by a factor of $\sqrt{5} \sim 2$. The overall impact is therefore relatively small (effectively the precision requirement is more stringent now by a factor of 1.6 (=2/1.25)). Therefore, we have not updated the Summary Table given in the Executive Summary.

Threshold requirement: precision unchanged; temporal resolution relaxed by a factor of 5 (=30/6); the horizontal resolution changed from 500 km x 500 km to 5^ox5^o (we assume that this is equivalent to 500 km x 500 km) and is therefore essentially unchanged . As a result 5 times more satellite data can be averaged now corresponding to a change (increase) of the precision of the averaged data by a factor of $\sqrt{5} \sim 2$. The overall impact is therefore relatively small (effectively the precision requirement is relaxed by a factor of 2). Therefore, we have not updated the Summary Table given in the Executive Summary.

Methane (CH_4)

For methane columns the requirements are *[REQ-GHG-2004]*: target precision: 10 ppbv or 0.6% (1 day average for 50 km horizontal resolution), threshold precision: 35 ppbv or 2% (6 days average for 500 km resolution). The precisions are relaxed by about a factor of two for the range resolved measurements which are required to provide independent information on three regions (boundary layer, free troposphere, stratosphere).

According to the latest requirement update given in *[REQ-GHG-2004Update1]* the following target requirements for the columns of CH_4 should be used:

- Temporal resolution: 6 days (instead of 1 day)
- Horizontal resolution: 500 km (instead of 50 km)

According to the latest requirement update given in [REQ-GHG-2004Update2] the target and threshold requirements for the columns are:

- *target requirements for columns: precision unchanged; temporal resolution: one week; horizontal resolution: $2^o x 2^o$*
- *threshold requirements for columns: precision unchanged; temporal resolution: one month; horizontal resolution: $5^o x 5^o$*

The conclusions that can be drawn from this study are:

- The first global maps of measured methane distributions from satellite have been generated from IMG/ADEOS-1 measurements (see, e.g., *Kobayashi et al., 1999; Clerbaux et al., 2003*). The data show qualitatively the expected variability, for example a strength North-South gradient, but also some problems which migh be related to the algorithm (e.g., treatment of surface emissivity).
- Methane total columns can also be retrieved from AIRS/AQUA. CH_4 total columns from AIRS are not an operational Level 2 core product of AIRS but a scientific data product under development by members of the AIRS science team (we are not aware of any published results based on real AIRS data).
- The (IMG, AIRS, IASI, etc.) TIR nadir measurements have their maximum sensitivity in the middle troposphere and are insensitive to the lower troposphere.
- Currently, there are two instruments in space which measure reflected sun light in spectral regions which correspond to the near-infrared (NIR) absorption bands of CH_4, namely MOPITT onboard EOS-Terra and SCIAMACHY on ENVISAT. These NIR nadir measurements are sensitive to CH_4 concentration changes at all altitude levels, including the boundary layer (see, e.g., *Buchwitz and Burrows, 2004*). Both instruments have a theoretical single pixel CH_4 column retrieval precision of ~1% *[Deeter et al., SPIE; Buchwitz et al., 2000a]*. Due to problems with the near-infrared retrievals MOPITT has not delivered any CH_4 column data products.
- Preliminary analysis of SCIAMACHY data *[Buchwitz and Burrows, 2004; Buchwitz et al., 2004c; Buchwitz et al., 2004d]* indicates that a precision of 1-6% has been achieved for single cloud free measurements over land using the WFM-DOAS Version 0.4 retrieval algorithm. Assuming that the precision improves with the square root of the number of measurements added the following precisions can be achieved (over land):
  - 0.25-1.5% to be compared with the target requirement of 0.6%
  - 0.25-1.5% to be compared with the threshold requirement of 2%
  - More analysis is needed to confirm these estimates. In addition, biases need to be better quantified.
- TES/AURA (launch mid 2004): Methane total columns are a standard operational data product from TES. The predicted precision for methane total columns and vertical profiles (vertical resolution: 2-6 km) to be retrieved from TES is ~3% for (quasi) single measurements (5.3 x 8.5 km^2 ground pixel size) *[TES web page]*. If this will be confirmed

using real flight data and assuming that the precision improves with the square root of the number of measurements averaged only a small number of measurements have to be added to get a precision better than the required threshold precision of 2%.

- Future systems:
  - IASI/METOP (launch 2005): Methane total columns are a standard operational data product from IASI. The required precision for methane total columns to be retrieved from IASI is < 5-10% for single measurements (12 km pixel size at direct nadir) *[Diebel et al., 1996; Clerbaux et al., 1998; Hadji-Lazaro et al., 2003]*. If this will be confirmed using real flight data and assuming that the precision improves with the square root of the number of measurements averaged only a small number of measurements have to be added to get a precision better than the required threshold precision of 2%.

- *Main conclusion:* Currently, no passive satellite systems exist for which it has been demonstrated that the requirements given in *[REQ-GHG-2004]* can be met. There are, however, satellite systems which have the potential to meet at least the threshold requirement for the column measurements in the near future (e.g., SCIAMACHY over land (requires more studies), AIRS, TES, and IASI (launch 2005)).

Impact of latest requirement update given in [REQ-GHG-2004Update2] (only impact on columns has been assessed relative to [REQ-GHG-2004Update1]):

Target requirement: precision unchanged; temporal resolution relaxed by a factor of 1.2 (=7/6); horizontal resolution changed from 500 km x 500 km to 2^ox2^o (we assume that this is equivalent to 200 km x 200 km) resulting in a change by a factor of 0.16 (=40000/250000). As a result 5 (=1/(1.2x0.16)) times less satellite data can be averaged now corresponding to a change (reduction) of the precision of the averaged data by a factor of $\sqrt{5} \sim 2$. The overall impact is therefore relatively small (effectively the precision requirement is more stringent now by a factor of 2). Therefore, we have not updated the Summary Table given in the Executive Summary.

Threshold requirement: precision unchanged; temporal resolution relaxed by a factor of 5 (=30/6); the horizontal resolution changed from 500 km x 500 km to 5^ox5^o (we assume that this is equivalent to 500 km x 500 km) and is therefore essentially unchanged . As a result 5 times more satellite data can be averaged now corresponding to a change (increase) of the precision of the averaged data by a factor of $\sqrt{5} \sim 2$. The overall impact is therefore relatively small (effectively the precision requirement is relaxed by a factor of 2). Therefore, we have not updated the Summary Table given in the Executive Summary.

Nitrous oxide (N_2O)

For nitrous oxide columns the requirements are *[REQ-GHG-2004]*: target precision: 0.1 ppbv or 0.03% (1 day average for 50 km horizontal resolution), threshold precision: 1 ppbv or 0.3% (6 days average for 500 km resolution). The precisions are relaxed by about a factor of three for the range resolved measurements which are required to provide independent information on three regions (boundary layer, free troposphere, stratosphere).

According to the latest requirement update given in *[REQ-GHG-2004Update1]* the following target requirements for the columns of N_2O should be used:

- Temporal resolution: 6 days (instead of 1 day)
- Horizontal resolution: 500 km (instead of 50 km)

According to the latest requirement update given in [REQ-GHG-2004Update2] the target and threshold requirements for the columns are:

- *target requirements for columns: precision unchanged; temporal resolution: one week; horizontal resolution: $2^o x 2^o$*
- *threshold requirements for columns: precision now 0.5 ppb instead of 1 ppb; temporal resolution: one month; horizontal resolution: $5^o x 5^o$*

The conclusions that can be drawn from this study are:

- Until now only a limited amount of IMG/ADEOS data have been processed to retrieve N_2O columns *[Lubrano et al., 2003]*. Based on simulated IMG retrievals *Lubrano et al., 2003*, conclude that a measurement precision of 1-3% should be possible (single 10 s measurements, 8 x 8 km^2). The sensitivity maximum is between 300 – 700 hPa with no information from the boundary layer. *Lubrano et al., 2003*, estimate that the single pixel retrieval precision for AIRS/AQUA and IASI/METOP is similar as for IMG but with more data points available for averaging.
- *Chedin et al., 2002*, present first results concerning the retrieval of N_2O atmospheric mixing ratios from space. Their method relies on the analysis of the difference between NOAA/TOVS observations (radiances) and simulations using collocated radiosonde data. The collocated radiosondes were necessary as not all the necessary informations can be derived from TOVS. No precision/accuracy values are given in *Chedin et al., 2002.*
- The near-infrared (NIR) nadir measurements of SCIAMACHY are sensitive to N_2O concentration changes at all altitude levels, including the boundary layer. Preliminary analysis of SCIAMACHY data *[Buchwitz et al., 2000; Buchwitz and Burrows, 2004; Warneke et al., 2004; Buchwitz et al., 2004d]* indicates that a precision of 10-20% can be achieved for single cloud free measurements over land. Assuming that the precision improves with the square root of the number of measurements added the following precisions can be achieved (over land):
  - 2.5-5% to be compared with the target requirement of 0.03%
  - 2.5-5% to be compared with the threshold requirement of 0.3%
  - More analysis is needed to confirm these estimates. In addition, biases need to be better quantified.
- TES/AURA: N_2O is not a standard operational TES data product. We are not aware of any publications where (scientific) N_2O retrieval from TES has been investigated and accuracy/precision values are given.
- Future systems:
  - IASI/METOP (launch 2005): N_2O is not a standard operational IASI data product. For scientfic retrievals see statement given above from *Lubrano et al., 2003.*

- *Main conclusion:* Currently, no passive satellite systems exist for which it has been demonstrated that the requirements given in *[REQ-GHG-2004]* can be met. For existing

instruments (e.g., SCIAMACHY and AIRS) more studies are required in order to assess if at least the threshold requirement can be met (this is not very likely as even the threshold observational requirements are demanding). Concerning future systems such as IASI more studies are needed to reliably assess if the requirements can be met.

Impact of latest requirement update given in [REQ-GHG-2004Update2] (only impact on columns has been assessed relative to [REQ-GHG-2004Update1]):

Target requirement: precision unchanged; temporal resolution relaxed by a factor of 1.2 (=7/6); horizontal resolution changed from 500 km x 500 km to $2^o x 2^o$ (we assume that this is equivalent to 200 km x 200 km) resulting in a change by a factor of 0.16 (=40000/250000). As a result 5 (=1/(1.2x0.16)) times less satellite data can be averaged now corresponding to a change (reduction) of the precision of the averaged data by a factor of $\sqrt{5} \sim 2$. The overall impact is therefore relatively small (effectively the precision requirement is more stringent now by a factor of 2). Therefore, we have not updated the Summary Table given in the Executive Summary.

Threshold requirement: precision changed from 1 ppb to 0.5 ppm, i.e., a factor of 2 more stringent; temporal resolution relaxed by a factor of 5 (=30/6); the horizontal resolution changed from 500 km x 500 km to $5^o x 5^o$ (we assume that this is equivalent to 500 km x 500 km) and is therefore essentially unchanged . As a result 5 times more satellite data can be averaged now corresponding to a change (increase) of the precision of the averaged data by a factor of $\sqrt{5} \sim 2$. The overall impact is therefore relatively small (effectively the precision requirement is unchanged). Therefore, we have not updated the Summary Table given in the Executive Summary.

Ozone (O_3):

The target observational requirement according to *[REQ-O3-2004]* for vertical profiles of the dry air O_3 volume mixing ratio are: precision < 10%, accuracy < 5%, vertical resoution 1 km; horizontal resolution 10 km. The threshold requirements are: troposphere: precision < 20%; accuracy < 10%, vertical resolution 3 km; horizontal resolution: 20 km; UTLS: precision < 20%; accuracy < 10%, vertical resolution 2 km; horizontal resolution: 50 km; stratosphere: precision < 20%; accuracy < 10%, vertical resolution 2 km; horizontal resolution: 100 km.

The conclusions that can be drawn from this study are:

- Ozone vertical profiles are retrieved from nadir looking instruments measuring in the UV/visible such as SBUV/2 and GOME. The vertical resolution is about 6 km in the middle stratosphere (20-25 km) and worse (about 10-12 km resolution) above and below. The precision and accuray of the stratospheric profiles is in the range 5-15%.
- Tropospheric information from SBUV and GOME is, however, limited. According to *Bhartia et al., 1996,* SBUV profiles are strongly influenced by a-priori assumptions outside the range 1-20 hPa (~26-50 km). For the GOME instrument more information is available as (continuous) spectra are recorded *[Munro et al., 1998; Hoogen et al., 1999]*. Nevertheless, the errors on the retrieved tropospheric ozone columns are quite large. According to *Siddans et al., 1997,* agreement with ozone sonde measurements is within 30-40%.
- Similar results can be expected from their successor instruments SCIAMACHY (nadir mode), OMI/AURA and GOME-2/METOP but with faster global coverage (one day for OMI and GOME-2) and smaller ground pixel size (e.g., 13 x 24 km^2 for OMI).
- Maps of tropospheric ozone have also been generated from IMD/ADEOS measurements *[Clerbaux et al., 2003]*. These data have been compared with ozone sondes and model results. A high correlation has been found but also biases (mean bias: ~15 DU) which might result from the decreasing sensitivity of IMG in the boundary layer.
- Tropospheric ozone has also been determined using a combination of sensors (e.g., TOMS / SAGE or TOMS / SBUV). *Fishman et al., 2003*, used a method, which essentially subtracts the stratospheric column measured by SBUV from the total column as measured by TOMS. *Fishman et al., 2003*, report on agreement with ozone sonde measurements within 13-20%. *de Laat and Aben, 2003,* however, point out that the method used *by Fishman et al., 2003*, is not unproblematic. *de Laat and Aben, 2003*, report that they can produce similar maps of tropospheric ozone using (mainly) tropopause height information.
- Tropospheric information can also be derived from SCIAMACHY due its quasi simultaneous limb and nadir observation of the same air mass. The theoretical retrieval precision has been estimated to ~10% *[Bovensmann et al., 1999]*. At present, however, no detailed information based on comprehensive theoretical analyisis or validation of real data is available.
- In summary, retrieval of tropospheric ozone information from space is still in its initial stages and uncertainties are large. The best that has been obtained so far is one piece of information for the troposphere (i.e.,no vertical resolution within the troposphere).
- Many limb viewing instruments exist that measure vertical profiles of ozone in the stratosphere and mesosphere by solar, lunar or stellar occultation (e.g., SAGE, POAM, SCIAMACHY, GOMOS), measurements of scattered limb radiance (e.g., SCIAMACHY) or limb thermal emission (e.g., the TIR measurements of MIPAS/ENVISAT or the microwave measurements of MLS/UARS).
    - Solar occultation measurements may have high precision and vertical resolution (SAGE III: ~6% precision, ~1 km vertical resolution) but cannot provide global coverage.

- Stellar occulation: GOMOS/ENVISAT has a field of view of ~1.7 km in the vertical direction but the resolution of the operational products have a resolution of ~3 km due to regularization. Preliminary validation of selected GOMOS ozone profiles showed agreement with independent data within 5-15% in the altitude range ~18-50 km *[ACVE-2/GOMOS, 2004]*.
- Limb microwave emission sounding: MLS/UARS ozone profiles cover the pressure range from 100 hPa to 0.22 hPa with a resolution of 4-6 km. Precision is best in the range 2-20 hPa (~4%; accuracy ~6%). At 100 hPa the accuracy is ~15% and the precision > 50% *[Livesey et al., 2003]*.
- Limb TIR emission sounding: MIPAS/ENVISAT has a vertical resolution of ~3 km. Preliminary validation of the MIPAS ozone operational data product indicates that there are no obvious biases and that the precision is ~10-15% in the altitude region ~20-55 km *[ACVE-2/MIPAS, 2004]*.
- Using SCIAMACHY limb observations of scattered light stratospheric (and mesospheric) ozone profiles have been retrieved with a vertical resolution of 3 km and an accuracy of ~10% *[von Savigny et al., 2004]*. The lowest altitude that can be observed is determined by clouds.
- TES/AURA (launch mid 2004): TES will operate in nadir and limb mode. For the nadir measurements *Clough et al., 1995*, estimate the ozone profile retrieval precision to approximately 5% (1 sigma) for a vertical resolution of 5 km in the middle and upper troposphere (corresponding to 2-3 independent pieces of information, see also *Luo et al., 2002*). If boundary layer ozone can be retrieved depends on the (thermal) contrast between the boundary layer and the surface. The vertical resolution in limb mode is about 2-6 km.
- OMI/AURA (launch mid 2004) and GOME-2/METOP (launch 2005): see GOME/ERS-2 discussion given above
- MLS/AURA (launch mid 2004): Similar as MLS/UARS (see above).
- IASI/METOP (launch 2005): The required ozone total column precision is 5-10% and for ozone in the troposphere 10-20% *[Clerbaux et al., 1998; Hadji-Lazaro et al., 2003]*.

- *Main conclusion*: No passive satellite systems have been identified for which it has been demonstrated that the target requirements given in *[REQ-O3-2004]* can be met (especially 1 km vertical resolution with global coverage and a horizontal resolution of 10 km). No passive satellite systems have been identified for which it has been demonstrated that the threshold requirements given in *[REQ-O3-2004]* can be met (troposphere: especially 3 km vertical resolution with global coverage and a horizontal resolution of 20 km, UTLS: especially 2 km vertical resolution with global coverage and a horizontal resolution of 50 km, stratosphere: especially 2 km vertical resolution with global coverage and a horizontal resolution of 100 km).

Pressure:

The threshold observational requirements for pressure are *[REQ-PT-2004]:* Surface pressure: precision < 1 hPa, accuracy < 0.5 hPa, horizontal sampling 50 km; lower troposphere: precision 0.6 hPa, accuracy < 0.5 hPa, horizontal sampling 50 km, vertical sampling 1 km; upper troposphere: precision 0.2 hPa, accuracy < 0.2 hPa, horizontal sampling 100 km, vertical sampling 1 km; lower stratosphere: precision 0.1 hPa, accuracy < 0.1 hPa, horizontal sampling 200 km, vertical sampling 2 km. The height assignment requirement is 10 m. The target requirements are even more stringent, e.g., horizontal sampling 15 km, precision surface pressure 0.5 hPa. In addition, there are near-real time data delivery requirements of 1 or 3 hours.

The conclusions that can be drawn from this study are:

- *Surface pressure*: In principle, the (dry air) surface pressure can be determined by measuring the total column of a well mixed gas, for example O_2 or CO_2, from which the (dry) air column can be computed and hence surface pressure.
  O'Brian, 2002, has reviewed recent and past attempts to measure surface pressure (or, basically equivalent, the geopotential height of pressure levels in the troposphere, e.g., the 500 hPa level) from space. He summarizes his findings as follows: *"While satellites now provide routine measurements of many important meteorological and geophysical parameters, measurements of surface pressure has remained elusive, despite its importance for … NWP. The difficulty is principally one of accuracy …"*.
  The review of *O'Brian, 2002*, covers various techniques, including microwave, thermal infrared, and visible/near-infrared passive sensors as well as active sensors (GPS occultations, DIAL, milimeter radar). The main part of his study is devoted to surface pressure retrieval using oxygen A band measurements from a geostationary orbit.
  As discussed in, e.g., *O'Brian, 2002*, the O_2 column can be determined, for example, from nadir radiance measurements in spectral regions corresponding to its visible/near-infrared absorption bands. The band that has been investigated in most studies is the O_2 A band located at 760 nm. The problem in retrieving the O_2 column is not a principal one but one of accuracy due to the demanding accuracy requirements for NWP applications. A 1 hPa surface pressure change corresponds to a 0.1% air column change which corresponds to a 0.1% O_2 column change. This means that the O_2 column (or the column of any other well mixed gas) needs to be determined with an accuracy of better than 0.1%. This is (at least) one order of magnitude better than what has been achieved for other gases which have been extensively studied over many years (e.g., ozone). The main problem in accurately determining the O_2 column using, for example, the O_2 A band, are uncertainties resulting from highly variable atmospheric scatterers (aerosols and clouds) which influence the path length of solar photons in the atmosphere. In addition, there are many other radiative transfer effects that affect accuracy such as the dependence of the retrieved column on surface reflectivity. There are also demanding requirements on the instrument: high stability, high signal to noise ratio, high spectral resolution, high spatial resolution, to mention the most important ones.

- *3-D pressure field*: There are a number of limb viewing instruments that measure or aim at measuring pressure as a function of altitude in the stratosphere and above. For all these systems the horizontal resolution (in the line-of-sight direction) is ~200-250 km basically for geometrical reasons. SAGE III, for example, aims at measuring pressure with a with a precision and accuracy of 2% (vertical resolution ~1 km). MIPAS/ENVISAT determines pressure levels from its CO_2 measurements with a precision of ~2% (vertical resolution ~3 km). Pressure as a function of altitude is a planned operational data product from SCIAMACHY (vertical resolution ~3 km). The operational algorithm is, however, currently only in its initial stage. In addition, the (platform) pointing knowledge

uncertainties are quite large (currently < 3 km, to be improved to ~1 km) which affects both MIPAS and SCIAMACHY. EOS-MLS has a Level 3 data product "Daily map of geopotential height". The expected precision (for 3 km vertical resolution) is < 30 m in the height range 5-30 km (~ 500-10 hPa) *[EOS MLS Science Objectives]*. The EOS-MLS geopotential height retrieval is based on the assumption of hydrostatic equilibrium (i.e., pressure and temperature are not retrieved independently). For a standard profile a 100 m increase in altitude corresponds to a 1.2% pressure decrease, i.e., 30 m correspond to a 0.36% pressure change. This means that the expected EOS-MLS retrieval precision is 1.8 hPa at 500 hPa (required 0.2 hPa), 0.36 hPa at 100 hPa hPa (required 0.1/0.2 hPa), and 0.036 hPa at 10 hPa hPa (required 0.1 hPa). If EOS-MLS reaches its expected performance it might be able to provide data in the middle stratosphere (30 km, 10 hPa) close to the required values.

- We are not aware of any passive satellite system that measures pressure as a function of altitude or of systems that measure the geopotential height of pressure levels in the troposphere with sufficient accuracy and precision (*O'Brian, 2002*). The troposphere is, however, the most important region for NWP.

- *Main conclusion*: In summary, no passive satellite systems exist for which it has been demonstrated that the target or threshold requirements given in *[REQ-PT-2004]* can be met. Furthermore, we are not aware of any such systems planned for the future (see also *Eyre et al., 2002, and O'Brian, 2002*).

Temperature:

The threshold observational requirements for temperature are *[REQ-PT-2004]:* troposphere: precision 1 K, accuracy < 0.5 K, vertical sampling 1 km, horizontal sampling 50-100 km; stratosphere: precision 2 K, accuracy < 0.5 K, vertical sampling 2-3 km, horizontal sampling 200-250 km. The target requirements are even more stringent, e.g., horizontal sampling 15 km, vertical sampling 0.5 km, precision 0.5 K. In addition, there are near-real time data delivery requirements of 1 or 3 hours.

The conclusions that can be drawn from this study are:

- The sensors that measure temperature profiles in the troposphere and stratosphere are nadir sounders operating in the microwave and thermal infrared spectral region. Temperature sounding from space has a relatively long history for NWP and other applications (e.g., the microwave instrument series MSU/AMSU on NOAA satellites and SSM/T / SSMIS series on DMSP satellites). SSM/T has a precision of 0.3 K, an accuracy of 2-3 K, a vertical resolution of 8-10 km, and a horizontal resolution of 175 km at direct nadir (~260 km at extreme swath) *[Grody, 1993; Goodrum, 2000; Redmann, 1992; Deblonde and English, 2002]*. AMSU-A/NOAA has a better performance, namely a precision better than 0.27 K, an accuracy of 1.5 K, a vertical resolution of 3 km in the height range 0-48 km and a horizontal resolution of 50 km at direct nadir (85x172 km^2 at extreme swath) *[Grody, 1993; Diak et al., 1992; Kidder et al., 2000; Goodrum, 2000; Goldberg, 2002; Goldberg, 2002b; Goldberg, 1999; Deblonde and English, 2002]*. An advantage of the microwave sounders is that they are quite insensitive to clouds and measure during day and night. The new generation of high resolution thermal infrared (TIR) nadir sounds such as AIRS/AQUA and IASI/METOP have a vertical resolution of 1 km and a (required) precision of 1 K, and a ground pixel size of 14 x 14 km^2 (AIRS) or 12 x 12 km^2 (IASI) *[Aumann et al., 2003; Susskind et al., 2003; Fetzer et al., 2003; Aires et al., 2002]*. The TIR measurements are also performed during day and night but are affected by clouds which reduces the number of useful measurements. 1 km / 1 K is also the performance of the sensor combination AIRS/AMSU-A onboard AQUA *[Grody, 1993; Diak et al., 1992; Kidder et al., 2000; Goodrum, 2000; Goldberg, 2002; Goldberg, 2002b; Goldberg, 1999; Deblonde and English, 2002]*. The predicted performance of the nadir/limb sounder TES/AURA is 1-2 K with a vertical resolution of 2-6 km in the height range 0-34 km (horizontal resolution 5 x 8 km^2, no scan) *[TES web page]*.

Main conclusion: There are several satellite sensors with global coverage with a performance or predicted performance close to or better than the required threshold performance (e.g., AIRS/AMSU-A/HSB on AQUA and IASI on METOP both with 1 K accuracy, 1 km vertical resolution, < 50 km horizontal resolution). The target performance of 0.5 K accuracy and precision, 0.5 km vertical resolution, and 15 km horizontal resolution is, however, not achieved.

3 List of Applicable Documents

Statement of work:

[SOW-2003] ESA/ESTEC, Concept study for advanced lidar instrument, Statement of work, EOPP-FP/2003-09-828, Issue 1, 17.10.2003

Technical proposal written in response to ESA RFQ/3-10880/03/NL/FF:

[PROP-DLR-2003] DLR and partners, Requirements Definition for Future DIAL Instruments, Technical Proposal, Reference: 3 472 749, 12. November 2003.

Observational requirements documents from Task 1:

Versions prepared for Mid Term Review (distributed via e-mail on 13-Aug-2004):

[REQ-GHG-2004] Martin Heimann and Sander Houweling, Analysis and Establishment of Threshold and Target Observation Requirements for Space-Based Measurements of CO_2, CH_4, and N_2O, Summary of WP 120 updates, Draft August 13, 2004.

[REQ-O3-2004] Jos Lelieveld, Ozone requirements, TN 130, Update 4, July 23, 2004.

[REQ-PT-2004] Hans Volkert and Gerhard Ehret, Analysis and Definition of Observation Requirements for Pressure and Temperature Measurements to be used In Numerical Weather Prediction (NWP), Version August 12, 2004.

The requirement tables from these documents are referred to and also used in:
[TN250-DLR-2004] Synthesis & comparison, selection of parameters for DIAL instrument analysis, TN 250, DLR/IPA, Draft.

Latest updates of GHG requirements:
[REQ-GHG-2004Update1] E-mail from G. Ehret, 5 October 2004.
[REQ-GHG-2004Update2] Summary of WP-120 updates, Sander Houweling, Draft October 7, 2004 (received via e-mail on October 8, 2004).

4 Introduction

The objective of the study “Requirements Definition for Future DIAL Instruments” is to provide the background for the definition of a future space-borne lidar system capable to monitore key atmospheric parameters relevant for climate change, atmospheric chemistry and/or meteorology.

Target species are the three greenhouse gases carbon dioxide (CO_2), methane (CH_4), and nitrous oxide (N_2O) (main goal: to better constrain their surface fluxes), ozone (O_3) (main goal: to improve our understanding of atmospheric chemistry), and atmospheric pressure and temperature (main goal: improvement of numerical weather prediction).

In order to identify the most important one or two of these parameters approriate for a future lidar system, it is necessary to assess to what extent the observational requirements can be met already now with existing passive systems or are likely to be met with passive systems in the near future. These aspects are addressed in this technote.

The focus of this passive systems analysis part of study “Requirements Definition for Future DIAL Instruments”, which is described in this technote, is

- to analyse the current status of operational[1] global passive sensors in the solar backscatter, thermal infrared, and microwave spectral regions for pressure (p), temperature (T), CO_2, N_2O, CH_4 and/or O_3 remote sensing systems,
- to assess by literature research the measurement methods, locations, accuracy, calibration and sampling schemes,
- to analyse the potential enhancements for p, T, CO_2, N_2O, CH_4 and O_3 measurements within the next decade; i.e. assess the potential of technological improvements, implementation of new technologies, new sensor combinations etc. to achieve worthwhile additional information w.r.t. the measurement objectives. Analyse the intrinsic limitations of solar backscatter, thermal infrared, and microwave sensors for p, T, CO_2, N_2O, CH_4 and O_3 measurements. The analysis shall be based on public available literature and relevant ESA studies if made available by ESA.
- to give recommendations on possible performance enhancement by synthesis with active sensors.

The input for this technote are the observational requirements for greenhouse gases *[REQ-GHG-2004]*, ozone *[REQ-O3-2004]*, and pressure and temperature *[REQ-PT-2004]*. They are briefly summarised in Section 5.

[1] The term “operational” is meant in a rather broad sense, covering for example both, ESA Earth Explorer and Earth Watch type missions, not in the restrictive sense of “near-real time data delivery” missions.

5 Summary of Observational Requirements

5.1 Requirements for greenhouse gases

The observational requirements shortly summarised in this section are described in detail in *[REQ-GHG-2004]*.

Table 3.2.1: Summary of technical user requirements for column content measurements

	CO_2 (ppm)		CH_4 (ppb)		N_2O (ppb)	
	Target	Threshold	Target	Threshold	Target	Threshold
Precision (line wing)	0.8	3.5	10	35	0.1	1
Syst. error	**					
Temporal res.	1 d	6 d	1 d	6 d	1 d	6 d
Horizon. res.	50 km	500 km	50 km	500 km	50 km	500 km
Vertical res.	column	column	column	column	column	column

**: still to be determined

Table 1: Requirements for CO_2, CH_4, and N_2O column measurements (dry air average mixing ratios). Table from: *[REQ-GHG-2004, TN250-DLR-2004]*.

Table 3.2.2: Summary of technical user requirements for range-resolved measurements

	CO_2 (ppm)		CH_4 (ppb)		N_2O (ppb)	
	Target	Threshold	Target	Threshold	Target	Threshold
Precision	1.2	7.2	17	68	0.3	3.2
Syst. error	**					
Temporal res.	1 d	6 d	1 d	6 d	1 d	6 d
Horizon. res.	50 km	500 km	50 km	500 km	50 km	500 km
Vertical res.	b, f, s	b, f,s	b,f,s	b,f,s	b,f,s	b,f,s

This table will be updated

Table 2: Requirements for CO_2, CH_4, and N_2O range resolved measurements. Table from: *[REQ-GHG-2004, TN250-DLR-2004]*.

According to the requirement update given in *[REQ-GHG-2004Update1]* the following target requirements for the columns of the Greenhouse gases (CO_2, CH_4, N_2O) should be used:

- Temporal resolution: 6 days (instead of 1 day)
- Horizontal resolution: 500 km (instead of 50 km)

This update has been taken into account for this version.

According to the latest requirements update given in in *[REQ-GHG-2004Update2] the requirements are:*

Table 4-1: Summary of technical user requirements for Hard Target LIDAR

	CO_2 (ppm)#		CH_4 (ppb)		N_2O (ppb)	
	Target	Threshold	Target	Threshold	Target	Threshold
Precision	1	3.5	10	35	0.1	0.5
Temporal res.	week	month	week	month	week	month
Horizon. res.	$2^{O}x2^{O}$	$5^{O}x5^{O}$	$2^{O}x2^{O}$	$5^{O}x5^{O}$	$2^{O}x2^{O}$	$5^{O}x5^{O}$
Vertical res.	column	column	column	column	column	column

#: dry air mixing ratio

These requirements are valid for a typical achievable weighting function (calculated for CO_2 at 2051.018nm).

Table 4-2: Summary of technical user requirements for DIAL (aerosol target)

	CO_2 (ppm)#		CH_4 (ppb)		N_2O (ppb)	
	Target	Threshold	Target	Threshold	Target	Threshold
Precision	5	10	100	100	0.5	1.0
Temporal res.	week	month	week	month	week	month
Horizon. res.	$2^{O}x2^{O}$	$5^{O}x5^{O}$	$2^{O}x2^{O}$	$5^{O}x5^{O}$	$2^{O}x2^{O}$	$5^{O}x5^{O}$
Vertical res.	bnd.layer	bnd.layer	bnd.layer	bnd.layer	bnd.layer	bnd.layer

#: dry air mixing ratio

Table 3: Requirements for CO_2, CH_4, and N_2O. Table from: *[REQ-GHG-2004Update2]*.

Important note:
Because these requirements became available on the same day where this document had to be delivered it was not possible to fully take these requirements into account. We have chosen the following approach to deal with this: In the Executive Summary short sections have been added to roughly assess the impact of these requirements for each of the three Greenhouse gases but only for the columns (text in italics). Also the Summary Table given in the Executive Summary has been adjusted to roughly take these new requirements (columns only) into account.

5.2 Requirements for ozone

The observational requirements shortly summarised in this section are described in detail in *[REQ-O3-2004]*.

Table 3.3: Threshold observational requirements for O3 measurements from space. Target Observational requirements are listed in parentheses.

Parameter	**Ozone measurements**		
Altitude range [km]	Troposphere	UTLS	Stratosphere
	0-10	8-16	10-50
Applications	1,2,6,7	1,4,5,6	1,3,4,6,7
Vertical resolution [km]	3(1)	2(1)	2(1)
Horizontal domain		global	
Horizontal resolution [km]	20 (10)	50 (10)	100 (10)
Dynamic range in mixing ratio [ppbv]	10-100	50-1000	10^3-10^4
Precision (1 standard deviation) [%]	< 20 (10)	< 20 (10)	< 20 (10)
Accuracy (systematic error) [%]	< 10 (5)	< 10 (5)	< 10 (5)
Timeliness [hr]	3	6	6

Table 4: Requirements for O_3 measurements. Table from *[REQ-O3-2004, TN250-DLR-2004]*.

5.3 Requirements for pressure and temperature

The observational requirements shortly summarised in this section are described in detail in *[REQ-PT-2004]*.

*Table 3.1.1: Observational requirements for **global NWP** for space borne temperature sensors broken down by the atmospheric layers **Lower Troposphere (LT)**, **Higher Troposphere (HT)**, **Lower Stratosphere (LS)**, and **Higher Stratosphere (HS)**.*

Parameter	***Temperature***			
Altitude range pressure height [hPa] approx. height range [km]	**LT** 1000–500 0 – 5	**HT** 500–100 5 – 15	**LS** 100–10 15 – 35	**HS** 10 – 1 35 – 50
Vertical sampling[1] [km]	1	1	2	3
Height assignment [km]	0.1	0.1	0.2	0.3
Horizontal domain	global			
Horizontal sampling[2] [km]	50	100	200	250
Dynamic range [K]	180 - 300			
Precision[3] (1 standard deviation) [K]	1	1	2	2
Bias [K]	< 0.5	< 0.5	< 0.5	< 0.5
Observation cycle[4] [h]	12	12	12	12
Timeliness[5] [h]	3	3	3	3

[1] vertical sampling requirement for regional NWP = 0.5 km
[2] horizontal sampling requirement for regional NWP = 15 km
[3] precision requirement for regional NWP = 0.5 °K
[4] observation cycle for regional NWP = 1 h
[5] timeliness for regional NWP = 1 h

Table 5: Observational requirements for temperature. From: *[REQ-PT-2004, TN250-DLR-2004]*. In the context of this technote the requirements for regional NWP are interpreted as target requirements and the requirements for global NWP are interpreted as threshold requirements

*Table 3.1.2: Observational requirements for **global NWP** for space borne pressure sensors broken down the Earth's **surface** and the atmospheric layers **Lower Troposphere (LT)**, **Higher Troposphere (HT)**, and **Lower Stratosphere (LS)**.*

Parameter	***Pressure***			
Altitude range pressure height [hPa] approx. height range [km]	**surface**	**LT** 1000-500 0 – 5	**HT** 500-100 5 – 15	**LS** 100-10 15 – 35
Vertical sampling [km]		1	1	2
Height assignment [km]	0.01	0.01	0.01	0.01
Horizontal domain	global			
Horizontal sampling[1] [km]	50	50	100	200
Dynamic range [hPa]	1050-950	1050-500	500-100	100-10
Precision[2] (1 standard deviation) [hPa]	<1	0.6	0.2	0.1
Bias [hPa]	<0.5	<0.5	<0.2	<0.1
Observation cycle[3] [h]	12	12	12	12
Timeliness[4] [h]	3	3	3	3

[1] horizontal sampling requirement for regional NWP = 15 km
[2] surface pressure requirement for regional NWP = 0.5 hPa
[3] observation cycle for regional NWP = 1 h
[4] timeliness for regional NWP = 1 h

Table 6: Observational requirements for pressure. From: *[REQ-PT-2004, TN250-DLR-2004]*. In the context of this technote the requirements for regional NWP are interpreted as target requirements and the requirements for global NWP are interpreted as threshold requirements

6 Overview Passive Systems

6.1 Study related general remarks

Existing or planned space borne passive system missions cover very different viewing geometries (nadir, limb, occultation). Each viewing geometry has its advantages and disadvantages (e.g., for solar occultation high precision but restricted coverage). As described in Section 4 the focus of this technote is to analyse systems for global observations. Global observation of the Earth can effectively be achieved (i.e., in typically a few days) with nadir and/or limb viewing geometries, not however with, e.g., solar or lunar occultation viewing geometries.

There are also different kinds of orbital configurations (low Earth orbits (sun-synchronized or not), geostationary orbits, etc.). The required global observation (plus the assumption that the mission to be defined shall be realized with not more than one satellite) basically leads to the requirement of a low Earth orbiting (LEO) satellite mission. Therefore, passive systems on LEO satellites will be the focus of this study.

From the observational requirements summarized in Section 5 it follows that primarily accurate measurements in the troposphere are required. Tropospheric measurements (including the middle troposphere and the boundary layer) require nadir observations. This is also the most likely viewing geometry of the envisaged lidar instrument to be specified in this study. Limb measurements are typically restricted (e.g., because of clouds) to the altitude range from the upper troposphere (or lower stratosphere) upwards. Because of this the focus of this study is on nadir observations (perhaps in combination with limb observations).

Therefore the focus of this technote will be on nadir looking passive sensors on LEO satellites.

6.2 Spectral regions overview

The passive systems analysed in this study cover a broad spectral range from the ultra violet to the microwave. For this study this large spectral region has been sub divided into three major parts, namely the solar backscatter spectral region, the thermal infrared spectral region, and the microwave spectral region. Concerning the parameters to be investigated in this study, each spectral region offers advantages and disadvantages with respect to, for example, information content (e.g., sentitivity to lower troposphere). This will be discussed in detail in Sections 7 - 9. A short overview is given in

Aspect	Solar	Thermal infrared	Microwave
Light source	Sun (stars)	Earth	Earth
Radiative transfer	Scattering, reflection, and absorption	Emission and absorption	Emission and absorption
Coverage	Dayside (stars: also nightside)	Day and night	Day and night
Clouds	Not transparent	Not transparent	Approx. transparent
Sensitivity w.r.t. lower troposphere	High	Low	Low
Nadir observation over land / ocean	Land: Possible Ocean: Difficult in NIR except for sun-glint	Possible	Land: Difficult Ocean: Possible
Gases	• O_3, CO_2, CH_4 • N_2O (weak)	O_3, CO_2, CH_4, N_2O	• O_3, N_2O • CH_4 (very weak) • No CO_2 lines
p/T sensitivity	p(z)+T(z): Low Surface pressure: possible	p: moderate T: high	p+T: High
Instrument types	Mainly grating spectrometers	FTIR, grating, filter, gas correlation	Heterodyne technique
Typical instruments	TOMS, SBUV, GOME, SCIAMACHY, OCO, …	TOVS, IMG, AIRS, TES, IASI, …	MSU, AMSU, SSM/T, MLS, …

Table 7: Spectral regions overview.

6.3 Satellite instruments overview

This section gives a short overview about the satellite instruments considered for this study.

6.3.1 Instruments operating in the solar spectral region

Instrument	Instrument Type	Platform	Orbit	Launch	Mission End	Spectral Range [nm]	Spectral Resol. [nm]	Spatial Foot-print [km]	Swath [km]	Cover-age
TOMS	Grating Spectrometer	Nimbus-7 Meteor-3 Earthprobe (EP)	LEO, sun-syn.	EP: 1996	EP: ongoing (2004: shows degradat.)	6 bands in UV	1	EP: 47 x 47	EP: 3100	EP: global: 1 day
SBUV/2	Grating Spectrometer	NOAA	LEO, sun-syn.	1996	2009	12 bands in UV	01. Jan	170	no scan	-
HALOE	Gas filter radiometer (Solar occ.)	UARS	LEO, non sun-syn.	1991	ongoing (only for special events)	Several channels 2.5-11 um	Broadband	Vertical: 2.5 km	-	-
POAM III	Photometer (Solar occ.)	SPOT-4	LEO, sun-syn.	1998	ongoing	9 bands 350-1030	2.05-17.7	Vertical: 1-2.5 km (O3: 1km)	-	~28 profiles per day
MOPITT	Gas correlation radiometer	TERRA	LEO, sun-syn., 10:30 AM	1999	2004	CH4: 2.2 um CO: 2.3 and 4.6 um	-	22 x 22	640	global: 3 days
SAGE III	Grating Spectrometer (Sol.+lunar occ.)	METEOR-3M 1	LEO, sun-syn., 9 AM (asc)	2001	2004	9 regions: 280 - 1550	0.2 - 0.5	Vertical: 0.5-2 km	-	-
GOME	Grating Spectrometer	ERS-2	LEO, sun-syn., 10:30 AM (desc)	1993	ongoing (2003: ERS download problems)	240 - 790	0.2 - 0.5	40 x 320	960	global: 3 days
SCIAMACHY	Grating Spectrometer (nadir, limb, sol.+lunar occ.)	ENVISAT	LEO, sun-syn., 10:00 AM (desc)	2002	2007	240 - 2400	0.2 - 1.6	Nadir: 30 x 60 30 x 120 30 x 240	960	global: 6 days
GOMOS	Grating Spectrometer (stellar occ.)	ENVISAT	LEO, sun-syn., 10:00 AM (desc)	2002	2007	250 - 675, 756 - 773, 926 - 952	0.1 - 0.9	Vertical: 1.7 km (FoV) 2-4 km (Level2)	-	~ 600 profiles per day
OMI	Grating Spectrometer	AURA	LEO, sun-syn., 1:45 PM (asc)	2004	2010	270 - 500	0.5	13 x 24	2600	global: 1 day
GOME-2	Grating Spectrometer	METOP 1-3	LEO, sun-syn., 9:30 AM	2005	2019	240 - 790	0.24-0.53	40 x 80	1920	global: 1 day
OCO	Grating Spectrometer	OCO	LEO, sun-syn., 1:15 PM (asc)	2007	2009	~760 nm, ~1610 nm, ~2060 nm	0.04, 0.08	1 x 1.5	no scan	16-day repeat
SOFIS	Fourier Trans. (solar occ.)	GCOM-A1	non sun-syn. 69 deg inclin.	2006 (cancelled)	-	760 nm, 3-13um	0.2 cm-1	Vertical: 1 km	-	28 profiles per day
GOSAT	Fourier Trans. (NIR+TIR)	GCOS	TBD	2007	TBD	~760 nm, ~1610 nm, ~2060 nm, 4-15 um	0.1-0.3 cm-1	TBD	TBD	TBD

Table 8: Instruments operating in the solar region: General overview.

Instrument	Links
TOMS/EP	http://jwocky.gsfc.nasa.gov/eptoms/ep.html
SBUV/2	http://www.cpc.ncep.noaa.gov/products/stratosphere/sbuv2to/
HALOE	http://haloedata.larc.nasa.gov/home.html
POAM III	http://spot4.cnes.fr/spot4_gb/poam_iii.htm
MOPITT	http://terra.nasa.gov/About/MOPITT/about_mopitt.html
SAGE III	http://www-sage3.larc.nasa.gov/
GOME	http://www.iup.physik.uni-bremen.de/gome
SCIAMACHY	http://www.iup.physik.uni-bremen.de/sciamachy
GOMOS	http://envisat.esa.int/instruments/gomos/
OMI	http://aura.gsfc.nasa.gov/instruments/omi/introduction.html
GOME-2	http://www.esa.int/export/esaME/gome-2.html
OCO	http://oco.jpl.nasa.gov
SOFIS	http://eos.nasda.go.jp
GOSAT	http://www.jaxa.jp/missions/projects/sat/eos/gosat/index_e.html

Table 9: Instruments operating in the solar region: Links.

Instrument	CO2	CH4	N2O	O3	p	T
TOMS				x		
SBUV/2				x		
HALOE		x		x		
POAM III				x		x
MOPITT		x				
SAGE III				x	x	x
GOME				x		
SCIAMACHY	x	x	x	x	x	x
GOMOS				x		x
OMI				x		
GOME-2				x		
OCO	x					
SOFIS	x					
GOSAT	x					

Table 10: Instruments operating in the solar region: Parameter overview.

6.3.2 *Instruments operating in the thermal infrared spectral region*

Instrument	Instrument Type	Platform	Orbit	Launch	Mission End	Spectral Range [cm-1]	Spectral Resol. [cm-1]	Spatial Foot-print [km]	Swath [km]	Cover-age
HIRS	IR Imager	POES NOAA	LEO PM	1985	ongoing	IR	filter	10	2200	global: 1 day
IMG	Interferometer	ADEOS	LEO descending node 10:15 - 10:45 AM	1996	1997	600 - 2000 2000 - 2326 2325 - 3000	< 0.1	8	8	TBD
NAST-I	Interferometer	ER-2, PROTEUS	Airborne	1998	several flights	590-2810	0,25	3	40	TBD
AIRS	Grating Spectrometer	AQUA	LEO Ascending node - 1:30 p.m. +/- 15 minutes	2002	ongoing	649 -1135 1217 - 1613 2169 -2674	~ nu/2400	14	1650	global: 2 days
TES	Interferometer	AURA	LEO 1:45 PM ascending node	2004	~2008	650 - 3050	0.1 Nadir 0.025 Limb	Nadir: 5 x 8 Limb: 55 x 170	Nadir: 5 Limb: 23	TBD
IASI	Interferometer	METOP-1/2/3	LEO 9:30 AM	2005	~2015	645 - 2760	0.25	12	2400	global: 1 day
CrIS	Interferometer	NPP NPOESS	LEO AM/PM	2006 (NPP) 2009 (NPOESS)	TBD	650 - 1095 1210 - 1750 2155 - 2550	0.625 1.25 2.5	14	2200	global: 1 day
GIFTS	Interferometer	TBD	GEO	< 2010	TBD	685 - 1130 1650 - 2250	0.3 - 36	4	TBD	full disk: 7min.
ABS/HES	Interferometer or Grating	GOES-R	GEO	~ 2012	TBD	650 - 1200 1210 - 1750 2150 - 2720	0.625 1.25 2.5	< 10	TBD	full disk: hour

Table 11: Instruments operating in the thermal infrared: General overview.

Instrument	Links
HIRS	http://poes.nesdis.noaa.gov/atovs http://daac.gsfc.nasa.gov/CAMPAIGN_DOCS/FTP_SITE/INT_DIS/readmes/tovs.html
IMG	http://www.eorc.nasda.go.jp/AtmChem/IMG/ http://www.eoc.nasda.go.jp/satellite/sendata/img_e.html
NAST-I	http://deluge.ssec.wisc.edu/~nasti/
AIRS	http://daac.gsfc.nasa.gov/atmodyn/airs/airs_products.html http://www-airs.jpl.nasa.gov/
TES	http://tes.jpl.nasa.gov/ http://aura.gsfc.nasa.gov/instruments/tes/introduction.html
IASI	http://smsc.cnes.fr/IASI/
CrIS	http://www.ipo.noaa.gov/Technology/cris_summary.html http://www.ipo.noaa.gov/Library/cris_NDX.html
GIFTS	http://asd-www.larc.nasa.gov/GIFTS/
ABS/HES	http://cimss.ssec.wisc.edu/goes/HES/

Table 12: Instruments operating in the thermal infrared: Links.

Instrument	CO2	CH4	N2O	O3	p	T
HIRS	x		x	x		x
IMG	x	x	x	x		x
NAST-I						x
AIRS	x	x	x	x		x
TES		x		x		x
IASI	x	x	x	x		x
CrIS						x
GIFTS	x			x		x
ABS/HES						x

Table 13: Instruments operating in the thermal infrared: Parameter overview.

6.3.3 *Instruments operating in the microwave spectral region*

Instrument	Instrument Type	Platform	Orbit	Launch	Mission End	Spectral Range [GHz]	Spectral Resol. [MHz]	Spatial Foot-print [km]	Swath [km]	Cover-age
SSM/T	Radiometer	DMSP	LEO	1978	TBD	50 - 60	TBD	175 (nadir) ~260 (edge)	1500	global
SSMIS	Radiometer	DMSP	LEO	2003	~2011+	19 - 183	240-390 (50-60GHz) <1.5MHz (60-65GHz)	38 (75 abv. 10mb)	1707	global
AMSU-A	Radiometer	NOAA AQUA METOP	LEO LEO LEO	1998 2002 ~2005	TBD	23 - 89	3-400	50 (nadir) 150(edge)	2200	global, 6hrs
CMIS	Radiometer	NPOESS	LEO	~2009	~2020	6 - 183	8.4-1280	40 (5)	1700 (3000)	global, 6hrs
ATMS	Radiometer	NPP, NPOESS	LEO LEO	~2005 ~2010	~2010 ~2020	23-183	3-400	50 (nadir) 150(edge)	2200	global
MLS	Radiometer	UARS AURA	LEO LEO	1991 2004	1997 (63GHz T sounder)	63, 183, 205 118,183,626, 2500	2-128 6-96	TBD 165	TBD TBD	34N-80S 34S-80N (2x36d) global

Table 14: Instruments operating in the microwave: General overview.

Instrument	Links
SSM/T	http://dmsp.ngdc.noaa.gov/html/sensors/doc_ssmt.html
SSMIS	http://www.aerojet.com/program/detail/about_ssmis.htm http://www.aoc.noaa.gov/article_SSMIS_Underflight_Studies.htm
AMSU-A	http://orbit-net.nesdis.noaa.gov/crad/st/amsuclimate/ http://amsu.cira.colostate.edu/ http://daac.gsfc.nasa.gov/atmodyn/airs/guide/amsu_instrument_guide.html
CMIS	http://www.npoess.noaa.gov/Technology/cmis_summary.html http://npoesslib.ipo.noaa.gov/S_cmis.htm
ATMS	http://www.npoess.noaa.gov/Technology/atms_summary.html
MLS	http://mls.jpl.nasa.gov/
EOS-MLS	http://aura.gsfc.nasa.gov/instruments/mls/datapro.html

Table 15: Instruments operating in the microwave: Links.

Instrument	CO2	CH4	N2O	O3	p	T
SSM/T						**x**
SSMIS						**x**
AMSU-A						**x**
CMIS						**x**
ATMS						**x**
EOS-MLS			**x**	**x**	**x**	**x**

Table 16: Instruments operating in the microwave: Parameter overview.

7 Passive Systems in the Solar Spectral Region

7.1 Introduction

The solar irradiance closely follows in magnitude and spectral dependence a black body emission curve at 6000 K. The term solar spectral region corresponds to the spectral region where the solar irradiance is large compared to the effective black body emission of the Earth (~290 K). The term solar spectral region as used in this study covers the wavelength region from approximately 200 nm to approximately 4000 nm (2500 cm^{-1}). The solar spectral region, therefore, covers the spectral region from the ultra violet (UV) to the near (or short wave) infrared region (NIR, SWIR) and includes the visible spectral region.

Spectral lines overview

Figure 1 shows the spectral positions and strength (line intensities) of the absorption lines of all gases relevant for this study in the solar spectral region (spectroscopic line parameters from Hitran 2000/2001 *[Rothman et al., 2003]*). For ozone the "continuum" absorption cross section in the UV/visible is shown in addition (as measured with the GOME flight model). As can be seen, all gases relevant for this study have many absorption lines in the solar spectral region covering a wide range of line strength from very weak to very strong. As the solar irradiance is quite low for wavelength larger than about 2500 nm (4000 cm^{-1}) it is important to focus on the region below 2500 nm (except for direct sun observation using solar occulation technique where a high signal can be obtained even for wavelength larger than 2500 nm). Below 2500 nm basically all gases show many strong and weak lines. The only exception is N_2O which only exhibits rather weak lines in this region. This can be better seen in Figure 2 which shows the atmospheric transmission in the spectral region 400 – 2400 nm.

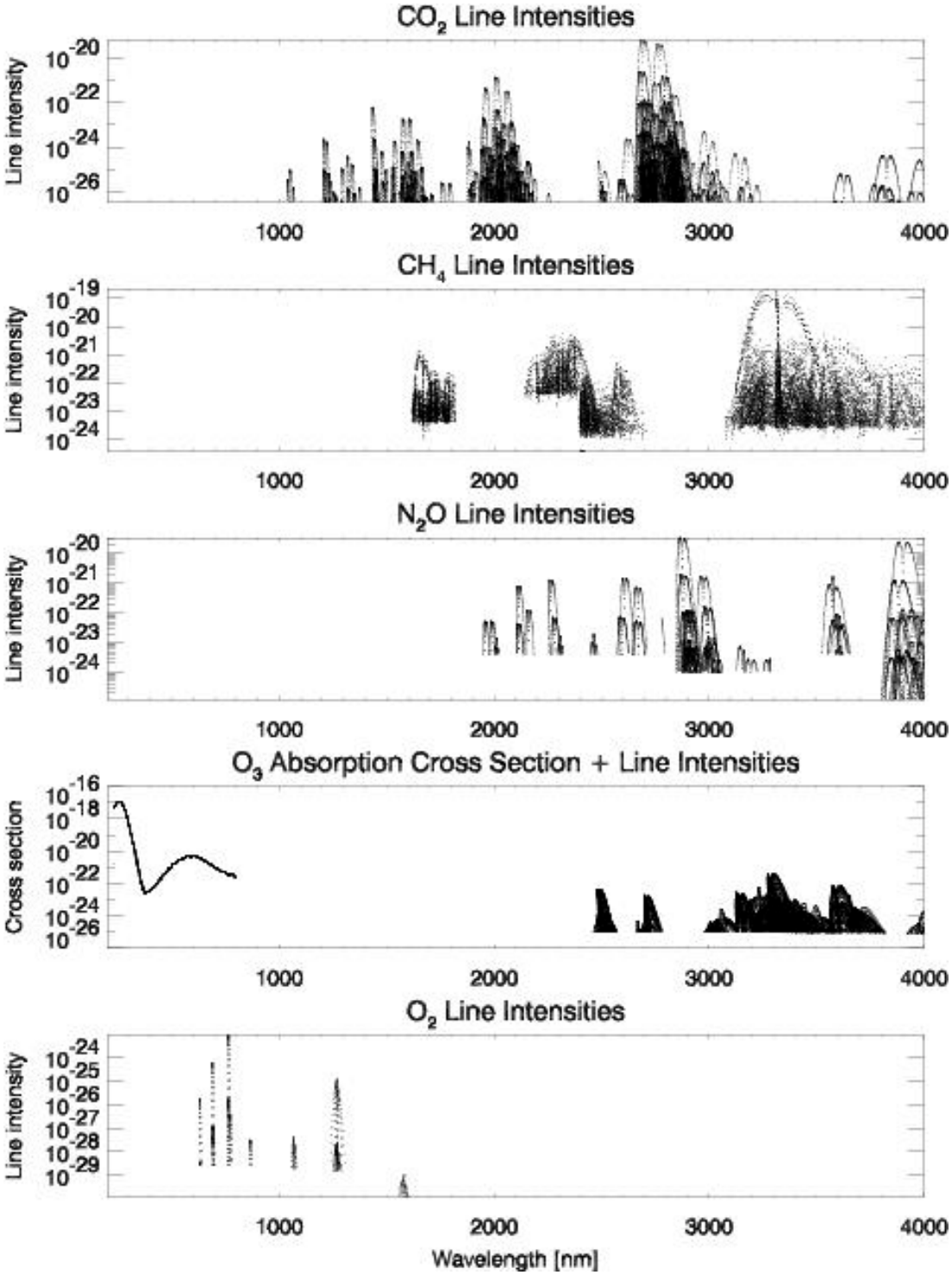

Figure 1: Molecular line intensities (line strength) of the atmospheric gases relevant for this study in the solar spectral region (for ozone in addition the UV/visible absorption cross section as measured with the GOME fligh model is shown). Figure generated by M. Buchwitz using Hitran spectroscopic line parameters *[Rothman et al., 2003]*.

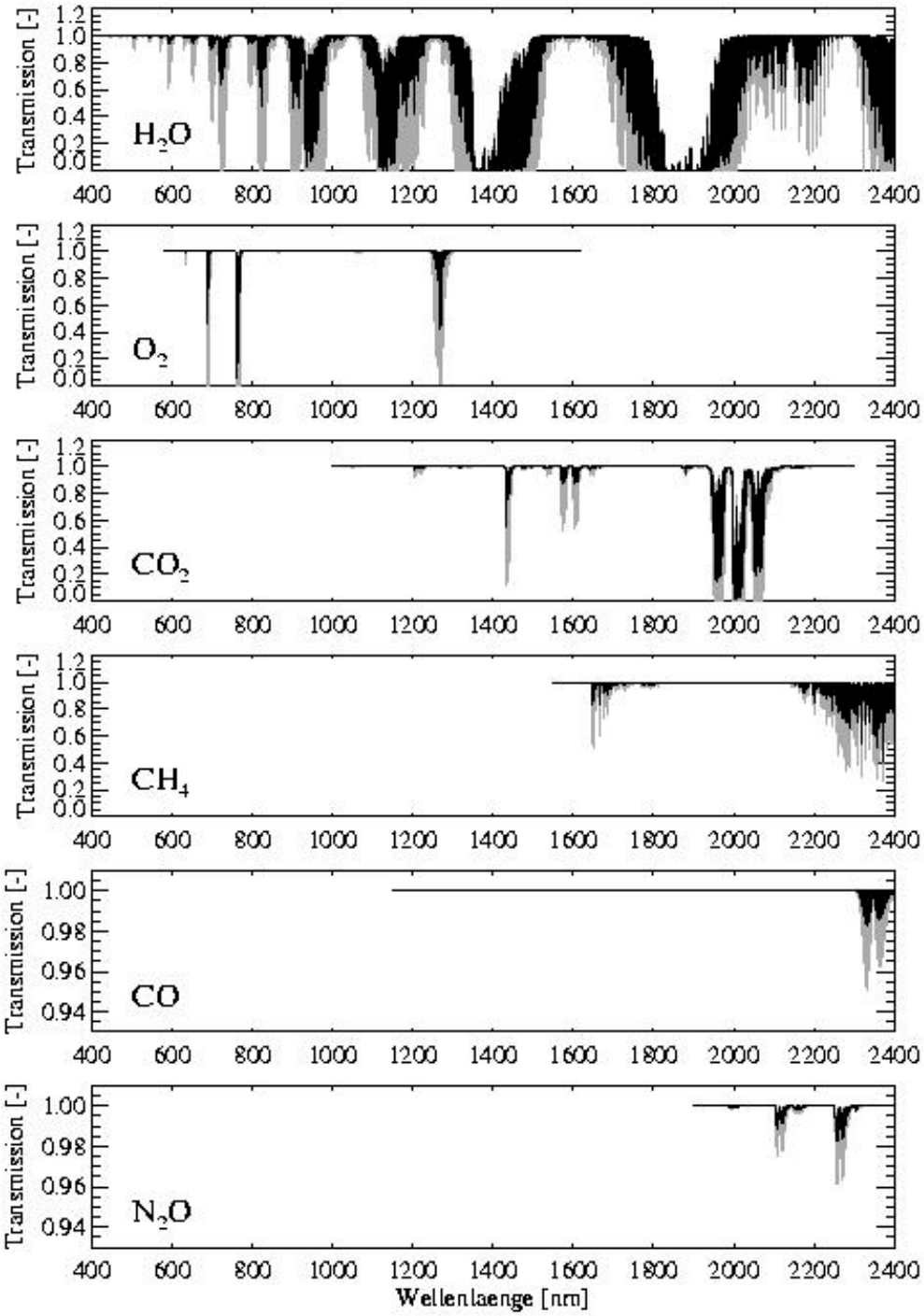

Figure 2: Transmission of various gases in the solar spectral region from 400 nm to 2400 nm (from *Buchwitz, 2000*). The transmissions have been calculated for an airmass of one (i.e., for a trace gas column equal to its vertical column) assuming a US Standard Atmosphere (with greenhouse gas concentrations scaled to year 2000 concentrations), a pressure of 900 hPa and a temperature of 270 K. The grey lines correspond to the monochromatic transmission, the black lines are for lower spectral resolution (Gaussian slit function with 0.2 nm full width at half maximum (FWHM)).

Radiative transfer and retrieval aspects

Passive sensors operating in the solar spectral region typically determine the amount (e.g., the vertical column or the concentration profile) of an atmospheric trace gas from characteristic spectral absorption structures resulting from the absorption of solar light as it passes through the terrestrial atmosphere.

The appropriate viewing geometrie for the determination of trace gas vertical profiles is the limb viewing geometrie (using scattered light or direct solar/lunar observations). Limited profile information can also be derived from the nadir view (e.g., ozone profiles from SBUV/2 or GOME). In limb viewing geometrie the vertical resolution is mainly determined by the field-of-view (FoV) of the instrument in the vertical direction. Therefore a good vertical resolution is possible. Profiles can be obtained from the lower stratosphere or upper troposphere upwards. Clouds constitute a major problem. They determine the lowest altitude that can be observed. The horizontal resolution in viewing direction is relatively low (~250 km) for geometrical reasons. Radiative transfer for the simulation of limb measurements of scattered light is complex and time consuming if multiple scattering in a curved (e.g., spherical shell) atmosphere needs to be accurately considered. This is not a primary issue for solar and lunar occultation measurements but here the spatial spatial coverage is restricted.

The appropriate viewing geometry for the determination of a trace gas total column by a passive sensor is the nadir mode where the atmospheric region below the instrument is observed. A high spatial resolution is advantageous as this increase the probability for cloud-free observations. Remote sensing in the solar spectral region using nadir viewing enables the entire troposphere and in particular the planetary boundary layer to be probed. Especially at longer wavelength (i.e., in the near-infrared (NIR) or short wave infrared (SWIR)) the sunlight penetrates down to the Earth surface, resulting in high measurement sensitivity for all altitude levels down to the ground.

Instruments such as GOME and SCIAMACHY measure both, the extraterrestrial solar irradiance and the backscattered Earthshine radiance. In the retrieval process an inversion method is used to determine the concentration of the absorber from the ratio of upwelling radiance to solar irradiance (“sun-normalized radiance”).

Typically trace gas (vertical or slant) column retrieval methods used for remote sensing in the solar spectral region are based on the Differential Optical Absorption Spectroscopy (DOAS) methode as described in, e.g., *Burrows et al., 1999a*. The earthshine radiance is normalized to the solar irradiance. Broadband contributions are separated from differential (absorption) features by approximating the spectrally slowly varying components (Rayleigh and Mie scattering, surface albedo) by a low order polynomial. In standard DOAS (used for, e.g., current operational ozone retrieval from GOME and SCIAMACHY) reference cross sections are fitted to the remaining differential absorption component. This results in the slant column density, which represents the absorber amount integrated along the (average) light path. A radiative transfer model (e.g., GOMETRAN, *Rozanov et al., 1997*) is used to compute a so-called air mass factor (AMF) by which the slant column density is converted to the desired vertical column density. The AMF can roughly be interpreted

as the length of the average light path relative to the vertical extent of the atmosphere. The AMF not only depends on the line-of-sight (LOS) scan angle and the sun position but also on distribution of atmospheric scatterers and absorber (and their detailed optical properties) and the surface spectral reflectance. Because of, e.g., multiple scattering and/or narrow absorption lines radiative transfer calculations are typically very time consuming. Many retrieval algorithms therefore use pre-calculated radiative transfer quanties such as AMFs (look-up table (LUT) approach).
Whereas standard DOAS might be considered appropriate for a "continuum" absorber such as ozone, more complex ("modified DOAS") algorithms (e.g., WFM-DOAS, *Buchwitz et., 2000a*, *Buchwitz and Burrows, 2004*) are applied for the retrievals of "line absorbers" such as CO_2 and CH_4 because of the much stronger dependence of their absorption cross section on wavelength, pressure, and temperature (see, e.g., *Buchwitz et al., 2000a*).

DOAS based algorithms are typically very robust and numerically fast (especially when using look-up tables) which makes them well suited for operational data processing. For example, the operational trace gas nadir data products of GOME and SCIAMACHY are produced using DOAS-type methods.

For more complex quanties to be retrieved, e.g. vertical profiles, typically more complex (and also time consuming) retrieval algorithms are used. Profile retrieval is an underconstrained inversion problem. Additional information or assumputions are needed to make the problem well posed. Many retrieval methods are based on "Optimal Estimation" (*Rodgers, 1976; Rodgers, 2000; Hoogen et al., 1999*) which enables the use of more or less detailed *a-priori* information of the quantities to be retrieved to constrain the retrieval.

7.2 Instrument overview

7.2.1 TOMS

The Total Ozone Mapping Spectrometer (TOMS) instrument series started in 1978 with the Nimbus-7 satellite and continued with the TOMS aboard a Russian Meteor-3 satellite until the instrument stopped working in December 1994. This NASA-developed instrument measures ozone indirectly by mapping ultraviolet light emitted by the Sun to that scattered from the Earth's atmosphere back to the satellite. TOMS main product is the total column of ozone.

The TOMS instrument currently in operation is the TOMS instrument onboard the Earth Probe (EP) Satellite (TOMS/EP) launched in July 1996. Currently TOMS/EP suffers from degradation (scan bias problems).

7.2.2 SBUV

The Solar Backscatter UltraViolet (SBUV) instruments (SBUV on Nimbus 7 and later SBUV/2 on the NOAA satellites) are nadir-viewing instruments that infer total column ozone and the ozone vertical profile by measuring sunlight scattered from the atmosphere in the middle ultraviolet.

One of the instruments currenly in operation is SBUV/2 on NOAA-16. Ozone profiles and total column amounts are derived from the ratio of the observed backscattered spectral radiance to the incoming solar spectral irradiance, which is referred to as the backscattered albedo. The only difference in the radiance and irradiance observations is the instrument diffuser used to make the solar irradiance measurement; the remaining optical components are identical. An important improvement of SBUV/2 over the SBUV was the ability to measure changes in solar diffuser reflectivity in flight, using a mercury lamp as a light source (this lamp also provides wavelength calibration).

7.2.3 HALOE/UARS

The Halogen Occultation Experiment (HALOE) was launched on the Upper Atmosphere Research Satellite (UARS) spacecraft in September 1991 as part of the Earth Science Enterprise (ESE) program. HALOE measurements covers the spectral range from 2.45 to 10.04 μm. Broadband and gas filter channels are used in the instrument. A detailed description of the instrument, scientific goals, and first results can be found in *[Russel et al., 1993]*. The UARS orbit is non sun-synchronous, polar, 585 km altitude, inclination 57 deg. Coverage is from 80 deg North to 80 deg South. The vertical resolution is determined by the IFOV which is 0.033 deg (~1.5 km). The main HALOE products relevant for this study are vertical profiles of ozone and CH_4.

7.2.4 POAM/SPOT

The first Polar Ozone and Aerosol Measurements (POAM) instrument was a three-channel spectrometer mainly dedicated to ozone measurements. It failed immediately after launch in 1985. The successors POAM II and POAM III were launched in 1993 and 1998 onboard SPOT-3 and SPOT-4 (Satellite Pour l'Observation de la Terre), respectively. Both consists of nine channels equipped with photometers coverning the UV-visible-NIR wavelength range. The SPOT orbit parameters are: sun-synchronous, polar, inclination 98.7 deg, 833 km altitude. The spatial coverage is: 54-71 deg North (sunrise), 63-88 deg South (sunset). The main targets parameters relevant for this study are vertical profiles of ozone and temperature.

7.2.5 MOPITT/TERRA

MOPITT (Measurements Of Pollution In The Troposphere) is the first satellite sensor to use gas correlation spectroscopy. MOPITT has been launed in 1999 onboard TERRA. The sensor measures emitted and reflected radiance from the Earth in three spectral bands. As this light enters the sensor, it passes along two different paths through onboard containers of carbon monoxide and methane. The different paths absorb different amounts of energy, leading to small differences in the resulting signals that correlate with the presence of these gases in the atmosphere. MOPITT's spatial resolution is 22 km at nadir and it 'sees' the Earth in swaths that are 640 km wide. MOPITT operates by sensing infrared radiation from either the thermal emission/absorption at 4.7 µm for CO profiles, or reflected sunlight at about 2.2 and 2.3 µm for CH_4 and CO column measurements in daylight.

So far only CO data products (profiles and columns) have been released which have been retrieved from the TIR channel of MOPITT. No methane data products (columns) have been released due to problems with the NIR channel data.

7.2.6 SAGE

SAGE (Stratospheric Gas and Aerosol Experiment) stands for a series of spaceborne occultation instruments. It started in the seventies of the last century with the SAM experiments (Stratospheric Aerosol Measurement) and continued with SAGE I onboard "Applications Explorer Mission B" (1979-1981), SAGE II on ERBS (Earth Radiation Budget Satellite) launched in 1984, and SAGE III on Meteor-3M (launched in December 2001).

SAGE III is a multi-channel grating spectrometer covering the UV-visible-NIR wavelength region and performs solar and lunar occulatation measurements. Previous instruments including SAGE II were broadband instruments. A detailed description of the SAGE III retrieval algorithms and the instrumental design can be found in *[McCormick et al., 2002]*.

7.2.7 GOME/ERS-2

The Global Ozone Monitoring Instrument (GOME) is the first European passive remote sensing instrument operating in the ultraviolet, visible, and near infrared wavelength regions whose primary objective is the determination of the amounts and distributions of atmospheric trace constituents. The main parameters relevant for this study are ozone total columns and vertical profiles.

GOME is part of the payload of the second European Remote Sensing satellite ERS-2 launched on April 21, 1995. The GOME instrument is a double monochromator which combines a predisperser prism and a holographic grating in each of the four optical channels as dispersing elements. The irradiance and radiance spectra are recorded with four linear Reticon Si-diode arrays with 1024 spectral elements each. Peltier elements attached to the diode arrays and connected to passive deep space radiators cool the detectors to about -40ºC. Except for the scan mirror at the nadir view port, all spectrometer parts are fixed and the spectra are recorded simultaneously from 240 nm to 790 nm. The spectral resolution varies between 0.2nm (UV, Channel 1) and 0.4 nm (VIS, channel 4). Part of the light which reaches the predisperser prism is branched out and recorded with three broadband polarization monitoring devices (PMD), which approximately cover the spectral range in channels 2 (300-400 nm), 3 (400-600 nm), and 4 (600-800 nm), respectively. The ERS-2 satellite moves in a retrograde, sun-synchronous, near polar orbit at a height of about 795km. The maximum scan width in the nadir viewing is 960km and global coverage is achieved within three days (after 43 Orbits). The local crossing time at the equator is 10:30am. An across track scan sequence consists of four ground pixel types called East, Nadir, West, and Backscan with 1.5 sec integration time.

Due to a permanent failure of the ERS-2 tape recorder, the availabilty of GOME data coverage is limited to the region where ERS-2 is in direct contact with ground stations (North Atlantic sector and north polar region) starting 22nd June 2003.

7.2.8 SCIAMACHY/ENVISAT

SCIAMACHY is part of the atmospheric chemistry payload of ENVISAT launched in March 2002. ENVISAT is in a sun-synchronous low Earth orbit (inclination: 98.55 deg, altitude: ~800 km, equator crossing descending node: 10:00am). SCIAMACHY observes the Earth's atmosphere in nadir, limb, and solar and lunar occultation viewing geometries. SCIAMACHY consists of eight spectral channels (each one effectively being a separate grating spectrometer) covering nearly the entire solar spectral region with moderate spectral resolution (0.2-1.5 nm FWHM). SCIAMACHY uses eight linear detectors arrays (1024 detector diodes per array or channel). A detailed overview about SCIAMACHY is given in *Bovensmann et al., 1999*.

SCIAMACHY is a flexible but complex instrument. For example the size of a nadir ground pixel is not constant but depends on spectral region (defined by up to 64 spectral clusters) and orbital position and is typically 30x60 km^2 or 30x120 km^2.

On the illuminated part of the orbit (dayside) SCIAMACHY mainly performs alternating limb and nadir observations (approx. one minute limb viewing followed by

approx. one minute nadir viewing). The vertical resolution in limb is about 3 km, the horizontal resolution approx. 250 km. Global coverage is achieved in six days (at the equator, faster at higher latitudes).

The operational data products of SCIAMACHY are listed in the table shown in Figure 3. As can be seen, all parameters relevant for this study are listed in this table. The operational algorithms for generating these data products are described in *[ATBD SCIA Lv1-2]*. Currently the quality of several of these products is preliminary. The operational products relevant for this study that have currently (mid 2004) reached a quality good enough for validation are ozone total columns from nadir and ozone profiles from limb. The operational data products derived from the near-infrared channels (CH_4, CO_2, N_2O) still need significant improvements. The same is true for the pressure and temperature data products from the limb observations also to be derived from the near-infrared channels (via CO_2).

There are a number of groups working on the development of scientfic retrieval algorithms in order to produce scientific data products from SCIAMACHY, including CH_4, CO_2, and N_2O columns from nadir. There is already detailed information available concerning the quality of these products and this information will be summarised in this technote. According to our knowledge, no scientific group is currently working on the retrieval of pressure and temperature profiles from SCIAMACHY.

	Nadir Total Column Amount and Distribution			Limb Stratospheric Profile and Distribution		
	UV/Vis	IR	UV to IR	UV/Vis	IR	UV to IR
Near Real-Time	O_3 NO_2 OClO * SO_2 * H_2CO * BrO **	H_2O N_2O CO CH_4 #	Clouds Aerosol			
Off-Line	O_3 NO_2 BrO OClO * SO_2 * H_2CO * UV Index**	H_2O N_2O CO CO_2 CH_4	Clouds Aerosol	O_3 NO_2 BrO**	H_2O CO_2 CH_4 Pressure Temp. N_2O** CO**	Aerosol

*observed under special condition
(volcanic eruption, ozone hole, heavy tropospheric pollution)

#reduced quality at CO fitting window

**recommended by Science Advisory Group,
implementation under negotiation with agencies

Figure 3: List of SCIAMACHY's operational data products.

The in-flight optical performance of SCIAMACHY is overall as expected from the on-ground calibration and characterization activities. One exception is the time dependent optical throughput variation in the SCIAMACHY near-infrared (NIR) channels 7 and 8 due to ice build-up on the detectors. This effect is minimized by regular heating of the instrument. This „ice issue“ is relevant for CO_2, CH_4, N_2O, and CO retrieval from SCIAMACHY as channels 7 and 8 cover absorption bands of CO_2, CH_4, N_2O, and CO. It affects the precision of the measurements (lower signal to noise ratios due to lower throughput) but also introduces bias (changing slit function). The SCIAMACHY measurements are currently limited in quality (e.g., preliminary calibration especially of the NIR channels) and quantity (not all orbits have been made available yet).

7.2.9 GOMOS/ENVISAT

GOMOS (Global Ozone Monitoring by Occultation of Stars) on board ENVISAT performs, for the first time, atmospheric measurements using the occultation technique with stars. There are roughly 25 stars which are bright enough for appropriate measurements resulting in good spatial coverage on the Earth’s night side. GOMOS is a moderate resolution spectrometer covering the UV and visible spectral range. The main target parameters relevant for this study are vertical profiles of ozone and temperature.

7.2.10 OMI/AURA

The Ozone Monitoring Instrument (OMI) is a contribution of the Netherlands's Agency for Aerospace Programs (NIVR) in collaboration with the Finnish Meteorological Institute (FMI) to the EOS Aura mission (launch mid 2004). The main OMI data products relevant for this study are ozone total columns and vertical profiles. The OMI instrument employs hyperspectral imaging in a push-broom mode to observe solar backscatter radiation in the visible and ultraviolet. OMI combines a wide swath (2600 km) with a high spatial resolution. A new feature of the OMI instrument is its capability to simultaneously record the complete swath and the spectrum of every ground pixel in the swath, which is achieved by employing a 2D CCD detector. The spatial information is imaged on one dimension of the CCD detector while the spectrum is projected along the other dimension of the CCD detector. This new design obliterates the need for a scan mirror, which is employed in similar satellite instruments like GOME and SCIAMACHY that are currently operational. The Earth will be viewed in 740 wavelength bands along the satellite track with a swath large enough to provide global coverage in 14 orbits (1 day). The nominal 13 x 24 km spatial resolution can be zoomed to 13 x 13 km for detecting and tracking urban-scale pollution sources.

7.2.11 GOME-2 series / METOP

As GOME the Global Ozone Monitoring Experiment-2 (GOME-2) is a spectrometer that measures both the radiance component of the light reflected by the Sun-illuminated Earth's atmosphere and the direct Sun light. GOME-2 is a payload instrument of the three MetOp satellites, which will be launched sequentially over 14

years starting in 2005. The main atmospheric parameters measured by GOME-2 which are relevant for this study are ozone columns and ozone vertical profiles.

GOME-2 is similar but not identical with GOME onboard ERS-2. For example, GOME-2 contains two spectrometers - one to measure the radiance component of light that is reflected from the Earth atmosphere in the direction of the satellite (the main channels), in the spectral range 240-790 nm with a resolution of 0.24-0.53 nm and another spectrometer to characterize simultaneously the state of polarization of the same spectrum (the Polarization Measurement Unit). GOME-2 also has a more complex Polarization Measurement Unit (PMU) than GOME, which measures simultaneously s- and p-polarized light on a spectral resolution between 2.8 nm at 312 nm and about 40 nm at 790 nm. To achieve an accurate radiometric in-orbit calibration of the instrument, GOME-2 has two internal calibration light sources, one of which offers well-isolated spectral lines in the required wavelength range and a white light source (WLS) for the broadband continuum. The WLS, which is not part of the GOME calibration unit, is used to monitor the etalon that is present on the cooled Reticon detectors, due to freezing water vapor. The maximum swath width is increased to 1920km across track in order to address the user requirement of global coverage in one day. In conjunction with this change the scan speed is adjusted to minimise the effect of oblique viewing and provide a constant scan rate on the ground. However, the scans is completely reprogrammable in-flight allowing different scan profiles. The width of the entrance slit is increased from 0.1 mm for GOME to 0.2 mm fro GOME-2, which avoids the spectral undersampling of the spectrometer. The coating of the different optical elements is changed to reduce both a steady out-gassing of the coating experienced with GOME and the straylight component measured by the detectors. Due to a different groove profile of the gratings the polarization sensitivity of the main channels is considerable lower than for GOME.

7.2.12 OCO

OCO (Orbiting Carbon Observatory) is a near future NASA/JPL satellite mission (launch planned for 2007) designed to measure highly accurate and precise CO_2 columns for surface source/sink quantification. Details are given in section 7.3.2.1.

7.2.13 SOFIS

SOFIS (Solar Occultation FTS for Inclined-orbit Satellite) is a Japanese satellite project aimed at measuring atmospheric CO_2 to quantify CO_2 sources and sinks (*Patra et al., 2003; Kuze et al., 2000*). Due to the solar occultation geometry the number of profiles per day is limited to 28 starting at an altitude of 5 km or higher (*Shimoda, 2003*). In 2003 it was concluded that these measurements do not provide sufficient information to significantly constrain the inversion (*Shimoda, 2003*). Focus is now on the GOSAT satellite (see below).

7.2.14 GOSAT

GOSAT (Greenhouse gas Observing SATellite) is a Japanese satellite for global measurements of carbon dioxide. GOSAT is a project that is jointly developed by the Japanese space agency JAXA (formerly NASDA) and Japan's Ministry of the Environment. JAXA is responsible for the development of the satellite itself and an

observing sensor, while the ministry is mainly in charge of the utilization of the data obtained. GOSAT is scheduled to be launched in 2007. GOSAT aims at accurate measurements of tropospheric mixing ratios of carbon dioxide in order to quantify the geographical distribution of CO_2 sources and sinks. GOSAT will carry Fourier Transform Spectrometers (FTS) to conduct both absorption spectrometry in the NIR and emission spectrometry in the TIR (O_2 A band, 1.6 μm, 2.0 μm, 4-15 μm). It is the intention to discriminate boundary layer CO_2 from free tropospheric CO_2 by combining NIR and TIR measurements (*Ogawa et al., 2004*).

7.3 Passive systems / solar spectral region: CO_2

7.3.1 Existing systems

7.3.1.1 SCIAMACHYENVISAT

Currently the only existing satellite instrument that measures spectra of CO_2 in the solar spectral region is SCIAMACHY. The SCIAMACHY spectra contain information on the CO_2 total column (from nadir) and on CO_2 vertical profiles (upper troposphere, stratosphere) from the limb observations of scattered sunlight and from transmitted sunlight and moonlight detected during solar and lunar occultation. Total columns of CO_2 from the nadir measurements and vertical profiles of CO_2 from the limb measurements are operational products of SCIAMACHY. The quality of these products is currently poor. They have not been considered good enough for validation for the second ENVISAT validation workshop ACVE-2 in May 2004. Therefore the following discussion is based on non-operational retrievals.

So far the development of scientific (i.e., non-operational) retrieval algorithms mainly focussed on the nadir observations and the current status of this activity is summarized below. For the limb mode detailed analysis is currently restricted to the estimation of the theoretical retrieval precision *[Kaiser et al., 2002]*. For solar occultation measurements CO_2 has primarily been used to improve the tangent height knowledge *[Meyer, 2004]*.

SCIAMACHY CO_2 columns from measurements:

Although SCIAMACHY has not been designed to measure CO_2 columns accurate enough for quantifcation of CO_2 surface sources and sinks early studies indicated that the single pixel retrieval precision for CO_2 column measurements is quite high, namely on the order of 1% (1-sigma) if the entire channel 7 is used as a spectral fitting window for CO_2 retrieval [*Buchwitz et al., 2000a*]. This precision has been estimated from radiative transfer and SCIAMACHY instrument simulations taking into account detailed instrument characteristics (throughput, spectral resolution, detector performance, signal-to-noise performance, etc.). The simulations have been performed for a variety of conditions covering a range of solar zenith angles (40-85 degs) and surface albedos (0.03-1.0).

Several (quasi random and systematic) error sources, however, have not been fully taken into account in that study, such as errors introduced by residual calibration errors and atmospheric variability (temperature, aerosols, undetected cirrus clouds, etc.). In *Buchwitz and Burrows, 2004*, the error analysis has been extended covering also (at least in parts) these type of errors. The error analysis in *Buchwitz and Burrows, 2004*, has been performed for the WFM-DOAS retrieval algorithm developed at the University of Bremen. The error analysis has been made for the (small) spectral fitting windows currently used for CO_2 retrieval from the real SCIAMACHY nadir spectra (main fitting window: 1558-1594 nm located in channel 6 (see Figure 4); in addition fitting window 2030-2040 nm located in channel 7 has been studied). The results are summarized in Table 18. They show that the currently implemented WFM-DOAS retrieval algorithm may result in CO_2 column retrieval errors on the order of several percent. Under certain conditions, however, the error

can be larger, especially over low albedo scenes such as over the oceans. It has to be pointed out that most of these errors can be significantly reduced by improving the WFM-DOAS algorithm (for example, the current implementation is only based on a single reference atmosphere and a single surface albedo of 0.1).

Error source	**Fitting window channel 6 1558-1595 nm**	**Fitting window channel 7 2030-2040 nm**
Atmospheric profile variability (mainly temperature and water vapor)	< 0.4 %	< 2.3 %
Aerosols	< 0.9 %	< 0.8 %
Subvisual cirrus clouds	< 1.4 %	< 3.7 %
Surface albedo		
0.300	+1.4 %	+0.9%
0.200	+0.9 %	+0.6 %
0.100 (reference)	0.0 %	0.0 %
0.050	-0.3%	-1.0%
0.030	-2.6 %	-2.0 %
0.003	-10.3 %	-9.0 %
Scan angle dependence	< 2-3 %	< 2-3 %
Solar zenith angle interpolation	<< 1%	<< 1%
Surface elevation	~ 1 %	~ 1 %

Table 17: Estimated CO_2 column retrieval errors for the University of Bremen WFM-DOAS Version 0.4 retrieval algorithm (from *Buchwitz and Burrows, 2004*).

WFM-DOAS has also been applied to simulated SCIAMACHY nadir measurements to determine the CO_2 averaging kernels. The averaging kernels describe how the sensitivity of a remote CO_2 measurement depends on altitude. They are shown in Figure 5. These averaging kernels indicate that SCIAMACHY is highly sensitive throughout the troposphere including the boundary layer.

The SCIAMACHY CO_2 column smoothing error resulting from “imperfect” averaging kernels (i.e., averaging kernels that deviate from 1.0) has been estimated in *Connor et al., 2003*. It is relatively small: 0.5 ppmv (~0.14%).

A promising approach for CO_2 source/sink detection/quantification from satellite is the retrieval of O_2 column normalized CO_2 columns followed by inverse modelling (see, e.g., EU research project EVERGREEN, http://www.knmi.nl/evergreen). The ratio of the CO_2 column divided by the simultaneously measured O_2 column (and multipication of this quantity with the O_2 mixing ratio of dry air, i.e., 0.2095) is called *column-averaged dry air CO_2 mixing ratio* (or mole fraction) denoted XCO_2. This XCO_2 approach is expected to help filtering out, e.g., surface pressure / surface elevation induced column variations that interfere with the (weak) column variation due to sources and sinks. Detailed results concerning CO_2 / XCO_2 retrieval from SCIAMACHY using the WFM-DOAS algorithm are given in *Buchwitz and Burrows, 2004,* and *Buchwitz et al., 2004c*.

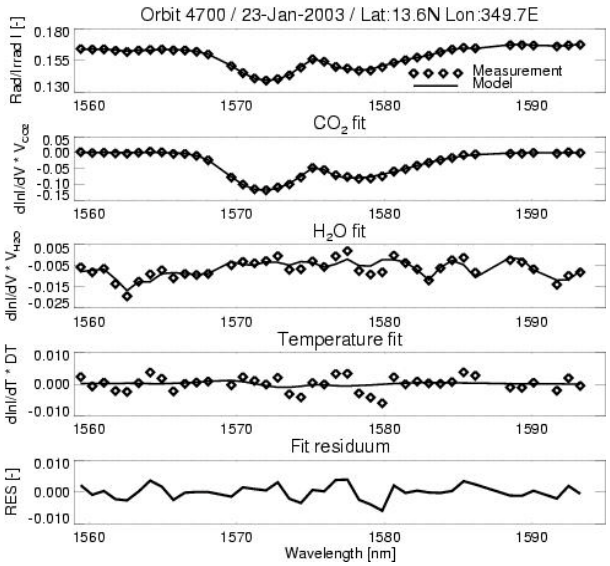

Figure 4: WFM-DOAS example fit for CO_2. From: *Buchwitz and Burrows, 2004*. The retrieved CO_2 column is 7.82 10^{21} molecules/cm^2 +/- 1.7%.

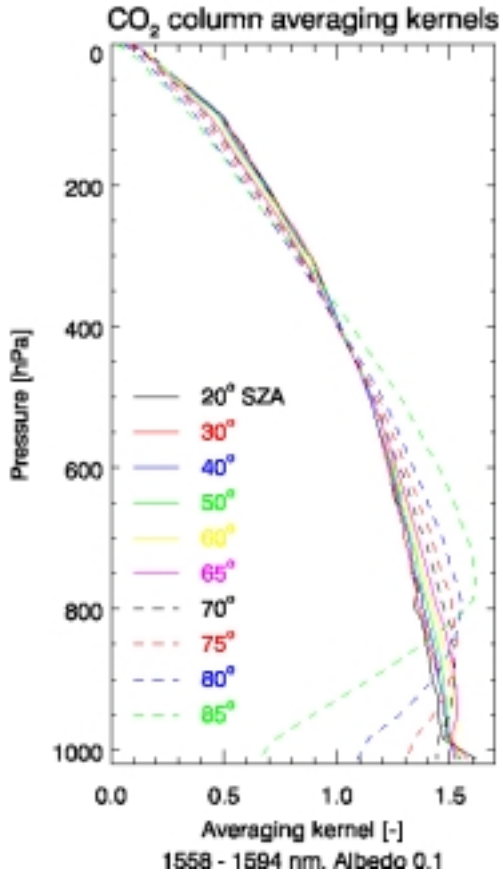

Figure 5: SCIAMACHY WFM-DOAS averaging kernels for CO_2 column retrieval for various solar zenith angles (*Buchwitz et al., 2004c*).

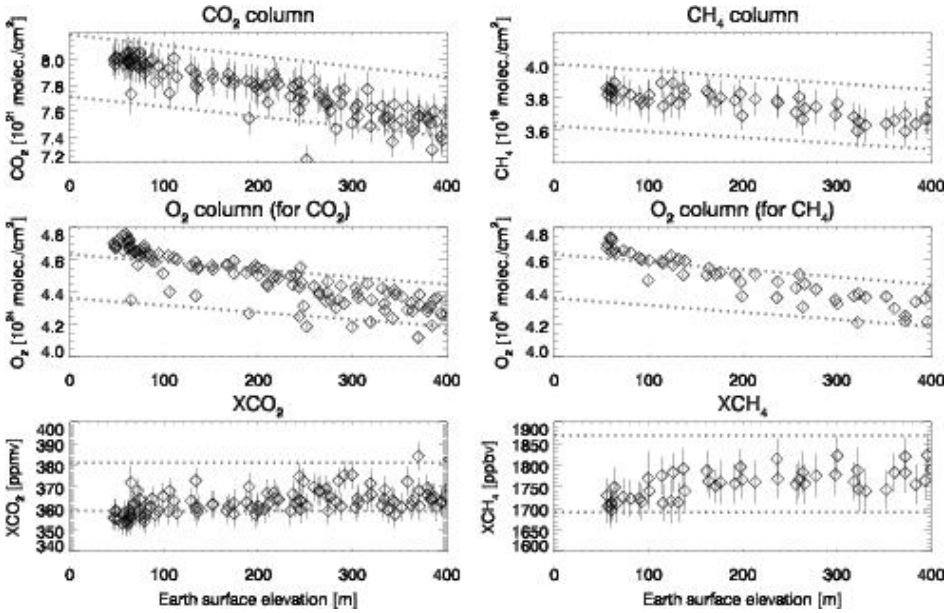

Figure 6: Left: Retrieved CO_2 and O_2 columns for a cloud free scene over Africa (Senegal) with surface elevation increasing from near sea level to 400 m (from: *Buchwitz and Burrows, 2004*.). Right: as left hand side but for methane. These results demonstrate the high sensitivity of SCIAMACHY for small column changes in the boundary layer.

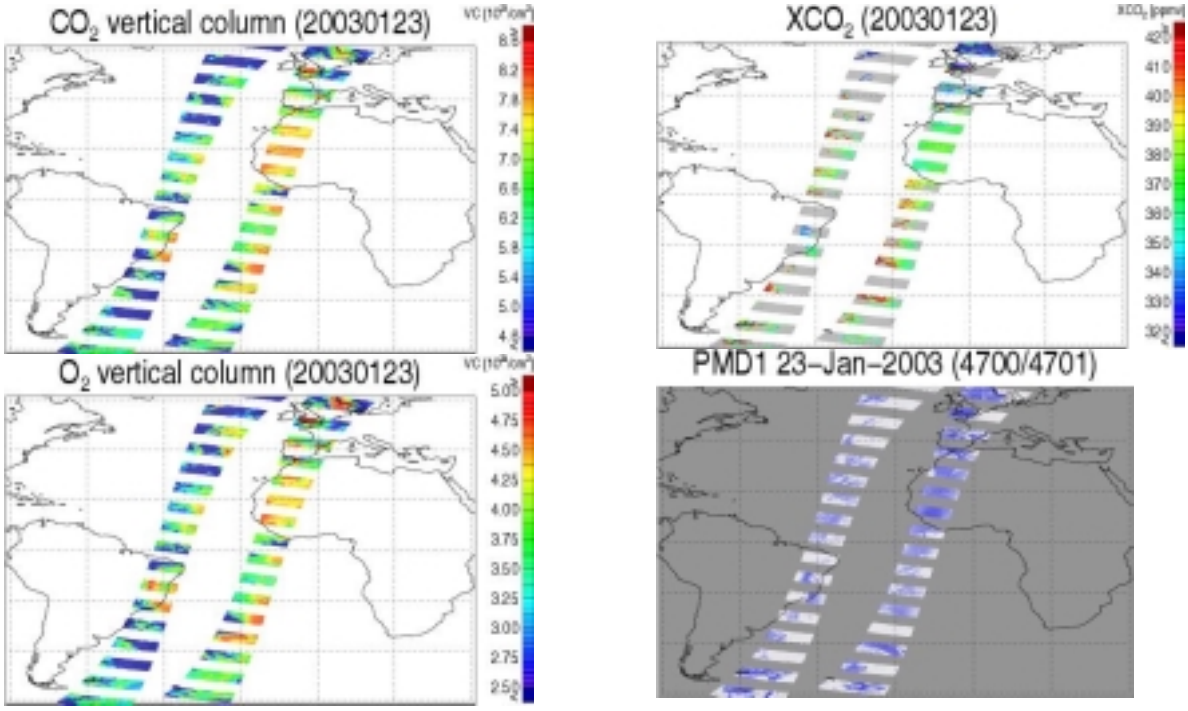

Figure 7: Preliminary CO_2 retrievals from SCIAMACHY nadir observations (from: *Buchwitz and Burrows, 2004*). Top left: CO_2 vertical columns retrieved from (verification) orbits 4700 (right orbit) and 4701 (left orbit) measured on January 23, 2004. Spectral fitting window: 1558-1594 nm. No cloud correction has been performed. Top right: O_2 vertical columns retrieved from the oxygen A-band (755-775 nm). Bottom left: Oxygen normalized CO_2 columns (XCO_2) with cloudy pixels shown in grey. Bottom right: Subpixel image produced from SCIAMACHY's polarization measurement device (PMD) (white = clouds, blue = cloud free) used to get subpixel information on clouds.

Initial verification and validation:

So far only a limited number of comparions have been made with independent measurements. FTIR solar occultation validation measurements have been made during a Polarstern ship cruise beginning of 2003 *[Warneke et al., 2004]*. The comparison with the FTIR measurements is shown in Figure 8. From this comparison it can be concluded that the SCIAMACHY CO_2 measurements agree with the FTIR solar occultation column measurements within about 5%.

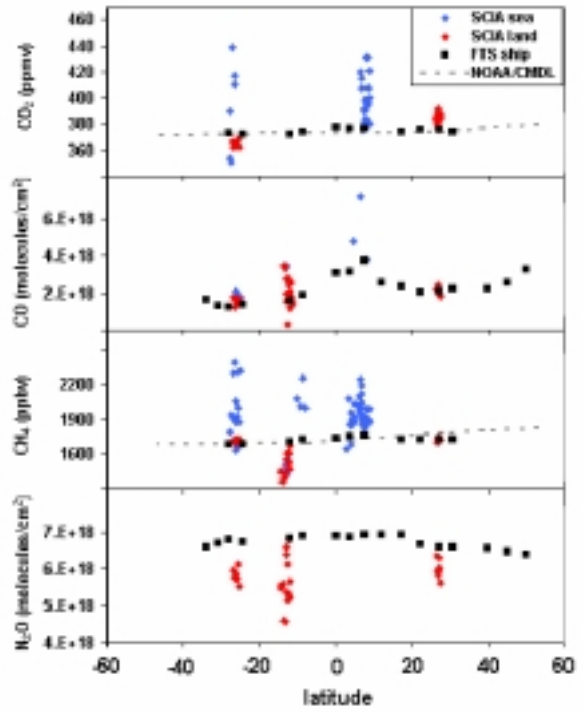

Figure 8: Comparison of various SCIAMACHY/WFM-DOAS data products with independent FTIR solar occultation measurements obtained during a Polarstern cruise beginning of 2003 *[Warneke et al., 2004]*.

Buchwitz et al., 2004c, present a comparison of the WFM-DOAS Version 0.4 CO_2 data products with a global model (see Figure 9) for the time period January 2003 to October 2003. They found that the SCIAMACHY CO_2 columns and mixing ratios for cloud free scenes over land are in reasonable agreement with the model. Over the ocean, as a result of the lower surface spectral reflectance and resultant low signal to noise ratios (with the exception of sun glint conditions), the accuracy of the individual data products is poorer. The standard deviation of the difference of the retrieved XCO_2 and the corresponding model values was 15 ppmv (4%). Relative to the model biases of up to about 20 ppmv have been found (~5%).

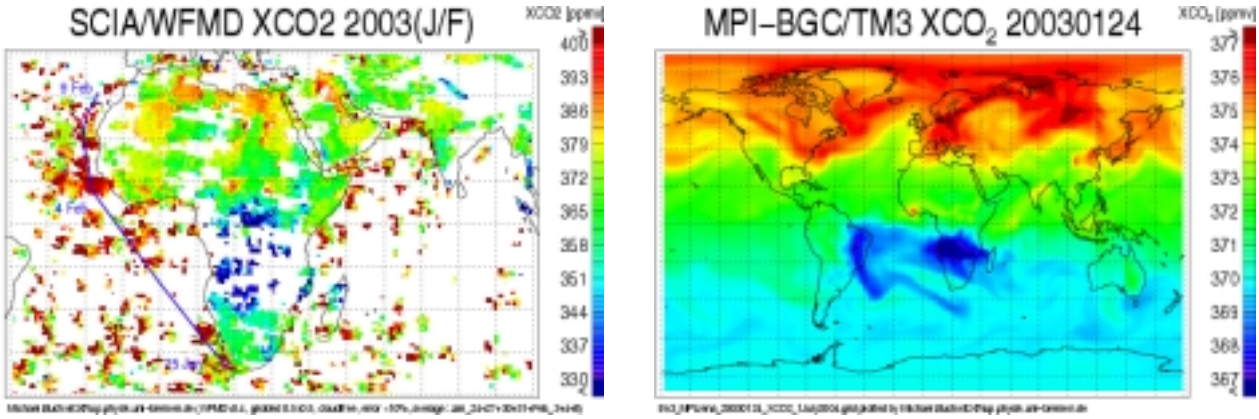

Figure 9: Left: XCO_2 as measured by SCIAMACHY (WFM-DOAS Version 0.4) over Africa end of January / beginning of February 2003. Shown are only the results for the cloud free pixels with fit error less than 10%. The line at the west coast of Africa indicates the ship track of the German research vessel Polarstern with an FTS on board for the validation of the SCIAMACHY measurements (see Figure 8). Right: XCO_2 from the TM3 model of the MPI for Biogeochemistry, Jena, Germany (group of M. Heimann; figure courtesy of S. Körner).. The most prominent feature in both figures is an extended region of low CO_2 mixing ratios around Zambia/Congo. The measured depth of the "CO_2 hole" is about 20 ppmv (TM3: ~ 5 ppm). From: *Buchwitz et al., 2004c*

SCIAMACHY CO_2 profiles from limb measurements:

Currently only one study has been published where the theroretical retrieval precision of CO_2 profiles has been estimated *[Kaiser et al., 2002]*. The results can be summarized as follows: the precision is better than 10% (1 sigma) in the altitude range 5-20 km (the precision decreases with increasing altitude).

SCIAMACHY CO_2 profiles from solar and lunar occultation measurements:

Currently the CO_2 absorption bands from SCIAMACHYs solar occultation spectra have only been used to improve the tangent height knowledge *[Meyer, 2004]*.

7.3.2 Future systems

7.3.2.1 Orbiting Carbon Observatory (OCO)

The OCO mission (*Crisp et al., 2004*) is planned to be launched as an ESSP mission in 2007 (http://oco.jpl.nasa.gov). The OCO instrument is specifically designed to monitor the column-averaged dry-air mole fraction of CO_2 (denoted XCO_2) with an a precision of 0.3% (1 ppmv) on regional scales (~4^ox5^o; semi-monthly). The instrument makes spectrally high resolved measurements in the 1.6 µm and 2.0 µm bands of CO_2 in combination with spectrally high resolution measurements in the O_2-A band (see Figure 10). The latter helps to correct for surface pressure and atmospheric scattering (*Kuang et al., 2002*).

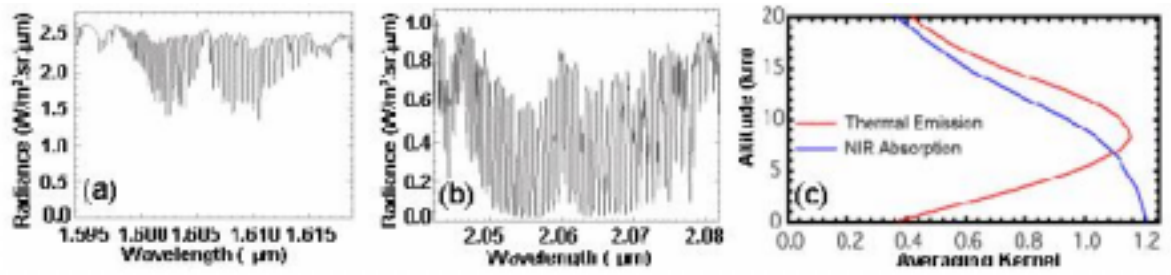

Figure 10: Spectral regions as observed by OCO (a and b) and CO_2 column averaging kernels (c) (from *Crisp et al., 2004*).

Why XCO_2 rather than CO_2 absolute column measurements? Even if the CO_2 column can be measured accurately enough at ground pixel resolution this would not be sufficient for source/sink retrieval as the CO_2 column not only depends on surface sources and sinks but also on surface topography, weather systems (surface pressure), etc. To better separate the weak source/sink signal from these disturbing (larger) signals a promising approach is to simultaneously retrieve the column of a well-known tracer, i.e., a well-mixed gas free of (significant) sources and sinks, and to divide the CO_2 column by the column of this reference gas. A gas that fulfils these requirements is O_2. For this reason the quantity XCO2 := (CO_2 column) / (O_2 column) x 0.2905, the so called “column-averaged CO_2 dry air mole fraction”, is the target quantity to be measured by OCO.

Clouds are an issue for a nadir looking instrument. Taking into account the high accuracy requirements for the CO_2 measurements probably only (nearly) cloud free measurements are useful. Therefore, the ground pixels size must be small enough to have a high probability for cloud free scenes (OCO: 1 x 1.5 km^2) even if the inverse modelling is done on a much coarser grid.

The OCO instrument will fly in a polar sun-synchronous orbit at an altitude of 705 km with an equatorial crossing time of 1:15 PM local time (just ahead of the EOS AQUA satellite in the so called afternoon constellation or A-train). The instrument will provide continuous 1 km across-track by 1.5 km along-track observations at a rate of 4.5 Hz (illustrated in Figure 10) with a 16-days ground-track repeat cycle. OCO has a swath width of 10 km. OCO will fly over each 1000 km x 1000 km region at least five times during each 16-day orbit track repeat cycle. The observatory will collect approximately 3500 soundings in each region per pass. The OCO team assumes

that 25% of these soundings will be sufficiently clear. This yields ~875 soundings in each region per pass.

As the diffuse component of the ocean reflectivity in the SWIR is low (< 1%) sun glint observations are needed to get higher signals and corresponding higher signal to noise ratios over the ocean. This requires to take Doppler shifts into account, especially at higher latitudes. OCO has nadir (for land), glint (for ocean) and target (for validation) viewing modes.

The current OCO measurement strategy is to produce monthly global maps of the column-averaged CO_2 dry-air mole fraction (XCO_2) averaged on a 4° - 5° grid with a precision of 0.3%. Results from an error analysis are shown in Figure 12.

The width of the (pressure broadened) absorption lines at sea level is about 0.1 cm^{-1} corresponding to 0.006 nm at 760 nm and 0.026 at 1600 nm. The Doppler width is approximately a factor of 8 smaller at 760 nm and a factor of 16 smaller at 1600 nm. The spectral resolution of OCO is much higher than, for example, SCIAMACHY. For the CO_2 channel OCO has a resolving power of 21,000 for the CO_2 channel 17,500. This resolution is worse than, e.g., for ground based FTIR measurements but significantly higher than in the corresponding SCIAMACHY channels. The higher the spectral resolution the more sensitive is the (nadir) radiance w.r.t. CO_2 concentration changes. The more (relevant) spectral points are being measured the more disturbing interfering parameters can be constrained resulting in more precise CO_2 concentrations. The measured (relative) depth of CO_2 absorption lines is the main source of information from which the CO_2 column can be retrieved. The relative depth of the CO_2 (or O_2) absorption lines, however, does not only depend on the CO_2 concentration, but on many other parameters as well (on the highly variable altitude and wavelength dependent scattering properties of the atmosphere, on the concentration of spectrally interfering gases, most notably water vapor (highly variable), on the temperature and pressure profiles, surface albedo. Many of these parameters can be constrained by taking advantage of the detailed information present in high resolution spectra (*Christi et al., 2003; Crisp et al., 2004; Dufour et al., 2003; Kuang et al., 2002; Yang et al., 2002*).

Kuang et al., 2002, conclude that: “a 3-band, spectrometric approach using NIR reflected sunlight has the potential for highly accurate XCO_2 measurements”. They investigated the problem of XCO_2 retrieval under various conditions and conclude: “Simulation experiments show that precisions of ~0.3-2.5 ppmv for XCO_2 can be achieved from individual clear sky soundings for a range of atmospheric/surface conditions, when the scattering optical depth is less than ~0.3”. Similar precisions (“better than 0.5%”) have been obtained from (real) high-resolution (0.014 cm^{-1}) ground based FTIR measurements (*Yang et al., 2002*). The signal-to-noise ratios specified for OCO are (SZA 35^o,surface albedo ~0.06) 400 for the CO_2 channel and 600 for the O_2 channel.

Kuang et al., 2002, shortly discussed two systematic error sources, namely an uncorrected zero offset error due to excess dark current, and a sampling biases (“We briefly review the effect of systematic errors and biases, but defer a more comprehensive investigation to later publications.”). A bias due to a zero offset error depends on surface albedo, solar zenith angle, etc. For a solar zenith angle of 60

degs and an assumed offset error of 0.2% the resulting XCO_2 bias is about 1.5 ppmv for an albedo of 0.06 and about 0.5 ppmv for an albedo of 0.2. The errors increase with solar zenith angle. From this one may conclude that a scene dependent geophysical bias (differential bias) of ~1 ppmb due to dark signal zero offset errors can be expected. *Kuang et al., 2002*, shortly discussed another source of biases, namely the sampling bias resulting from the fact that XCO_2 will only be measured only under cloud free conditions but photolysis in many ecosystems is typically stronger under cloud free conditions than on average. *Kuang et al., 2002*, conclude that: *"To mitigate the impact of such sampling errors, the space based XCO_2 measurements must be combined with time-resolved in-situ data … and models …". Crisp et al., 2004,* showed retrieval accuray estimates from a large number of simulations covering many atmospheric and surface reflectivity conditions. They conclude that the systematic errors are typically below about 1 ppmv (see Figure 12).

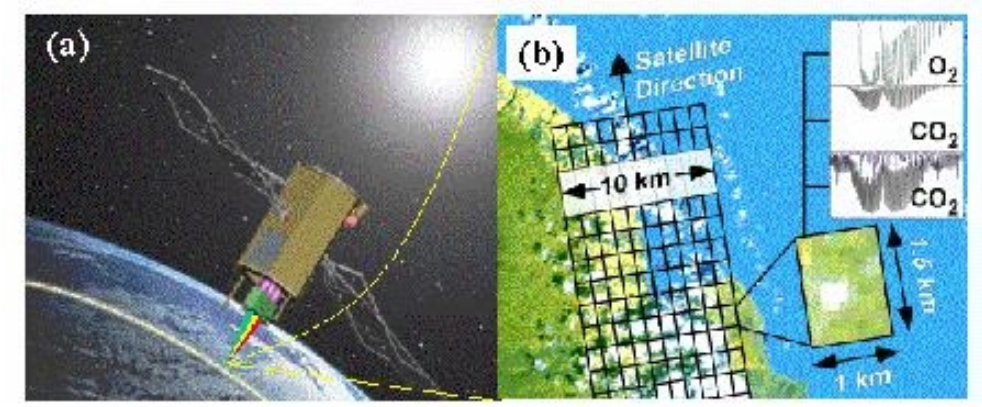

Figure 11: OCO satellite and nadir sampling (from *Crisp et al., 2004*).

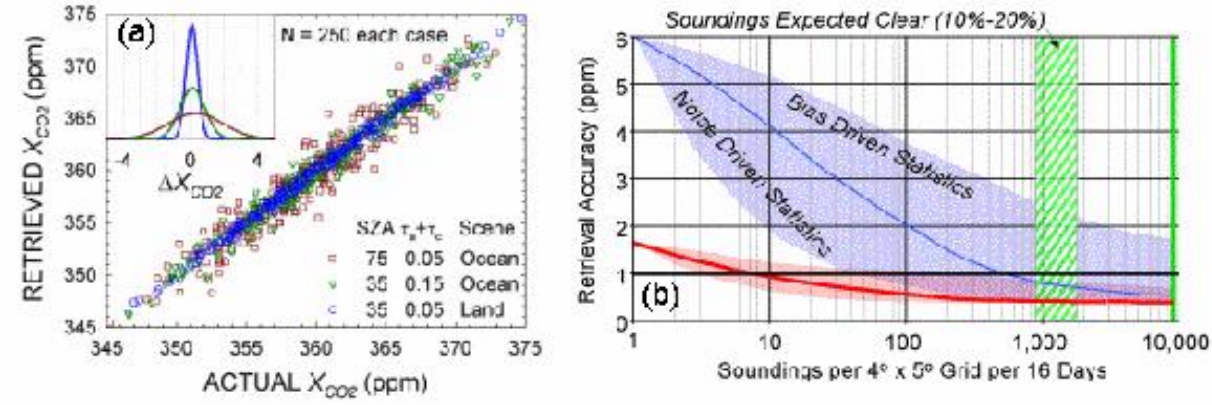

Figure 12: OCO error analysis (from *Crisp et al., 2004*). (a) Retrievals of XCO_2 from individual simulated nadir soundings at SZAs of 35 and 75 degs. (b) Predicted accuracy of XCO_2. Cases with (red) and without (blue) the 2.06-µm CO_2 channel. Results from sensitivity tests (solid lines) are shown with shaded envelopes indicating the range expected for error.

In *Crisp et al., 2004b,* the following is written concerning systematic biases: *"Systematic biases can be more problematic than random errors because their effects on flux inversions are not reduced by averaging large numbers of soundings. The results presented below demonstrate that the effects of XCO_2 measurement biases on CO_2 flux uncertainties depend on their spatial and temporal extent since CO_2 sources and sinks are inferred from regional-scale XCO_2 gradients. Steady-state*

global biases introduce no error in XCO_2 gradients and the inferred CO2 fluxes. Sub-regional scale biases are indistinguishable from random noise. Regional to continental scale biases are of greatest concern. This requires that the OCO validation program must identify and correct regional to continental scale XCO_2 measurement biases to within 1-2 ppm."

The OCO CO_2 column smoothing error resulting from "imperfect" averaging kernels (i.e., averaging kernels that deviate from 1.0) has been estimated in *Connor et al., 2003*. This smoothing error (which depends on solar zenith angle, albedo, and aerosol) in the range 0.15-1.33 ppmv.

7.3.2.2 GOSAT

The Japanese space agency JAXA also plans to build a satellite for CO_2 measurements accurate enough for source/sink quantification, namely GOSAT which is due for launch in 2007 *[Ogawa et al., 2004; Shimoda, 2003]*. GOSAT shall make high spectral resolution Fourier transform nadir measurements in the NIR and TIR spectral regions. These measurements shall allow a discrimination between boundary layer and free tropospheric CO_2 concentrations.

7.4 Passive systems / solar spectral region: CH_4

7.4.1 Existing systems

7.4.1.1 MOPITT/TERRA

MOPITT has been designed to measure methane columns from reflected solar radiation in the spectral region around 2.3 µm. The theoretical retrieval precision for single measurements is ~1% (Deeter et al., SPIE). Because of problems with the methane NIR channel retrievals no data have been delivered until now.

7.4.1.2 SCIAMACHY/ENVISAT

The SCIAMACHY spectra contain information on the CH_4 total column (from nadir) and on CH_4 vertical profiles (upper troposphere, stratosphere, mesosphere) from the limb observations of scattered sunlight and from transmitted sunlight and moonlight detected during solar and lunar occultation. Total columns of CH_4 from the nadir measurements and vertical profiles of CH_4 from the limb measurements are operational products of SCIAMACHY. The quality of these products is currently poor. They have not been considered good enough for validation for the second ENVISAT validation workshop ACVE-2 in May 2004. Therefore the following discussion is based on non-operational retrievals. So far only the nadir measurements have been analysed in quite some detail. Therefore, this section will focus on the SCIAMACHY nadir measurements.

SCIAMACHY CH_4 columns from nadir measurements:

In pre-launch studies it has been estimated that the single pixel retrieval precision for SCIAMACHY CH_4 column measurements is quite high [*Schrijver et al., 1998; Buchwitz et al., 2000a*], namely on the order of 1% (1-sigma) if the entire channel 8 is used as spectral fitting window for CH_4 retrieval. This precision has been estimated from radiative transfer and SCIAMACHY instrument simulations taking into account detailed and realistic instrument characteristics (throughput, spectral resolution, detector performance, signal-to-noise performance, etc.). The simulations have been performed for a variety of conditions covering a range of solar zenith angles and surface albedos.

Several (quasi random and systematic) error sources, however, have not been fully taken into account in those studies, such as errors introduced by residual calibration errors and atmospheric variability (e.g., temperature, aerosols, undetected cirrus clouds). In *Buchwitz and Burrows, 2004*, the error analysis has been extended covering (at least in parts) also these type of errors. The error analysis in *Buchwitz and Burrows, 2004*, has been made for the WFM-DOAS retrieval algorithm developed at the University of Bremen. The error analysis has been performed for the (small) spectral fitting windows used for CH_4 column retrieval from the real SCIAMACHY spectra (main fitting window: 2265-2280 nm located in channel 8). The results are summarized in Table 18. They show that the currently implemented WFM-DOAS retrieval algorithm may result in CH_4 column retrieval errors on the order of a few percent. Under certain conditions the error can be larger than 3%, especially over low albedo scenes such as over the oceans. It has to be pointed out that most

of these errors can be significantly reduced by improving the WFM-DOAS algorithm (e.g., the current implementation is based on a single reference atmosphere and a single surface albedo of 0.1 only).

Error source	**Fitting window channel 8 2265-2280 nm**
Atmospheric profile variability (mainly temperature, water vapor)	< 1.3 %
Aerosols	< 0.3 %
Subvisual cirrus clouds	< 3.7 %
Surface albedo	
0.300	+0.8 %
0.200	+0.5 %
0.100 (reference)	0.0 %
0.050	-0.7%
0.030	-1.5 %
0.003	-7.4 %
Scan angle dependence	< 2-3 %
Solar zenith angle interpolation	<< 1%
Surface elevation	~ 1 %

Table 18: Estimated CH_4 column retrieval errors for the first implementation of the University of Bremen WFM-DOAS retrieval algorithm (from *Buchwitz and Burrows, 2004*).

WFM-DOAS has also been applied to simulated SCIAMACHY nadir measurements to determine the CH_4 averaging kernels. They are shown in Figure 14. These averaging kernels indicate that SCIAMACHY is highly sensitive throughout the troposphere including the boundary layer.

In the following the status of CH_4 / XCH_4 retrievals from SCIAMACHY is summarised focussing on the results obtained at University of Bremen using the WFM-DOAS algorithm (*Buchwitz and Burrows, 2004*). The paper of *Buchwitz and Burrows, 2004*, is currently the only publication where CH_4 retrievals from real SCIAMACHY data have been reported in quite some detail.

Buchwitz and Burrows, 2004, report on first WFM-DOAS retrievals using so-called verification orbits (special Level 1 orbit files generated and made available by ESA/ESTEC) which have a better calibration than the current operational Level 1 data products. WFM-DOAS example fits are shown in Figure 13. The fit parameters are the desired CH_4 vertical column plus some additional parameters to account for spectrally interferring gas absorptions, atmospheric temperature effects and (by including a low order polynomial) atmospheric scattering and surface reflectivity as well as certain calibration errors.

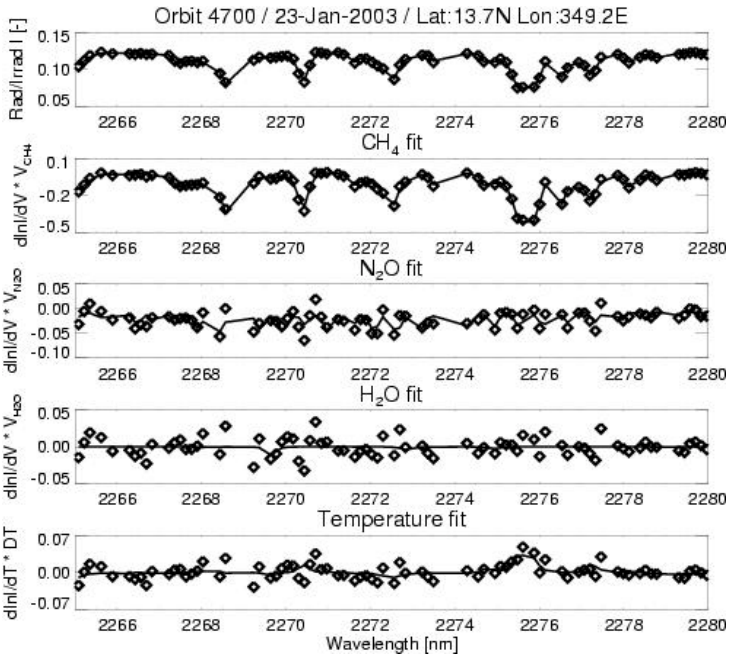

Figure 13: WFM-DOAS example fit for CH_4 (from: *Buchwitz and Burrows, 2004*). The retrieved CH_4 column is 3.83 10^{19} molecules/cm^2 +/- 2.2%, the simultaneously retrieved N_2O column is is 6.3 10^{18} molecules/cm^2 +/- 17%,

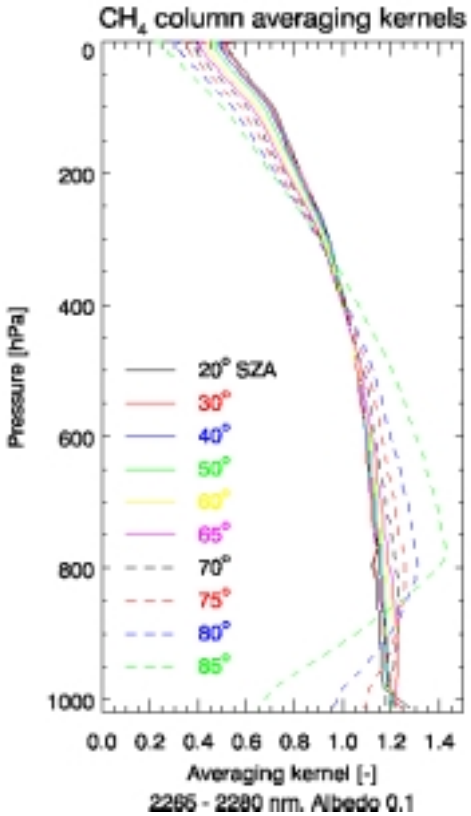

Figure 14: SCIAMACHY WFM-DOAS averaging kernels for CH_4 column retrieval for various solar zenith angles (*Buchwitz et al., 2004c*).

Initial verification and validation:

A limited number of comparions have been made using FTIR solar occultation measurements made during a Polarstern ship cruise beginning of 2003 *[Warneke et al., 2004]*. The comparison with the FTIR measurements is shown in Figure 8. From this comparison it can be concluded that the SCIAMACHY CH_4 measurements agree with the FTIR solar occultation column measurements within about 5%.

Initial results from a comparison of the WFM-DOAS Version 0.4 methane columns with the network of land based FTS ground stations are reported by *de Maziere et al., 2004*. In that study all available orbits from 33 days from the time period January 2003 to October 2003 have been compared with 12 stations. The FTS methane columns have a precision of ~1-3% and an accuracy of ~10%. Within that study it has been found that the agreement of the WFM-DOAS Version 0.4 methane columns with the FTS data is typically within 15%.

Buchwitz et al., 2004c, present a detailed comparison of the WFM-DOAS Version 0.4 methane data products with global models for four days from the time period January 2003 to October 2003. They found that the SCIAMACHY methane columns and mixing ratios for cloud free scenes over land are in reasonable agreement with the models. Over the ocean, as a result of the lower surface spectral reflectance and resultant low signal to noise ratios (with the exception of sun glint conditions), the accuracy of the individual data products is poorer. The measured methane column amounts agree with the model columns within a few percent. The mean differences between the measured and the modelled absolute columns (in molecules/cm^2) are +0.5% (see Figure 15) and +1.8% for two of the analysed days but -9.3% and -15.3% for the two other days. This shows that there is a time dependent bias. This bias seems related to time dependent instrument characteristics (mainly resulting from the ice build up on the detectors) that have not yet been considered good enough in the calibration and/or retrieval process. The inter-hemispheric difference of the methane mixing ratios, determined from single day cloud free SCIAMACHY measurements over land, is in the range 30-110 ppbv and in reasonable agreement with the corresponding model data (48-71 ppbv). For the set of individual measurements the standard deviations of the difference with respect to the models is in the range ~100-200 ppbv (5-10%) for XCH_4.

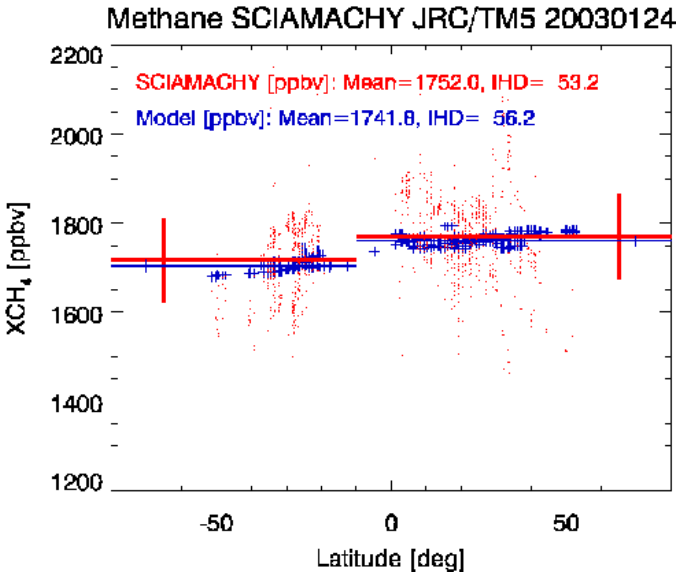

Figure 15: Comparison of SCIAMACHY WFM-DOAS XCH_4 measurements for January, 24, 2003, with the global model TM5 of JRC/Ispra (courtesy of P. Bergamaschi). IHD = InterHemispheric (methane mixing ratio) Difference. From: *Buchwitz et al., 2004c.*

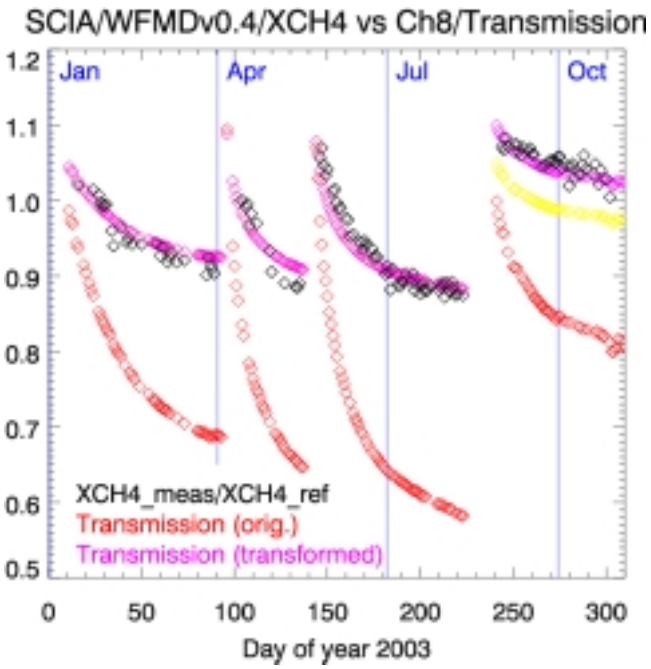

Figure 16: Black symbols: Average XCH_4 divided by a constant reference value as measured by SCIAMACHY using WFM-DOAS Version 0.4. Red symbols: SCIAMACHY channel 8 relative transmission as determined by the SOST (SCIAMACHY Operations Support Team) light path analysis. The magenta curves ("Transmission (transformed)") are a linear transformation of the "Transmission (orig.)" curves and are used for a first order bias correction of the retrieved methane columns to correct for problems introduced by the ice issue. From: *M. Buchwitz.*

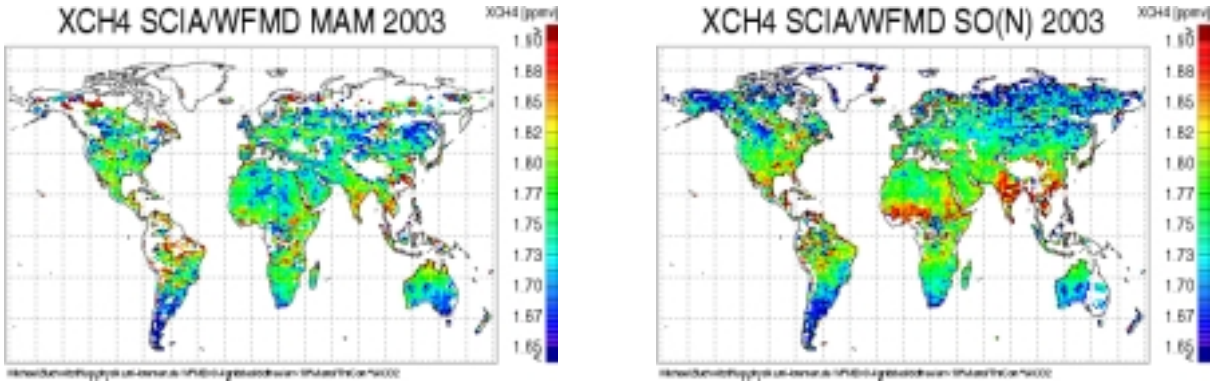

Figure 17: Left: XCH_4 as measured by SCIAMACHY averaged over the time periode March to May 2003. Right: The same but for September and October 2003 (for November no orbits were available). Before averaging the methane columns have been first order bias corrected (see Figure 16) to compensate for errors introduced by the "ice issue". Clearly visible are enhanced concentration of methane over India, south-east Asia, and central Africa, in good qualitative agreement with model results. XCH_4 as shown here has not been obtained by normalizing to the SCIAMACHY O_2 measurements but to the CO_2 measurements. *Copyright: M. Buchwitz*

SCIAMACHY CH_4 profiles from limb measurements:

Currently only one theoretical study has been published where the theroretical retrieval precision of CH_4 profiles has been assessed *[Kaiser et al., 2002]*. The precision is estimated to be better than 10% (1-sigma) in the altitude range 5-15 km (the precision decreases with increasing altitude).

SCIAMACHY CH_4 profiles from solar and lunar occultation measurements:

Currently no detailed results concerning CH_4 profile retrieval from the SCIAMACHY solar or lunar occultation measurements are available.

7.4.2 Future systems

According to our knowledge no passive systems are planned for measuring methane columns or profiles in the solar spectral region.

7.5 Passive systems / solar spectral region: N_2O

7.5.1 Existing systems

7.5.1.1 SCIAMACHY/ENVISAT

The SCIAMACHY spectra contain information on the N_2O total column (from nadir) and on N_2O vertical profiles (upper troposphere, stratosphere, mesosphere) from the limb observations of scattered sunlight and from transmitted sunlight detected during solar and lunar occultation. Total columns of N_2O from the nadir measurements and vertical profiles of N_2O from the limb measurements are operational products of SCIAMACHY. The quality of these products is currently poor. They have not been considered good enough for validation for the second ENVISAT validation workshop ACVE-2 in May 2004. Therefore the following discussion is based on non-operational retrievals. So far only the nadir measurements have been analysed in detail. Therefore, this section will focus on the SCIAMACHY nadir measurements.

SCIAMACHY N_2O columns from nadir:

Concerning N_2O column retrieval from the SCIAMACHY nadir measurements the situation is similar as described in Section 7.3.1.1 for CO_2 column retrieval and in Section 7.4.1.2 for CH_4 column retrieval (XN_2O concept analog to XCO_2 concept for surface source/sink detection, similar retrieval algorithms). The main difference is that N_2O retrieval is much more difficult because of the rather weak N_2O absorption lines (see Figure 2).

Therefore, the theoretical N_2O column retrieval precision is approximately one order of magnitude worse than for CO_2 and CH_4 (10% instead of 1%), see *Schrijver et al., 1998; and Buchwitz et al., 2000a.* This precision has been estimated from radiative transfer and SCIAMACHY instrument simulations taking into account detailed and realistic instrument characteristics (throughput, spectral resolution, detector performance, signal-to-noise performance, etc.). The simulations have been performed for a variety of conditions covering a range of solar zenith angles and surface albedos.

Several (quasi random and systematic) error sources, however, have not been fully taken into account in those studies, such as errors introduced by residual calibration errors and atmospheric variability (e.g., temperature, aerosols, undetected cirrus clouds). These errors still need to be quantified, e.g., by performing an error analysis as done in *Buchwitz and Burrows, 2004*, for CO_2 and CH_4.

A WFM-DOAS N_2O example fit is shown in Figure 13. For this typical example the N_2O fit error is 17% which is in broad agreement with the 10% precision mentioned above and additional errors that contribute and still need quantification.

Initial validation:

A limited number of comparions have been made using FTIR solar occultation measurements during a Polarstern ship cruise beginning of 2003 *[Warneke et al., 2004]*. The comparison with the FTIR measurements is shown in Figure 8. From this comparison it can be concluded that the SCIAMACHY N_2O measurements agree with the FTIR solar occultation column measurements within 30%.

Initial results from a comparison of the WFM-DOAS Version 0.4 N_2O columns with the network of land based FTS ground stations are reported by *de Maziere et al., 2004*. In that study all available orbits from 33 days from the time period January 2003 to October 2003 have been compared with 12 stations. The FTS N_2O columns have a precision of ~2-3% and an accuracy of ~2.5%. Within that study it has been found that the agreement of the WFM-DOAS Version 0.4 N_2O columns with the FTS data is within 30% for most stations but for some stations significantly larger deviations have been found.

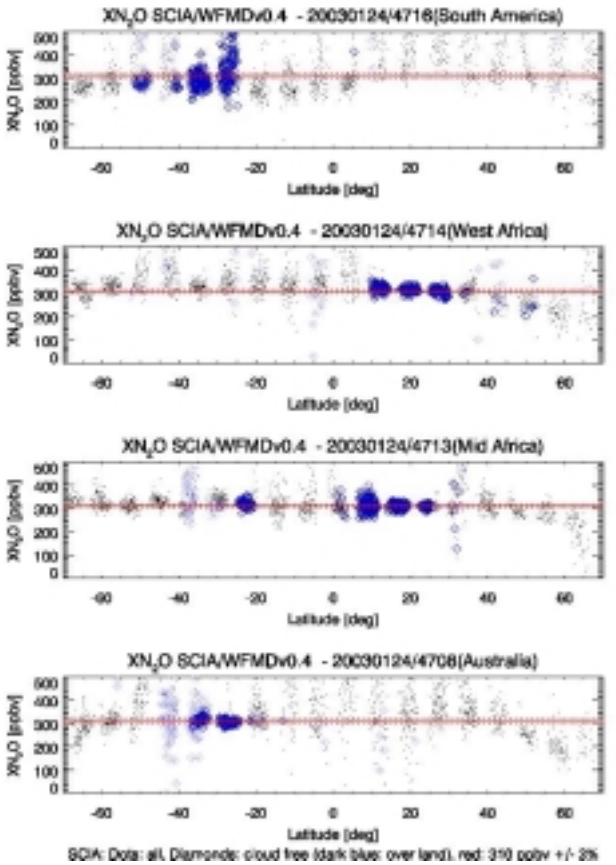

Figure 18: XN_2O as retrieved from four orbits (January 24, 2003) from SCIAMACHY by WFM-DOAS Version 0.4. Dots: all pixel; symbols: cloud free pixels; dark blue symbols: cloud free pixels over land. Red lines: 310 ppbv +/- 3%. *Figure: M. Buchwitz.*

SCIAMACHY N_2O profiles from limb measurements:

Currently only one theoretical study has been published where the theroretical retrieval precision of N_2O profiles has been assessed *[Kaiser et al., 2002]*. The precision is estimated to be better than 50% (1-sigma) in the altitude range 5-10 km (the precision decreases with increasing altitude).

SCIAMACHY N_2O profiles from occultation measurements:

Currently no results concerning N_2O profile retrieval are available.

7.5.2 Future systems

According to our knowledge no passive systems are planned for measuring N_2O columns or profiles in the solar spectral region.

7.6 Passive systems / solar spectral region: Ozone

7.6.1 Existing systems

7.6.1.1 TOMS

TOMS ozone columns:

Dataset and quality *[TOMS V7 web page]*:

The TOMS Version 7 dataset consists of 1 x 1 degree gridded monthly averaged total column ozone. It is derived from the Nimbus-7 TOMS monthly averaged total column ozone data gridded at 1.25 x 1 degree (lon/lat). The Nimbus-7 TOMS data is the only source of high resolution global information about the total ozone content of the atmosphere for the period November 1, 1978 - May 6, 1993. The ozone dataset was produced by the Ozone Processing Team (OPT) using final Nimbus-7, Version 7, OPT data reduction algorithm and was released in the Spring of 1996.

Validation: Differences range from 2% to 4% for Dobson network comparison, and 3 1/2% to 5% for the World Standard.

A new TOMS total ozone algorithm is currently in preparation (TOMS Version 8) but has not yet been officially released.

7.6.1.2 SBUV

SBUV ozone profiles:

An SBUV error summary is given in
Table 19 *[SPARC web page]*. The Table contains estimated errors (90% limits) for SBUV from the algorithm *[Bhartia et al., 1996]* and from the calibration, and an estimate of the error in maintaining the calibration. Since many of the components of these are errors that are systematic, they will not be completely eliminated by averaging profiles.

Pressure level **hPa**	***Algorithm*** **%**	***Calibration*** **%**	***Calibration drift*** ***%/year***
0.5	6	5	0.5
1.0	6	5	0.5
2.0	5	4	0.5
4.0	5	3	0.5
7.0	5	3	0.46
10.0	5	2	0.36
20.0	7	2	0.29
40.0	11	2	0.4
100.0	15	2	0.4

Table 19: SBUV ozone profile error summary according to SPARC.

According to *Bhartia et al., 1996*: "… it is shown that the BUV technique can capture short-term variabilities of ozone in 5-km vertical layers, between 0.3 mbar and 100 mbar, with a precision of 5-15%. However, outside the 1-20 mbar range, BUV-derived results are heavily influenced by a-priori assumptions. To minimize this influence, it is recommended that studies of long-term trends using BUV data be restricted to 1-20 mbar range". *(note: 1-20 mbar corresponds to approx. 26 – 50 km)*

Tropospheric ozone from combined SBUV and TOMS measurements:

Tropospheric ozone columns have been derived by combining measurements from different sensors, e.g., TOMS and SBUV or TOMS and SAGE II (see *Fishman et al., 2003*, and references given therein).

Fishman et al., 2003, have produced daily tropospheric ozone residual (TOR) maps between 50 deg N and 50 deg S from 1979 to 2000 (resolution: 1 deg latitude x 1.25 deg longitude). Basically, these maps have been generated by subtracting the stratospheric column as measured by SBUV from the total column as measured by TOMS. *Fishman et al., 2003,* report on agreement with ozone sonde measurements within 13-20% in line with other studies (see references given in *Fishman et al., 2003*) . However, *de Laat and Aben, 2003*, point out that they can produce similar tropospheric ozone distributions as shown in *Fishman et al., 2003,* without using any satellite ozone measurements. According to *de Laat and Aben, 2003*, the ozone variability observed by *Fishman et al., 2003,* seems to be mainly due to tropopause height variations rather than being a result of air pollution.

7.6.1.3 GOME/ERS-2

Parameter: Ozone total column (see Figure 19) and vertical profiles.

GOME ozone columns:

The current version of the operational data processor is GOME Data Processor (GDP) Version 3.0 which has been extensively validated [*GDP3ESA, 2002; Lambert et al., 2003*]. The accuracy of the GOME GDP V3.0 ozone columns is *[Lambert et al., 2003]*:

"GDP total ozone has been validated from pole to pole by comparison with well understood, controlled and documented ground-based measurements from SAOZ/DOAS UV-visible spectrometers, Brewer and Dobson spectrophotometers, and UV filter radiometers within the Network, and with global data from the TOMS satellite sensor and from modelling/assimilation tools. GDP retrievals have also been compared with retrievals from independent DOAS algorithms and from the TOMS V7 algorithm.

The spectral fitting of ozone slant columns in the UV region from 325 to 335 nm works well. GOME gives a consistent global picture of the total ozone field and results in temporal and spatial structures similar to those from other sensors. The studies do not reveal any long-term drift of quality.

The agreement of GDP level-2 total O_3 data product with the other sources of O_3 data varies with both latitude and season. At Northern middle latitudes, the average agreement is within ±2-3%. At higher latitudes, a solar zenith angle (SZA) dependent difference appears. In addition a dependence of the GDP data product on the ozone column values has been identified. Latitude, season, SZA and column dependences are coupled in the final data product.

The average deviation of GOME from ground-based data does not exceed ±2-4% for SZA below 70°. At lower sun elevation, the average error ranges from -8% to +5% depending on the season. Lowest total ozone values are overestimated by GOME by 5-10% during ozone hole conditions."

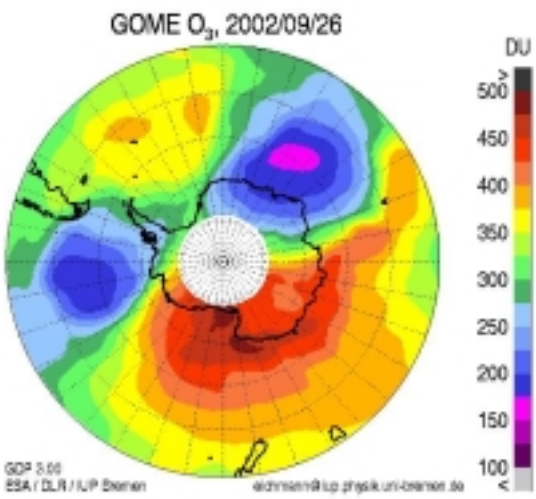

Figure 19: The antarctic "ozone hole" as measured by GOME (GDP V 3.0) on September 26, 2002. In 2002 the ozone hole has been split into two parts (blue colors) due to a major stratospheric warming event. This has never been observed before.

Future outlook - the next version of the GOME data processor: ESA/ESRIN has recently conducted a study in order to select a next generation algorithm for GOME. Three scientific algorithms have been (further) developed and validated. The results indicate that significant improvements can be expected for the next version. Basically agreement with ground stations within the uncertainty of the ground based Dobson and Brewer measurements has been reached overcoming some of the limitations of GDP V3.0 such as seasonally dependent differences with respect to ground stations (see, e.g., *Weber et al., 2004a; Weber et al., 2004b*).

GOME ozone profiles:

Height resolved ozone profiles can be derived from the GOME nadir measurements [*Siddans et al. 1997; Hoogen 1998; Munro et al., 1998; Siddans et al., 1998; Hoogen et al.,1999*]. Examples are shown in Figure 20.

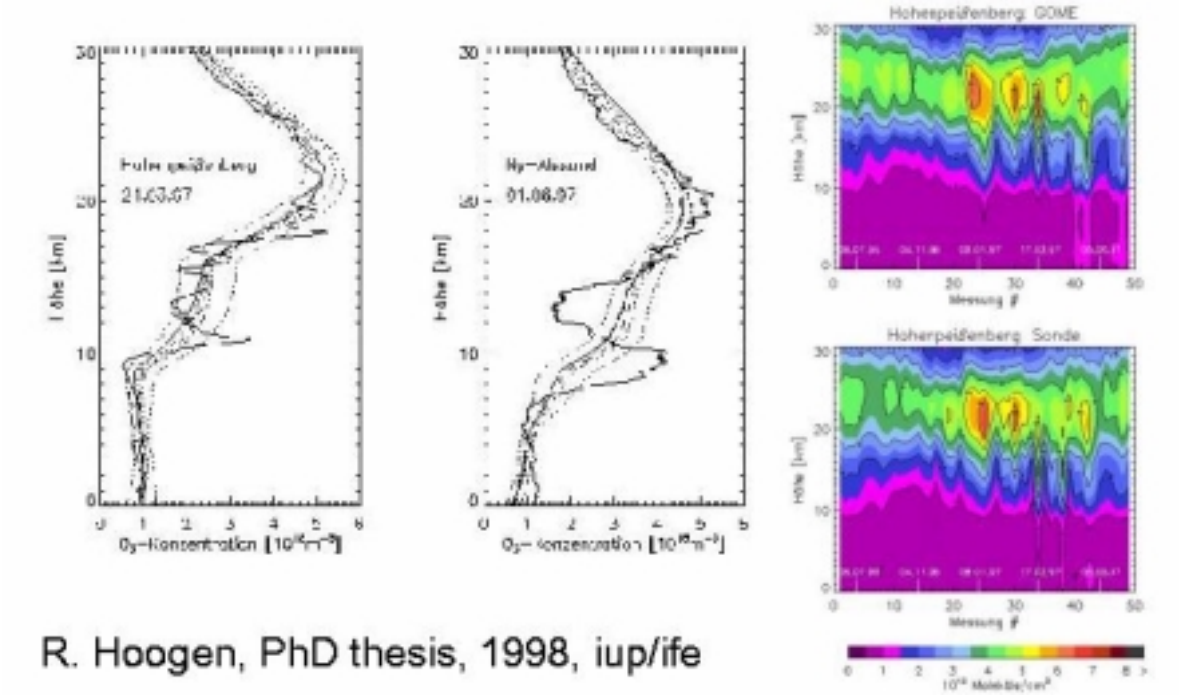

Figure 20: Ozone vertical profiles as measured with GOME compared to ozone sonde measurements *[Hoogen 1998]*.

Stratospheric information:

The vertical resolution of the GOME derived ozone profiles is estimated to be in the range 5 – 12 km with best resolution around 20-30 km and lower resolution above and below (see Figure 21). The accuracy of the profiles is <10% in the middle stratosphere and <20% in the lower stratosphere.

In detail: *[Hoogen et al., 1999]*: “The RMS difference between ozone subcolumn amounts in 10 km layers as measured by GOME and by the sondes is approximately 7-8% in the middle stratosphere and 15-20% in the lower stratosphere.”
[*Siddans et al., 1998*]: “Comparison of GOME to other satellite sensors (MLS and SSBUV) indicates biases < 10% in the stratosphere (above 40 mbar); comparison to colocated ozone sondes indicates biases of < 5% … and standard deviations of < 10% … above 12 km.”

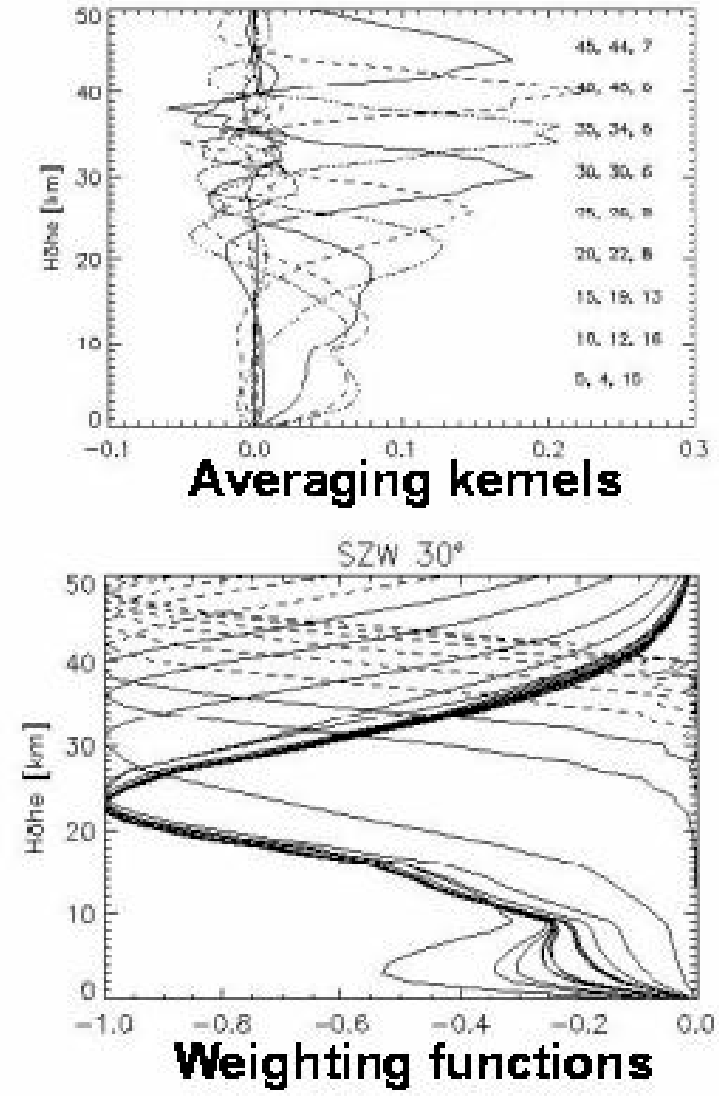

Figure 21: Averaging kernels (top) and weighting functions (bottom) for ozone profile retrieval from GOME nadir observations *[Hoogen, 1998]*. For each averaging kernel the nominal and the actual height of its maximum and the FWHM of the main peak are indicated.

Tropospheric information:

According to [*Siddans et al. 1997; Munro et al., 1998; Siddans et al., 1998, Hoogen et al.,1999*] it is possible to obtain information on ozone down to the ground, i.e., also in the troposphere. The estimated uncertainties are, however, quite large. According to Siddans et al., 1997, the biases are < 30% and the standard deviation as compared to ozone sonde measurements are < 40% below 12 km.

7.6.1.4 SCIAMACHY/ENVISAT

SCIAMACHY ozone columns from nadir:

Recently, results from an initial validation of the latest version of the SCIAMACHY operational data processor has been presented (ACVE-2 workshop, 3-7 May 2004). The results can be summarised as follows *[Kelder et al., 2004]*:

Operational ozone column product (NRT product Version 5.01):

The quality of the columns is comparable with GOME data processor version 2.x (an old version with known problems). The agreement with independent measurements is within 2-10% with an average underestimation of a few percent.

Scientific ozone column products:

During this workshop also the quality of scientific data products has been assessed. For these products (generated at KNMI and BIRA) an average deviation of 1.5% with respect to independent measurements has been identified and a standard deviation of ~5%.

SCIAMACHY ozone profiles from limb:

The vertical resolution of the SCIAMACHY limb measurements is mainly determined by the instruments FoV (2.6 km) and is about 3 km *[Bovensmann et al., 1999; von Savigny et al., 2004]*. The lowest altitude from which ozone information can be retrieved is determined by clouds (tropics: ~16 km).

The theroretical retrieval precision of ozone profiles from the SCIAMACHY limb measurements has been estimated to be better than 1% (1-sigma) in the altitude range 5-50 km *[Kaiser et al., 2002]*.

Recently, results from an initial validation of the latest version of the SCIAMACHY operational data processor has been presented (ACVE-2 workshop, 3-7 May 2004). It has to be noted that the SCIAMACHY limb profiles suffer from a to be improved ENVISAT pointing knowledge problem which results in errors in the altitude assignment of the limb profiles of up to 3 km resulting essentially in vertically “shifted” profiles. The validation workshop results can be summarised as follows *[Kelder et al., 2004]*:

Operational ozone profiles:

By comparison with groundbased measurements biases in the range –8% to +12% have been identified.

Scientific ozone profiles:

Version 1.6 ozone profiles generated at the University of Bremen *[von Savigny et al., 2004]* have been compared with HALOE measurements. Agreement is in the range –

7% to 15%. Figure 22 illustrates the capabilities of the SCIAMACHY limb observation.

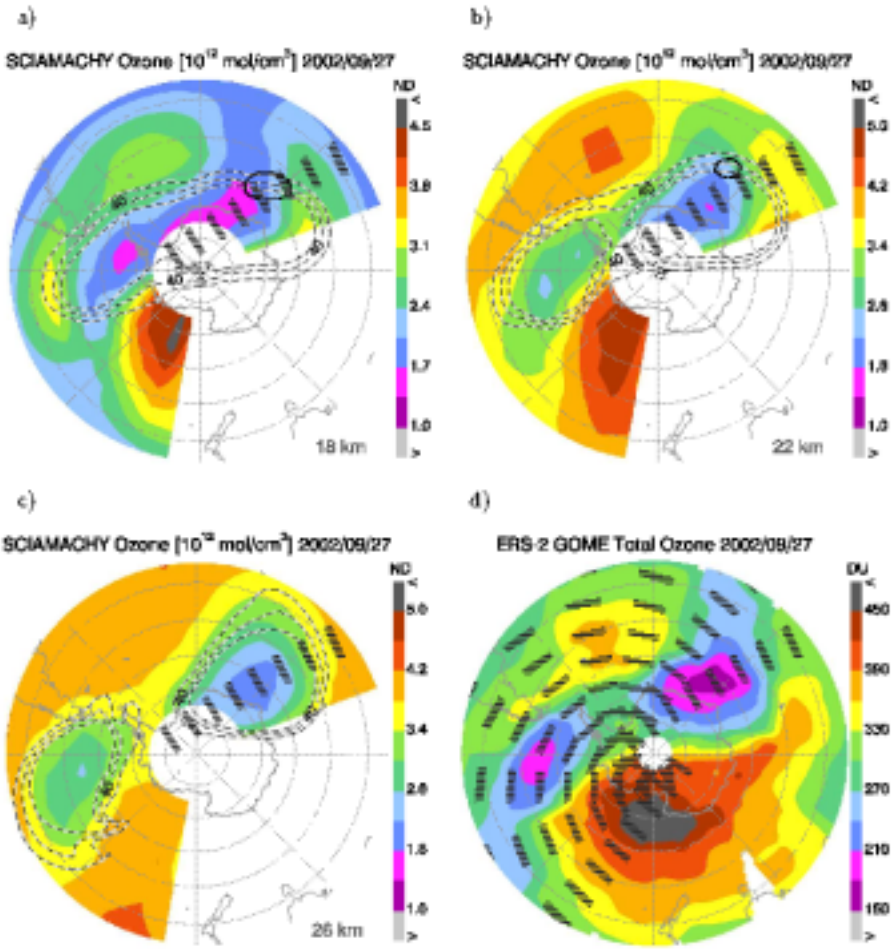

Figure 22: The antartic year 2002 "ozone hole split event" as seen by SCIAMACHY limb observations (altitudes: 18 km (top left), 22 km (top right), and 26 km (bottom left) *[Savigny et al., 2004]*.

SCIAMACHY tropospheric ozone columns from combined nadir/limb:

First results have been generated at the University of Bremen and are currently being analysed. No reliable precision/accuray values are available at present.

SCIAMACHY ozone profiles from solar occultation:

First results concerning ozone profile retrieval from the SCIAMACHY solar occultation measurements are described in *Meyer, 2004*. A comparison with independent satellite measurements is shown in Figure 23. An error analysis has been performed and summarized Table 20.

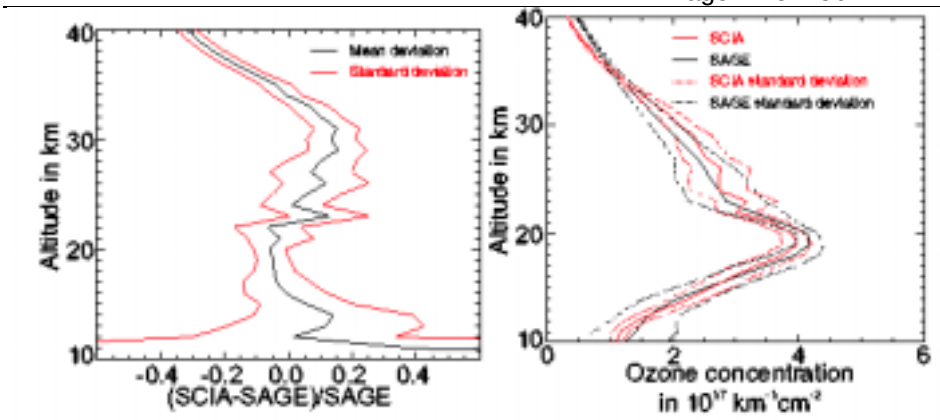

Figure 23: Comparison of ozone profiles retrieved from the SCIAMACHY solar occultation measurements compared to ozone profiles measured by SAGE II (from *Meyer, 2004*).

Error Description	Value	Type
Deviations from validation results		
O_3	$\sim 10\,\%$	random/bias
NO_2	$\sim 15\,\%$	random/bias
Error due to instrument noise	0.025–1 %†	random
Statistical errors (optimal estimation)		
O_3	$\sim 5\,\%$	random
NO_2	$\leq 10\,\%$	random
Horizontal Inhomogeneities		
photochemical (NO_2)	10–40 %‡	bias
dynamic	0–10 %‡	random
Uncertainties of cross-sections	$\leq 3\,\%$	random
Diffuse radiation	$\ll 0.1\,\%$†	bias
Increased aerosol loading (enhanced diffuse light)	$\ll 1\,\%$†	bias
Neglect of FOV height extension	$< 2\%$†	bias
Inhomogeneous illumination of detector	$\sim 1\,\%$§	spectral
Wavelength shifts	$\sim 1\,\%$§	spectral
Undersampling	$\sim 1\,\%$§	spectral
Model errors obtained from spectral residues		
with matching algorithm	$\sim 1\,\%$§	bias
without matching algorithm	1–6 %	bias
Sun spots	0–10 %¶	bias
Global limb darkening (due to pointing errors)	$\sim 7\,\%$¶	bias
Geometry errors		
Tangent height uncertainty		
with height retrieval	< 1 km	random
without height retrieval	1–3 km	random/bias
Height resolution	3–5 km	
Maximum pointing error	0.012°	random

Table 20: Error analysis and summary of validation results for ozone (and NO_2) profile retrieval from the SCIAMACHY solar occultation measurements (from *Meyer, 2004*).

7.6.1.5 OMI/AURA

Parameters: Ozone total columns and vertical profiles.
Expected precision and accuracy: as GOME but with improved spatial resolution (13 x 24 km^2 rather than 40 x 320 km^2).

7.6.2 Future systems

7.6.2.1 GOME-2/METOP

Parameters: Ozone total columns and vertical profiles.
Expected precision and accuracy: as GOME but with improved spatial resolution (40 x 80 km^2 rather than 40 x 320 km^2).

7.7 Passive systems / solar spectral region: Pressure

7.7.1 Existing systems

7.7.1.1 SAGE III

The required accuracy and precision of the SAGE III solar occultation pressure profiles is ~2% *[Pitts et al.; SAGE3-Val-Summary, 2001]*. The vertical resolution/sampling is 0.5-2 km. The height range covered by SAGE III is 0-85 km (if clouds are in the field-of-view the lowest altitude is the cloud top).

7.7.1.2 SCIAMACHY/ENVISAT

Stratospheric pressure profiles derived from the SCIAMACHY limb measurements are an operational data product from SCIAMACHY (see
Figure 3). The pressure as a function of (geometrical) altitude is planned to be derived from the CO_2 absorption bands in channel 7 (~2 μm) *[ATBD SCIA Lv1-2]*. At present, no detailed information on this data product is available. The engineering tangent heights as given in the operational SCIAMACHY data products suffer from (to be improved) ENVISAT pointing knowledge errors which currently might be as large as 3 km (to be improved to ~1 km).

7.7.2 Future systems

According to our knowledge, no future passive satellite systems operating in the solar spectral region systems are planned which will deliver pressure as a function of (geometrical or geopotenital) altitude with sufficient accuracy/precision as an operational or scientific data product (see also *O'Brian, 2002*).

7.8 Passive systems / solar spectral region: Temperature

7.8.1 Existing systems

7.8.1.1 SAGE III

The required accuracy and precision of the SAGE III solar occultation pressure profiles is ~2K *[Pitts et al.; SAGE3-Val-Summary, 2001]*. The vertical resolution/sampling is 0.5 km. The height range covered by SAGE III is 0-85 km (if clouds are in the field-of-view the lowest altitude is the cloud top).

7.8.1.2 SCIAMACHY/ENVISAT

Stratospheric temperature profiles derived from the SCIAMACHY limb measurements are an operational data product from SCIAMACHY (see
Figure 3). The temperature as a function of (geometrical) altitude is planned to be derived from the CO_2 absorption bands in channel 7 (~2 μm) *[ATBD SCIA Lv1-2]*. At present, no detailed information on this data product is available. The engineering tangent heights as given in the operational SCIAMACHY data products suffer from (to be improved) ENVISAT pointing knowledge errors which might be currently as large as 3 km (to be improved to ~ 1 km).

7.8.1.3 GOMOS

GOMOS delivers or plans to deliver two different sets of operational temperature profiles from its stellar occultation measurements, namely the High Resolution Temperature Profiles (HRTP) derived from the signal of two fast photometers (red and blue, 1 kHz sampling, vertical resolution of temperature profiles ~200 m) and lower resolution temperature profiles derived from the main channel spectra (via O_2 absoption and Rayleigh scattering). The lower resolution profiles have not yet reached a quality considered good enough for validation *[Fussen et al., 2004]* and for the HRTP product validation is currently too limited to derive firm conclusions. A limited comparison with independent measurements (e.g., SAOZ balloon) showed agreement within 2-4 K in the altitude range 20-30 km *[Goutail et al., 2004]* for selected profiles and larger discrepancies above and below.

7.8.2 Future systems

According to our knowledge, no future passive satellite systems operating in the solar spectral region systems are planned which will deliver temperature as a function of altitude in the troposphere with sufficient accuracy/precision as an operational or scientific data product.

8 Passive Systems in the Thermal Infrared Spectral Region

8.1 Introduction

In the thermal-infrared (TIR), molecules with a dipole moment have active vibrational rotational transitions, which can be observed both in emission and absorption (see Figure 24). For the observation of species down to the troposphere, pressure broadening of the spectral features is considerably less problematical than at MW wavelengths as the Doppler line width is proportional to the frequency of the light and is therefore larger in the mid-infrared than at longer wavelengths.

It has to be noted that sounding the troposphere in the TIR has often a low sensitivity to trace gas concentrations in the lowest troposphere, where the majority of Greenhouse gases (GHG) resides, due to the lack of temperature contrast.

Passive remote sensing by mid-infrared spectroscopy has been successfully applied to the measurement of a large number of stratospheric trace constituents and some upper tropospheric constituents by limb emission or absorption sounding.

There are only a few experiment flown up to the present, which specifically uses infrared information to probe GHGs in the troposphere: HIRS and IMG. In addition the AIRS experiment on NASA Aqua mission covers also the relevant spectral range as well as TES (Tropospheric Emission Spectrometer) on EOS-AURA.

In the near future there are new missions planned to measure GHG distributions in the IR, namely IASI on METOP and the GIFTS (Geostationary Imaging Fourier Transform Spectrometer) mission.

The GIFTS mission is the first attempt to fly and operate a FTIR in geostationary orbit with the primary focus of determining meteorological parameters like water vapour and temperature, but as a secondary objective it is intended to derive trace gas concentrations of O_3 and CO and other gases from GIFTS measurements.

Spectral lines overview

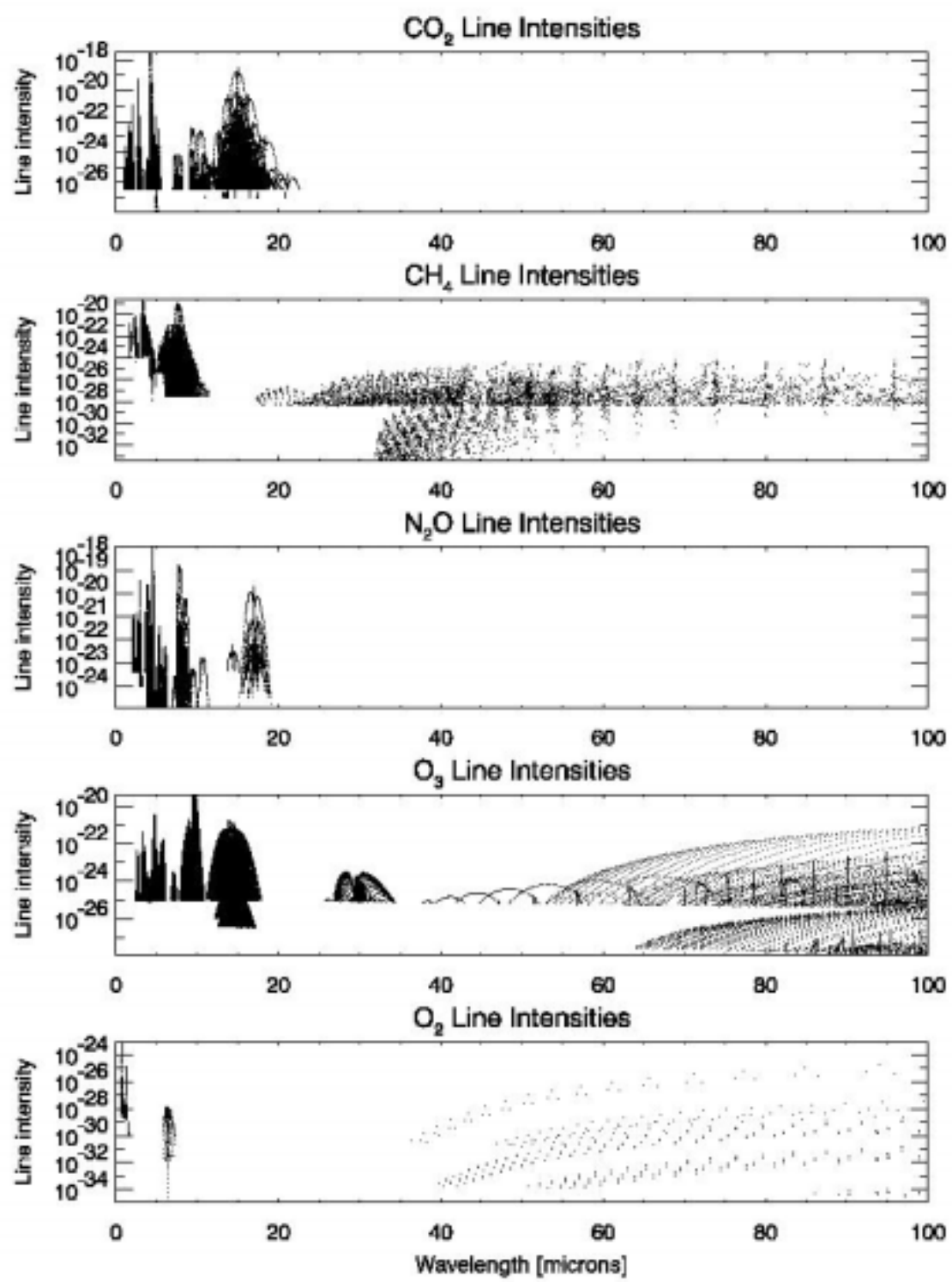

Figure 24: Molecular line intensities in the thermal infrared spectral region. Figure generated from Hitran 2000 spectroscopic line parameters by *M. Buchwitz [Rothman et al., 2003].*

8.2 Instruments overview

8.2.1 Scanning Radiometer

8.2.1.1 HIRS POES/NOAA/METOP

http://www2.ncdc.noaa.gov/docs/klm/html/c3/sec3-2.htm

The first High Resolution Infrared Radiation Sounder (HIRS) is a scanning radiometer instrument and was developed and flown in 1975 on the Nimbus 6 satellite. Results from the Nimbus 6 orbital data and system studies showed promise of obtaining data from which improved atmospheric soundings could be derived. The basic design for the Nimbus HIRS system was modified to accommodate the TIROS-N series of spacecraft with TIROS-N orbital requirements, to improve the sensor performance, and to increase the reliability of the filter wheel drive assembly. Additional improvements and operational changes were made for the HIRS/3. Three HIRS/3 were built for use on the NOAA KLM spacecraft. The HIRS/4 design is a modification of the HIRS/3 design, built to fly on the NOAA-N, -N' spacecraft.

The HIRS/3 is a twenty channel scanning sounding radiometer instrument which has an instantaneous field-of-view of 1.3 degrees providing a nominal spatial resolution at nadir of 18.9 km (11.7 miles). The antenna provides a cross-track stepped scan, scanning +/- 49.5 degrees from nadir with a total of 56 fields-of-view per scan. The instrument completes one scan line every 6.4 seconds. The HIRS/3 scan profile has been modified to eliminate the viewing of the cold blackbody internal calibration target from the automatic calibration sequence. The additional time has been used to perform another scan (38 per calibration sequence) of the Earth. The instrument measures scene radiance in the infrared spectrum. Data from the instrument is used, in conjunction with the AMSU instruments, to calculate the atmosphere's vertical temperature profile from the Earth's surface to about 40 km altitude. The data is also used to determine ocean surface temperatures, total atmospheric ozone levels, precipitable water, cloud height and coverage, and surface radiance.

HIRS/4 is a scanning sounding radiometer with 19 channels in the range 3.8–15.5 mm, and one visible channel. Scanning is performed in a cycle of 6.4 s, which provides 56 pixels spread over a swath width of 1080 km on each side of the sub-satellite point. Scan separation is 42 km, which corresponds to the satellite displacement during the cycle. Calibration scans on internal blackbodies take place in a cycle of 256 s or every 40 scans. For HIRS/4, the Instantaneous Field of View (IFOV) is reduced from 17.4 km (diameter at nadir for HIRS/2 and HIRS/3) to 10 km, thus providing better cloud free observation ratios. Main products from HIRS are temperature, Ozone, precipitable water, cloud height and coverage and surface radiance (albedo). HIRS/4 will also be flown on METOP (AM orbit).

8.2.2 Spectrometer/Interferometer

8.2.2.1 IMG/ADEOS-I

http://www.eorc.nasda.go.jp/AtmChem/IMG/

The Interferometric Monitor for Greenhouse gases (IMG) *[Kobayashi et al., 1999]* launched aboard ADEOS-I in August 1996 was the first high resolution nadir infrared instrument allowing the simultaneous measurement from space of a series of trace gases focusing on GHGs: H_2O, CO_2, N_2O, CH_4, CFCs, O_3, and CO. ADEOS-I is a sun-synchronous (equator local crossing time at descending node 10:30 AM) polar-orbiting satellite.

The IMG is a nadir-viewing Fourier transform interferometer that recorded the thermal emission of the Earth-atmosphere system between 600 and 3030 cm^{-1}, with a maximum optical path difference of 10 cm, resulting in a spectral resolution of 0.1 cm^{-1}. The footprint on the ground is approx. 8 km x 8 km, in three spectral bands (band 1 from 2387 to 3030 cm^{-1}, band 2 from 2000 to 2500 cm^{-1}, and band 3 from 600 to 2000 cm^{-1}), corresponding to three different detectors and three geographically adjacent footprints.

The IMG instrument performed a global coverage of the Earth, making 14 orbits per day with series of six successive measurements separated by 86 km (every 10 sec.) along the track, followed by the observation of deep space and of an internal blackbody for calibration purposes. Due to the huge data flow rate, the nominal operational mode of IMG was set to 4 days operation/10 days halt alternation.

Unfortunately, in June 1997, the ADEOS satellite ceased to collect and transmit data due to a power failure in its solar panel.

8.2.2.2 AIRS/AQUA

http://www-airs.jpl.nasa.gov/

The Atmospheric Infrared Sounder AIRS was launched on EOS Aqua, the first PM (1:30 PM Equatorial Crossing Time) EOS platform, in May 2002. The AIRS instrument is a high-spectral-resolution infrared grating spectrometer (3.74 - 4.61 µm, 6.20 - 8.22 µm, 8.80 - 15.4 µm) designed to sound the atmosphere w.r.t. global distributions of temperature and moisture. As research products O_3, CO_2 and CH_4 profiles are under development.

The heart of the instrument is a cooled (155 K) array grating spectrometer operating over the range of 3.7 - 15.4 µm at a spectral resolution (l/Dl) of 1200. The spectrometric approach uses a grating to disperse infrared energy across arrays of high sensitivity HgCdTe detectors operating at 58 K. The concept requires no moving parts for spectral encoding and provides 2378 spectral samples, all measured simultaneously in time and space. Simultaneity of measurement is an essential requirement for accurate temperature retrievals under partly cloudy conditions.

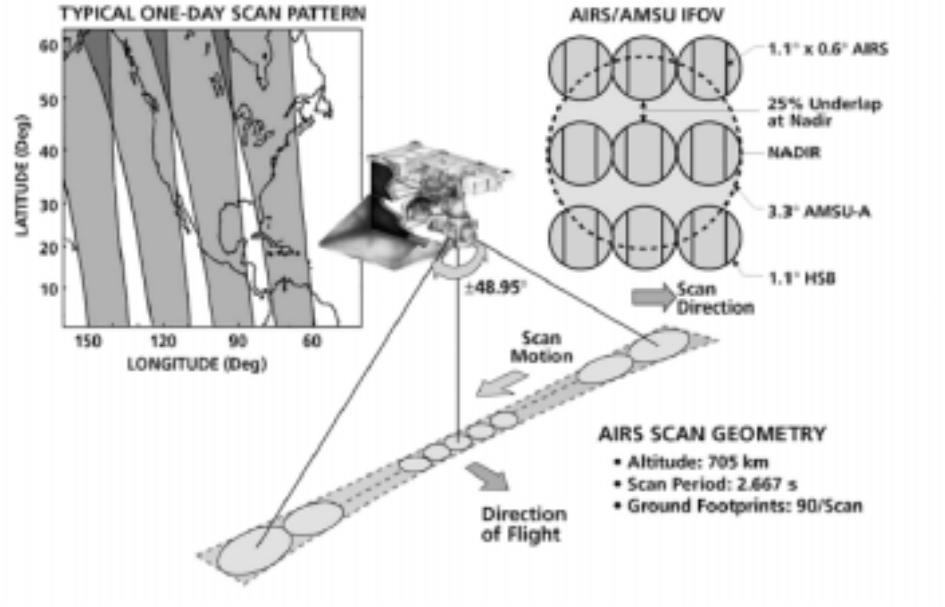

Figure 25: Alignment of AIRS/AMSU/HSB foorprints [Aumann et al. 2002].

AIRS views the ground through a cross track rotary scan mirror which provides ±49.5° ground coverage. A total of 90 ground footprints are observed each cycle with each 22.4 ms footprint containing all 2378 spectral samples. The AIRS IR spatial resolution is 13.5 km from the nominal 705.3 km orbit.

8.2.2.3 TES/AURA

http://aura.gsfc.nasa.gov/instruments/tes/introduction.html

http://tes.jpl.nasa.gov/

TES is a high-resolution infrared-imaging Fourier transform spectrometer with spectral coverage from 3.2 to 15.4 µm at a spectral resolution of 0.025 cm^{-1} , thus offering line-width-limited discrimination of essentially all radiatively active molecular species in the Earth's lower atmosphere. TES has been launched onboard NASAs AURA satellite in summer 2004 (sun-synchronous polar orbit, PM). TES has the capability to make both limb and nadir observations. In the limb mode, TES has a height resolution of 2.3 km, with coverage (scan range) from 0 to 34 km. In the down-looking mode, TES has a spatial resolution of 0.53 km x 5.3 km with a swath of 5.3 km x 8.5 km. TES is a pointable instrument and can access any target within 45° of the local vertical, or produce regional transects up to 885 km length without any gaps in coverage.

TES has the capability to measure the GHG O_3, CH_4 and H_2O.

8.2.2.4 IASI/METOP1-3

http://smsc.cnes.fr/IASI/

The Infrared Atmospheric Sounding Interferometer (IASI) consists of a Fourier Transform Spectrometer with an imaging system and will be flown on Metop 1 – 3 from 2005 onwards in a sun-synchronous polar orbit (AM). It is based on a Michelson Interferometer and is designed to measure the infrared spectrum emitted by the Earth and its atmosphere. The instrument provides spectra of high radiometric quality at 0.5 cm^{-1} resolution, from 645 to 2760 cm^{-1}. Data samples are taken at intervals of 25 km along and across track (nadir), each sample having a maximum diameter of about 12 km.

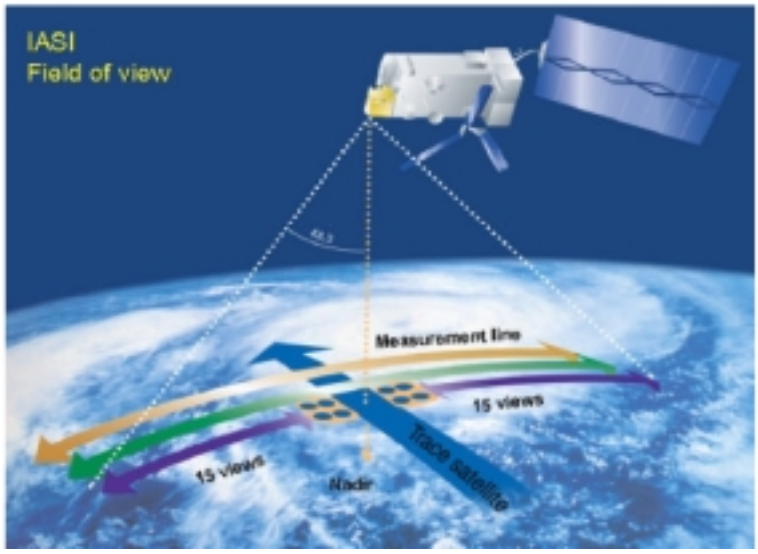

Figure 26: IASI viewing geometry [IASI web pages].

IASI will provide improved infrared soundings of the temperature profiles in the troposphere and lower stratosphere, moisture profiles in the troposphere, as well as some of the chemical components playing a key role in the climate monitoring, global change and atmospheric chemistry.

8.2.2.5 CrIS/NPOESS

http://www.ipo.noaa.gov/Library/cris_NDX.html

http://www.ipo.noaa.gov/Technology/cris_summary.html

http://nppwww.gsfc.nasa.gov/science/CrIS.html

The Crosstrack Infrared Sounder (CrIS) is a sensor under development for the National Polar-orbiting Operational Environmental Satellite System (NPOESS) program, which is the follow-on to the current POES meteorological satellite systems. In this context CrIS will be the follow on instrument of the successful HIRS series. CrIS is an infrared interferometric sounding sensor which accurately measures

upwelling earth radiances at very high spectral resolution (0.625-2.5 cm^{-1}), and uses this data to construct vertical profiles of atmospheric temperature, moisture and pressure. The first CrIS instrument is intended to be launched in 2007 within the NPOESS Preparatory Project NPP.

8.2.2.6 GIFTS

http://asd-www.larc.nasa.gov/GIFTS/

http://tellus.ssec.wisc.edu/outreach/gifts/gifts.htm

The Geosynchronous Imaging Fourier Transform Spectrometer (GIFTS) is a concept which combines large area format Focal Plane detector Array (LFPA) with the Fourier Transform Spectrometer (FTS) to image the infrared emission from geostationary orbit. The GIFTS measurement concept uses a large area format focal plane detector array (685 to 1130 cm^{-1} and 1650 to 2250 cm^{-1}) in a Fourier Transform Spectrometer (FTS) mounted on a geostationary satellite to enable the simultaneous gathering of high spectral resolution (as great as 0.3 cm^{-1}) and high spatial resolution (4 km x 4 km pixel) Earth infrared radiance spectra over a large area (512-km x 512-km) of the Earth within a 10 second time interval. A low visible light level camera provides quasi-continuous imaging of clouds at 1-km spatial resolution. Extended Earth coverage is achieved by step scanning the instrument field of view in a contiguous fashion across any desired portion of the visible Earth. The radiance spectra observed at each time step are transformed to high vertical resolution (1-2 km) temperature and water vapor mixing ratio profiles using rapid profile retrieval algorithms. In addition GIFTS spectral range covers emissions of O_3, CO_2 and CH_4.

8.2.3 Future geosynchronous IR sounder

8.2.3.1 HES/GOES

http://cimss.ssec.wisc.edu/goes/HES/

The Hyperspectral Environmental Suite (HES), previously named Advanced Baseline Sounder (ABS), will replace the current GOES sounder which has 18 spectral bands. A high spectral resolution interferometer or grating sounder is currently being considered for GOES-R and beyond (2012+). With high temporal resolution (better than 1 hour), high spatial resolution (better than 10 km), high-spectral-resolution (better than single wavenumber) and broad coverage (hemispheric), ABS/HES measurements will enable monitoring the evolution of detailed temperature and moisture structures in clear skies with high accuracy (better than 1 K root mean square) and improved vertical resolution (about 1 km) over the current GOES sounder. Improved high spectral resolution sounder and high spatial resolution imager on future geostationary weather satellite will greatly enhance nowcasting and forecasting capabilities for a wide variety of applications.

8.2.3.2 IR Sounder on MTG

http://www.eumetsat.de

The post MSG system is currently under specification.

8.3 Passive systems / thermal infrared spectral region: CO_2

8.3.1 Existing systems CO_2

8.3.1.1 HIRS/NOAA

Tropical (20°N-20°S) midtropospheric (5–13 km) mean atmospheric CO_2 concentration were retrieved from the observations of the NOAA series of polar meteorological satellites by *[Chedin et al., 2003a]*, using a nonlinear regression inversion scheme (trained by a neuronal network). For the 4 years of the present analysis (July 1987 to June 1991), monthly means of the CO_2 concentration retrieved over the tropics (20°N to 20°S) from NOAA 10 were evaluated. Maps of monthly mean midtropospheric CO_2 concentration have been produced at a resolution of 15° x 15°. A rough estimate of the method-induced standard deviation of these retrievals is of the order of 4 ppmv (around 1%) *[Chedin et al., 2003a]*. It has to be noted that the impact of biases in the single measurement on the monthly mean concentrations is not analysed in detail. In addition, as typical for all CO_2 derived from IR measurements, the measurements are not sensitive to CO_2 in the lowest troposphere (see also *[Engelen and Stephens, 2004]*).

8.3.1.2 IMG/ADEOS

IMG was especially designed to measure GHGs. Therefore IMGs spectral range covering CO_2 emissions and the spectral resolution as well as the spatial resolution is aqeuate to expect good CO_2 retrievals. Nevertheless, up to now unfortunately no result on retrieval from IMG data have been published. One reason for this seems to be that acurately measured global scale temperature and surface emissivity fields colocated with the IMG measurements are not available for the IMG measurement period *[Chedin et al., 2003b]*.

8.3.1.3 AIRS/AQUA

[Engelen and Stephens, 2004] used an information theory based anaysis to study the capability of the Atmospheric Infrared Sounder (AIRS) for retrieving atmospheric carbon dioxide and for contrasting these resulty with the current system of infrared sounders (Television and Infrared Observation Satellite (TIROS) Operational Vertical Sounder/High-Resolution Infrared Radiation Sounder (TOVS/HIRS)). It is argued that instruments like AIRS (and IASI) will be able to retrieve column-averaged CO_2 mixing ratios with high accuracy (order of 1–2 ppmv). On the other hand, the TOVS/HIRS system is only able to retrieve column-averaged CO_2 mixing ratios with an accuracy of the same order as the seasonal amplitude of atmospheric CO_2 variations (order of 10 ppmv). The impact of the constrains on the a-priori covariance matrix on the extractable information seems to be of importance *[Engelen and Stephens, 2004]*.

8.3.1.4 TES/AURA

TESs spectral range is covering CO_2 IR emissions and the spectral resolution as well as the spatial resolution is aqeuate to expect good CO_2 retrievals. A drawback of TES high horizontal resolution in combination with its combined limb-nadir measurements concept is the lack of coverage, as only a small strip along track is measured. CO_2 is currently not an operational TES data product. CO_2 emission are primarily used to derive temperature fields *[TES ATBD V 1.1]*.

8.3.2 Future systems CO_2

8.3.2.1 IASI/METOP

In a sensitivity study *[Chedin at al., 2003b]* investigated the potential to derive high precision CO_2 total column data from IASI and AIRS measurements. They show that although the carbon dioxide signal is below or at the instrument noise level for IASI and uncertainties in temperature and water vapor errors can dominate, a careful averaging of the retrieved carbon dioxide fields over areas of 500 x 500 km^2 and 2 weeks should allow to extract changes at the level of 1% or less in the total column carbon dioxide amount. They also show results from an information content study for AIRS data which suggests 50 channels are adequate for inferring the tropospheric carbon dioxide amounts but that they are not sensitive to CO_2 changes in the boundary layer *[Chedin et al., 2003b]*.

8.4 Passive systems / thermal infrared spectral region: CH_4

8.4.1 Existing systems CH_4

8.4.1.1 IMG/ADEOS

Clerbaux et al. 2003 reported on CH4 retrievals from IMG data. They give a measurement uncertainty of 4 % for a column measurement *[Clerbaux et al. 2003]*. Details on the method of error estimate are not given.

8.4.1.2 AIRS/AQUA

In *[Aumann et al. 2003]* it is claimed that CH_4 will be a AIRS L2 product, but is not one of the core products. Currently there is no error estimate availble on CH_4 from AIRS.

8.4.1.3 TES/AURA

TESs spectral range is covering CH_4 IR emissions and the spectral resolution as well as the spatial resolution is adequate to expect good CH_4 retrievals. A drawback of TES high horizontal resolution in combination with its combined limb-nadir measurements concept is the lack of coverage, as only a small strip along track is measured. CH_4 is a standard TES product *[TES ATBD V 1.1]* and the accurary is estimated with 3% (14 ppbv) [TES WWW]. Recently an information content analysis and sensitivity study was published by *[Worden et al. 2004]*. They conclude that TES CH_4 nadir measurements are sensitive to concentrations in the upper troposphere and lower stratosphere only and not to tropospheric CH_4. Below approx. 8 km the estimated total error equals the a-priori error (no gain in information). In the upper troposphere and the lower stratosphere the estimated error is about 3% *[Worden et al. 2004]*. The information content analysis reveals that 0.43 – 0.69 degrees of freedom are available from the measurement, with the consequence that for CH_4 an upper tropospheric and lower stratospheric sub-column can be determined from TES nadir emission spectra.

8.4.2 Future systems CH_4

According to the information availble from the TES web pages the error of CH_4 profiles determined from the limb sounding measurements is 3%. No detailed error assessement is currently available.

8.4.2.1 IASI/METOP

Based on retrieval results with IMG data Clerbaux et al. 2003 estimats the CH4 error to be approx. 4 % *[Clerbaux et al. 2003]*. The IASI web pages are claiming for an error on 5 –10% [IASI web page].

8.5 Passive systems / thermal infrared spectral region: N_2O

8.5.1 Existing systems N_2O

8.5.1.1 IMG/ADEOS

Lubrano et al 2003 reported on the retrieval of N_2O concentrations from IMG emission spectra. It was concluded there, that no information for N_2O can be obtained in the boundary layer by using spectra recorded over the sea surface, that the amount of information that can be obtained regarding the shape of the observed N_2O profile is very limited, that reliable information may be obtained for the N_2O total column amount and that the most appropriate pressure where the measurements are sensitive to is 300 to 700 hPa. In this range an accuracy of 1-3% can be reached from one single IMG nadir spectrum *[Lubrano et al. 2003]*.

8.5.2 Future systems N_2O

8.5.2.1 IASI/METOP

Lubrano et al 2003 reported on the retrieval of N_2O concentrations from IMG emission spectra degraded to IASI spectral resolution. It was concluded there, that no information for N_2O can be obtained in the boundary layer by using spectra recorded over the sea surface, that the amount of information that can be obtained regarding the shape of the observed N_2O profile is very limited, that reliable information may be obtained for the N_2O total column amount and that the most appropriate pressure where the measurements are sensitive to is 300 to 700 hPa. In this range an accuracy of 1-3% can be reached from IASI nadir spectrum *[Lubrano et al. 2003]*.

8.6 Passive systems / thermal infrared spectral region: Ozone

8.6.1 Existing systems O_3

8.6.1.1 TOVS/NOAA

A systematic analysis of the TIROS Operational Vertical Sounder (TOVS) used as a lower stratospheric ozone monitor over oceans is presented in *[Drouin et al. 2003]*. Poor information on ozone above 40 hPa is available and thus a partial ozone column over the atmospheric layer 400–40 hPa is derived. Systematic errors of the total and partial ozone column retrievals are investigated using comparisons with Total Ozone Mapping Spectrometer observations and four dimensional ozone fields derived from data assimilation experiments. The latitudinal and seasonal differences over the year 1998 are inside the interval (+35, -35) Dobson Units (DU) for the total ozone column *[Drouin et al. 2003]*.

8.6.1.2 IMG/ADEOS

Clerbaux et al. 2003 reported on O_3 retrievals from IMG data. They give a measurement uncertainty of 3-5 % (25 DU) for a total column *[Clerbaux et al. 2003]* and 13 % uncertainty for a tropospheric column (0-12 km). Details on the method of error estimate are not given. Turquety et al. 2002 reported a 10% accuracy of total column O_3 derived from IMG data determined by an intercomparison to TOME/ADEOS O3 data *[Turquety et al, 2002].*

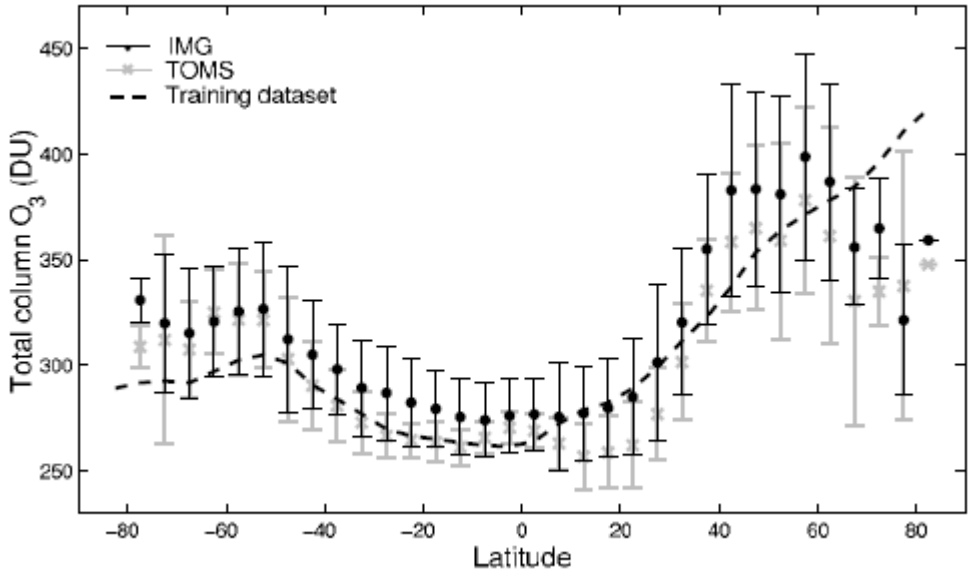

Figure 27: Total O_3 derived from co-located IMG/ADEOS and TOMS/ADEOS measurements zonally averaged over the four periods analyzed (with associated standard deviations). From Turquety et al. 2002 .

8.6.1.3 AIRS/AQUA

The AIRS web pages are claiming an accuracy of total ozone of 20% *[AIRS web page]*. From intercomparisons with TOMS data during validation of the AIRS total ozone product it was reported that total column ozone differs from TOMS globally by 4.4 ± 5.3% *[AIRS Validation Report 2003]*. It has to be noted that this preliminary analysis is based in data evaluation of one day.

8.6.1.4 TES/AURA

TESs spectral range is covering O_3 IR emissions and the spectral resolution as well as the spatial resolution is adequate to expect good O_3 retrievals. A drawback of TES high horizontal resolution in combination with its combined limb-nadir measurements concept is the lack of coverage, as only a small strip along track is measured. O_3 is a standard TES product *[TES ATBD V 1.1]* and the accurary is estimated with 3% (3-20 ppbv) [TES web page]. Recently an information content analysis and sensitivity study was published by *[Worden et al. 2004].* They conclude that TES O_3 nadir measurements are sensitive from the free troposphere (< 700hPa) up to the stratosphere but not to tropospheric O_3 below approx. 700 hPa. The estimated error for the profile is about 20-30% below 20 km and approx. 10% above 20 km *[Worden et al. 2004]*. The information content analysis reveals that approx. 5 degrees of

freedom are available from the measurement, with 2.4 degrees of freedom in the troposphere. This results in an achievable vertical resolution of 5-10 km from TES nadir measurements.

According to the information availble from the TES web pages the error of O_3 profiles determined from the limb sounding measurements is 3%. No detailed error assessement is currently available.

8.6.2 Future systems O3

8.6.2.1 IASI/METOP

The IASI web pages are claiming for an error on 3 % for total column ozone and 10-30% for tropospheric column ozone *[IASI Web]*. These numbers are roughly in line with the uncertainty estimates given in *[Clerbaux et al. 2003]*, based on IMG data analysis.

8.7 Passive systems / thermal infrared spectral region: Temperature

8.7.1 Existing systems T

8.7.1.1 AIRS/AQUA

Within the AIRS validation activities, retrieved SST are compared against ECMWF, with differences of -0.8 K ± 1.0 K *[AIRS Validation Report 2003]*. Differences against buoys are -0.8 K ± 1.1 K. SST comparisons with a ship-borne radiometer are -0.85 ± 1.2 K.

Retrieved temperature profiles are compared with ECMWF, and with dedicated radiosondes. Root-mean-square temperature differences against ECMWF vary from about 1.3 K just above the surface to less than 1 K in the troposphere when averaged over 1 km thick layers, with biases of 0.2 K or less *[AIRS Validation Report 2003]*. Dedicated radiosondes give uncertainties of less about 1 K in retrieved temperature in the free troposphere *[AIRS Validation Report 2003]*.

8.7.1.2 TES/AURA

TESs spectral range is covering CO_2 IR emissions and the spectral resolution as well as the spatial resolution is adequate to expect good temperature retrievals. A drawback of TES high horizontal resolution in combination with its combined limb-nadir measurements concept is the lack of coverage, as only a small strip along track is measured. T is a standard TES product *[TES ATBD V 1.1]* and the accurary is estimated with 1 K [TES WWW]. Recently an information content analysis and sensitivity study was published by *[Worden et al. 2004]* . They conclude that TES nadir measurements are sensitive to temperature from the surface up to the stratosphere. The estimated error for the T-profile is about 1 K above the surface and surface temperature error is approx. 0.5 K *[Worden et al. 2004]*. The information content analysis reveals that approx.10 degrees of freedom are available from the

measurement. This results in an achievable vertical resolution of 3-10 km from TES nadir measurements.

8.7.2 Future systems T

8.7.2.1 IASI/METOP

Aires et al. 2002 studied the retrieval of atmospheric and surface temperature from IASI measurements with a regularised neural net approach *[Aires et al. 2002a]*. They estimated with this approach that the surface temperature for tropical situations yields an rms error of 0.4 K for instantaneous retrievals. Results for atmospheric temperature profile retrievals are close to 1-K rms error for the instantaneous temperature retrieval with 1-km vertical resolution.

8.7.2.2 GIFTS

GIFTS aims to measure temperature with 1 K accuracy, 1 km vertical resolution and 4 km horizontal resolution [GIFTS web pages]. Detailed sensitivity studies are currently not availble.

9 Passive Systems in the Microwave Spectral Region

9.1 Introduction

The microwave region extends from about the millimeter wavelength range and below (sub-millimeter range) to about the centimeter wavelengths range, which corresponds to the 3 GHz to 3 THz spectral region. The most common spectral unit used by the microwave community is frequency.

In contrast to the visible spectral region, where energy flux is mainly induced by solar radiation, in the microwave (and thermal infrared) emission of the earth surface and the atmosphere is the primary source of energy.

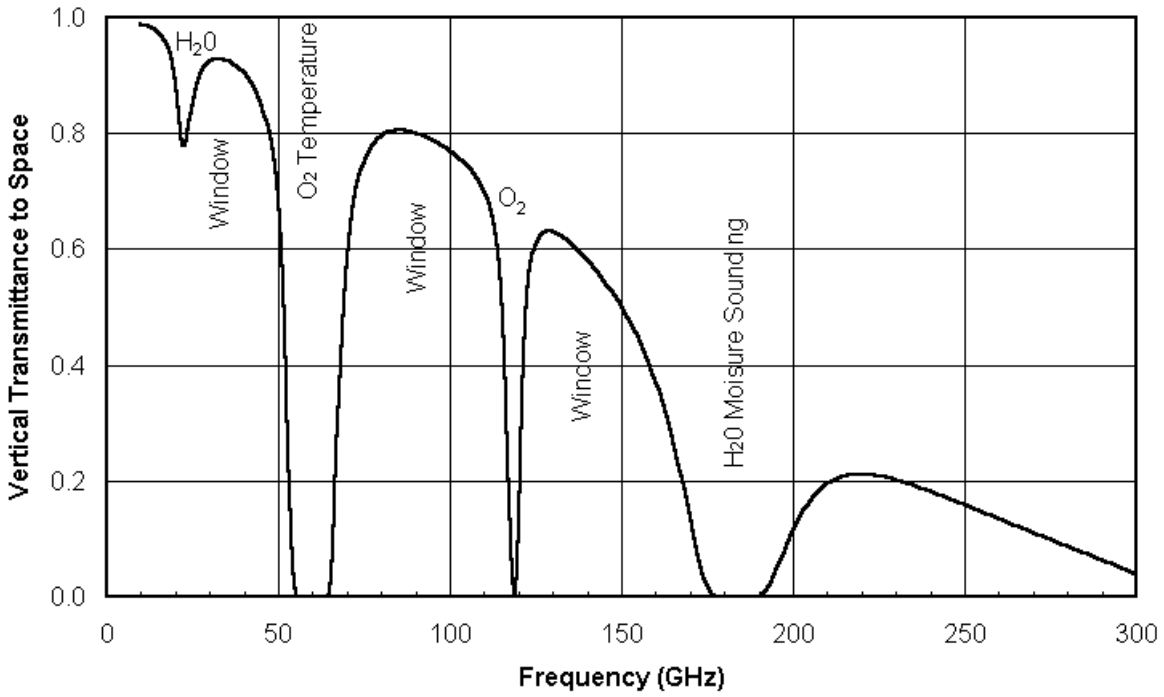

Figure 28: Absorption features in the microwave region: water vapor absorption centered at 22 and 183 GHz and oxygen absorption at 118 GHz and between 50 and 70GHz are dominating the microwave spectral region *[Cira's AMSU Website].*

Spectral lines overview

The microwave spectral region is dominated by absorption features due to oxygen and water vapor. Figure 28 shows the contributions to the absorption from these two sources. Absorption due to water vapor occurs at 22 and 183 GHz. Oxygen absorbs at 118 GHz and between 50 to 70 GHz due to a series of oxygen absorption lines.

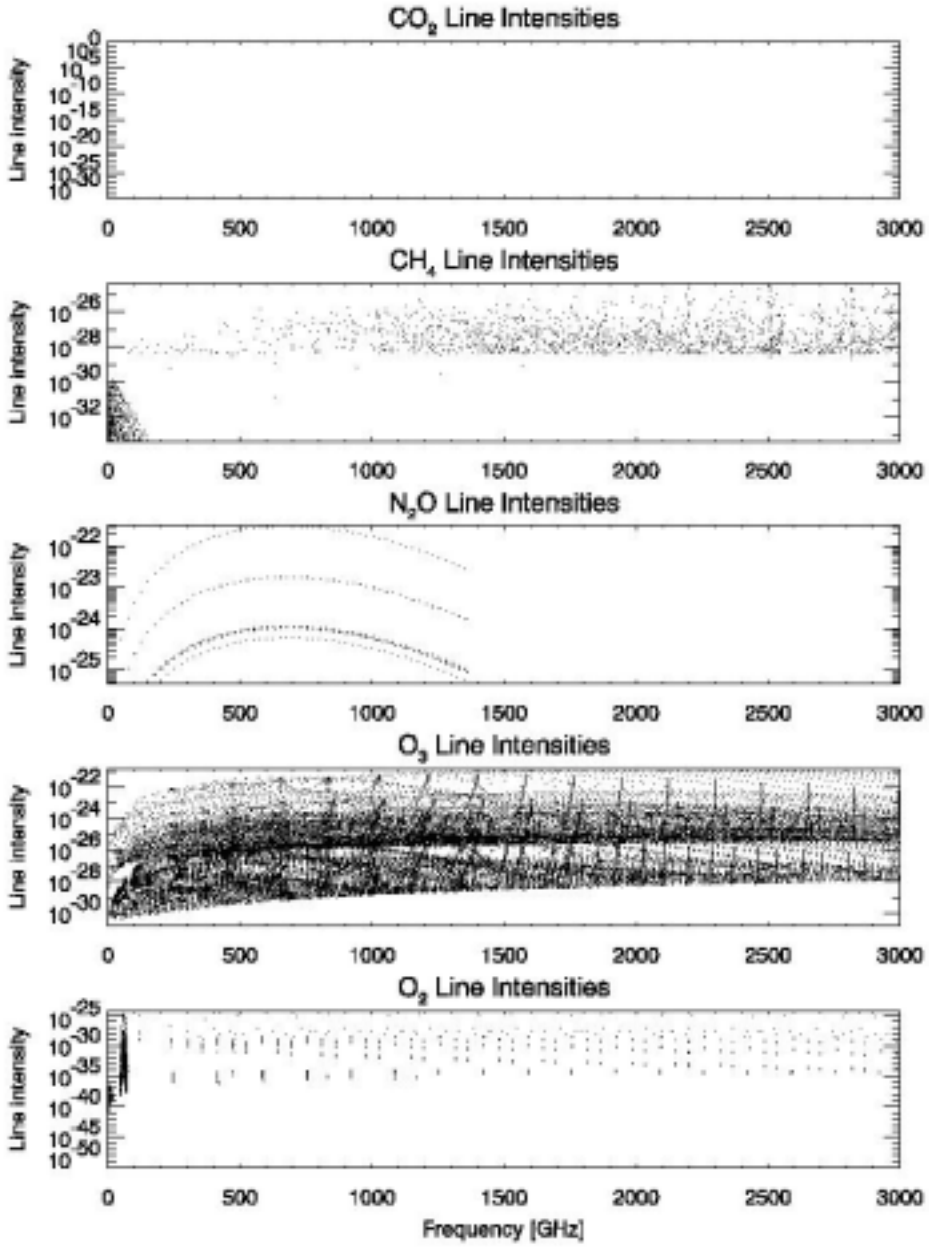

Figure 29: Molecular line intensities in the microwave spectral region. Figure generated from Hitran 2000 spectroscopic line parameters by *M. Buchwitz [Rothman et al., 2003]*.

As can be seen in Figure 29 there are also other molecules absorbing in the microwave like CH_4, N_2O, and O_3. CO_2 does not show up in this region due to its missing permanent dipol moment as absorption in the microwave is induced by rotational transitions. CH_4 absorption line intensities are, with respect to its atmospheric abundance, too small to be detectable. N_2O absorption is moderate, however, its abundance is relatively weak in order to be detectable in nadir geometry. Only limb sounders like EOS-MLS have the ability to spectrally resolve emission lines at all altitudes, which allows measurements of very weak lines in the presence of nearby strong ones and thus measurements of chemical species with very low atmospheric abundances *[EOS-MLS-ATBD]*, like N_2O. O_3 absorption line strengths are similar or even weaker than those of N_2O, it is the large quantity of molecules that makes ozone atmospheric absorption one of the most absorbing trace gases. It also has a large number of features throughout the microwave spectrum.

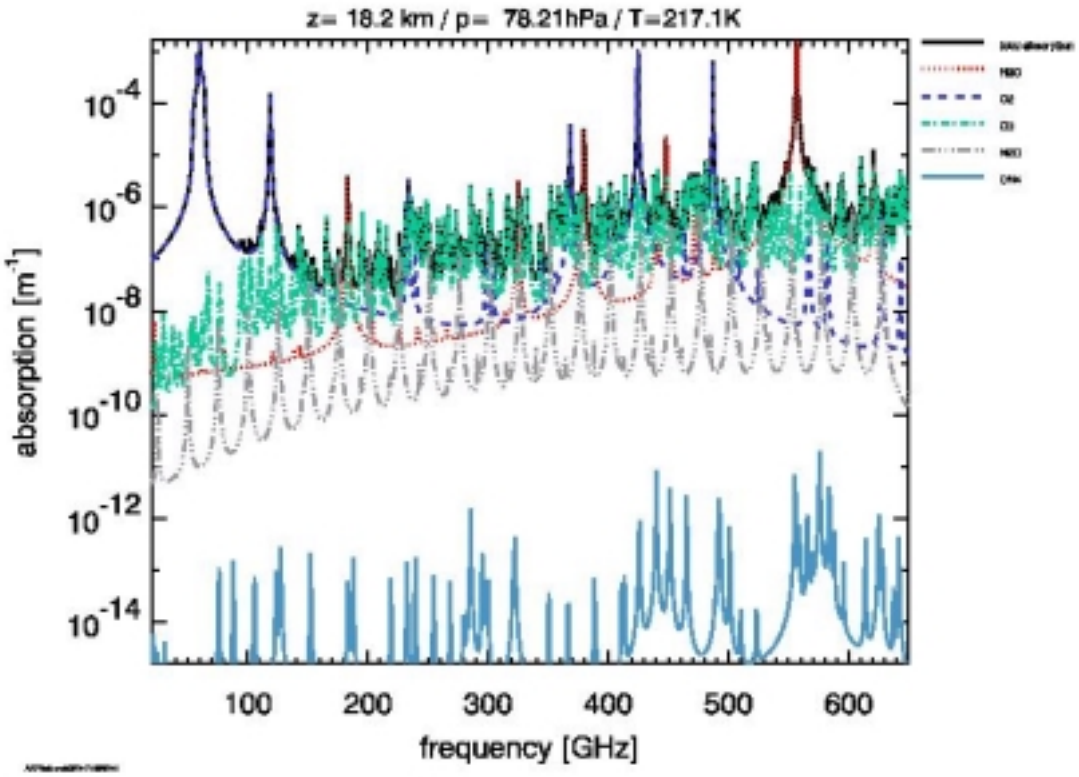

Figure 30: Absorption spectra in the microwave spectral region for limb viewing mode (Source: *Axel von Engeln, IUP/IFE, Bremen*).

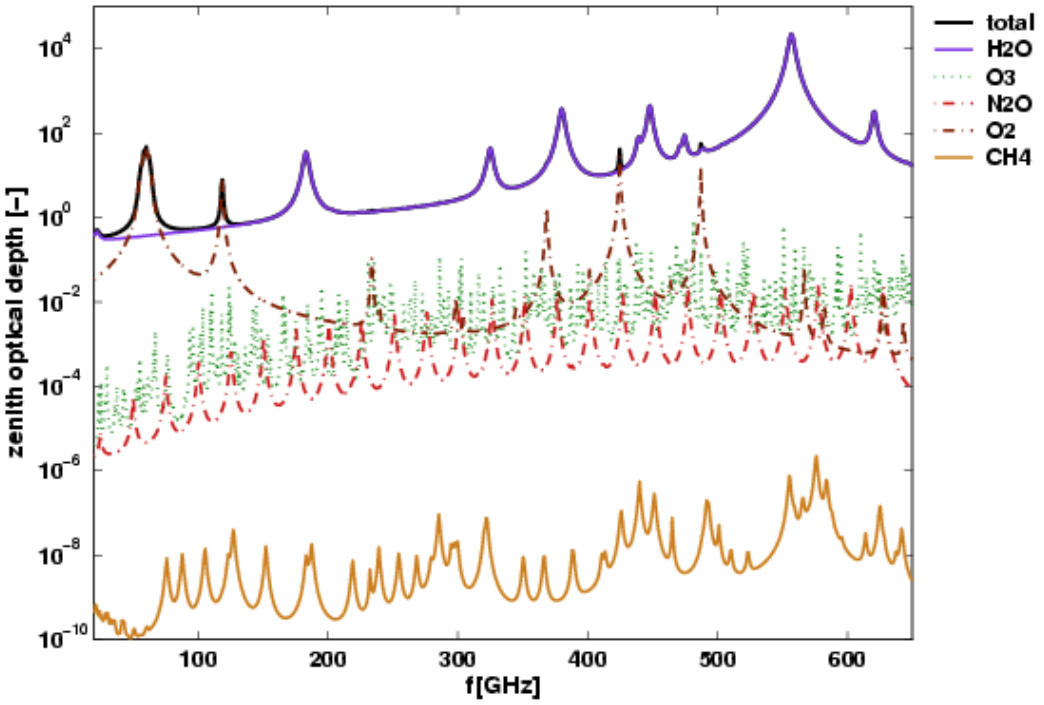

Figure 31: Zenith optical depth in the microwave spectral region appropriate for the nadir viewing mode (Source: *Carmen Verdes, IUP/IFE, Bremen*).

Both, the strong and evident absorption features of O_3 can be clearly seen in Figure 30 (dashed dotted green line), showing calculated atmospheric absorption coefficients for the considered gases plus the corresponding total absorption, as an example simulated for typical atmosperic conditions at 18.2 km altitude. However, the determination of O_3 from nadir observations is very difficult due to the small thermal contrast of the atmosphere relative to the ground. The relatively weak CH_4 features can be seen at the bottom of Figure 30. Figure 31 shows the zenith optical depth for various gases appropriate for the nadir mode. As can be seen the total optical depth is almost entirely determined by water vapour and oxygen absorption lines. Therefore, as also described in *Grody, 1993*, only water vapour and temperature (via oxygen) can be derived from nadir microwave spectra. Global 3D-field operational products from passive microwave sounders can only be achieved for temperature retrievals using oxygen absorption mainly around 60 GHz and 118 GHz.

Radiative transfer and retrieval aspects

When satellite observations are made at a number of frequencies along the edges of an absorption line, a set of weighting functions occur, with peaks at various altitudes. The observations may then be analyzed together to retrieve the temperature profile from the brightness temperatures. The ability to resolve temperature variations along the line of sight (in the vertical or slant path) depends on the width of the weighting functions, with broader weighting functions providing less vertical resolution. For monochromatic radiation, the width is dictated by the pressure structure of the atmosphere along with the physics of radiative transfer. When a satellite channel averages radiation over some finite band of frequencies, the weighting functions are broadened further if the optical properties of the atmosphere vary across the band, as they tend to do near absorption lines.
For temperature sounding, it is preferable to use frequencies where the absorption is dominated by a gas that has a fixed, well-known concentration. If the gas is highly variable, such as with water vapor, the temperature weighting functions vary with the gas concentration and it is difficult to associate a temperature signal with a specific level of the atmosphere. In the microwave spectrum, only molecular oxygen provides suitable absorption lines for temperature sounding. There is a complex of lines in the range of 50 to 70 GHz and a single line at 118.75 GHz. Many nadir viewing temperature sounders rely on the spectrum near 60 GHz because 1) the line complex provides spectral bands where the optical properties vary little over a significant range of frequencies, helping to narrow weighting functions, 2) contamination from cloud and rain water (liquid and ice) is less at lower frequencies, and 3) receiver technology allows for lower instrument noise at 60 GHz than at 118 GHz *[NPOESS-CMIS-ATBD].*

Prior to the development of microwave sounders, temperature soundings were derived using infrared measurements in the 15μm carbon dioxide band and were limited to clear areas *[Grody, 1993]*. In contrast, microwave observations between 50-60 GHz are ideal for monitoring temperature because atmospheric temperature and microwave radiance is highly linear and they are not affected by precipitation free clouds due to the large frequency separation between the water vapor line and the oxygen complex. Areas of precipitation can be easily detected using lower frequency window channels. Microwave absorption by liquid water clouds increases monotonically with frequency. Frequencies below 20 GHz enable observations of

surface parameters through clouds and in the 20 to 40 GHz region the extraction of liquid water content.
Unlike infrared measurements the weighting function does not vary significantly for different atmospheric temperature profiles. Absorption by clouds cuts off the infrared weighting function below the cloud tops. In contrast, microwave measurements enable to retrieve the true temperature patterns of clouds *[Grody, 1993; Goldberg, 2002].*

Using AIRS simulated data, *Goldberg et al., 2003,* found 4.5% of the fields of view over ocean with less than 0.6% cloud contamination. Since the European Centre for Medium Range Weather Forecasting (ECMWF) and the National Centers for Environment Prediction (NCEP) currently use only “clear” data from IR sounders for assimilation into forecast analysis fields, the small fraction of “clear” data from IR sounders has had little impact on the forecast *[Aumann et al., 2003].*
As an example, Figure 32 shows weighting functions of the Advanced Microwave Sounding Unit (AMSU) for each of its 15 channels. The height range of operational temperature profile products is 0-45 km. At the very low pressures above about 50 km Zeemann splitting of the oxygen lines due to the Earth’s magnetic field is noticeable, which would make polarisation measurement necessary in order to accurately sound the atmosphere *[Grody, 1993]*.

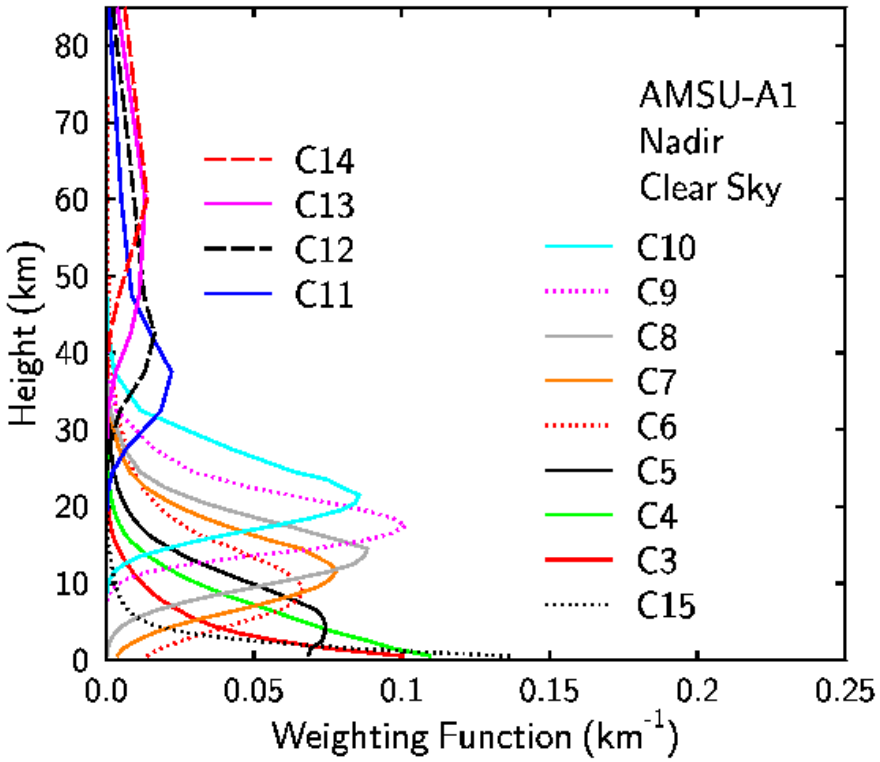

Figure 32: Weighting functions of the 15 AMSU channels (change of measured brightness temperature for small changes of atmospheric layer temperature) *[Cira’s AMSU Website]*.

Compared to imagers like the Special Sensor Microwave / Imager (SSM/I), temperature sounders are designed with poorer spatial resolution, as the horizontal variability of atmospheric temperature for large-scale events is smaller than it is for surfaces. In order to obtain wide swath widths resulting in greater areal coverage, sounders like AMSU scan cross-track rather than conical *[Grody, 1993]*. However,

there are new sensors for temperature profile sounding like SSMIS and CMIS which are conical scanning instruments (see Sections 9.4.3 and 9.4.5, respectively).

9.2 Error Sources

The microwave emissivity is strongly frequency and surface dependent. Due to the residual emissivity uncertainty microwave sounders alone cannot provide the accuracy required for NWP.

For temperature sounding, the vertical resolution achievable in the troposphere from the microwave region is low compared to that achievable in the 4.3μm CO_2 band.
The Field-Of-Views are larger compared to IR *[Aumann, 2003]*.

With coarser spectral resolution, the measurements average over weighting functions spanning a broader range of pressure levels, degrading the vertical resolution of temperature profiling. Microwave temperature sounding frequencies do not provide sufficient vertical resolution to resolve sharp vertical gradients that occur in the atmosphere. Vertical gradients near the surface are often very sharp and of high amplitude, because of the strong energy fluxes that occur at the surface. Temperature retrieval errors tend to increase, therefore, near the surface wherever such gradients are present. This effect is diminished over ocean and other water surfaces, because the surface energy fluxes are buffered by the large heat capacity of water and the transfer of energy between the surface and subsurface water *[NPOESS-CMIS-ATBD].*

Precipitating clouds are another significant error source in the microwave. However, areas of precipitation are easily detectable using lower frequency window channels *[Goldberg, 2002].*

Conversion of antenna temperatures to brighness temperature removes the contribution from the instrument and space. Insufficient knowledge about the instrument's antenna pattern introduces biases, which (for cross-tracking instruments) depend on FOV position.

Limb adjustment removes the effect of angle and scan-line asymmetry and the need to bias adjust measurtements as a function of angle. For AMSU-A, limb adjustment errors are generally within instrumental noise *[Goldberg, 1999].*
Large temperature errors generally occur at pressure levels where weighting functions are inadequate and strong correlation is lacking between level temperatures and the weighted temperatures sensed by the instrument *[Grody, 1993].*

Uncertainties, e.g., in the AIRS/AMSU/HSB observations originate from several sources. Radiance errors arise from noise processes within the instruments themselves and from imperfect calibration, but particularly from cloud contamination or residuals from the cloud-clearing process.

The errors in retrieved products have several sources. Uncertainties in the radiances used in the retrieval are one source of retrieval errors. Another error source is limitations of the forward model used in the retrieval software. (Some systematic

biases that may be discovered during forward model validation could be explained by errors in the calibration process. Other errors due to poorly understood spectroscopy or flaws in the initial forward model are being corrected by updating the forward model itself). Incomplete truth data, such as limited observations of skin temperature and emissivity, or limited temperature soundings above 50 hPa (a typical upper altitude for weather balloons), are another source of uncertainty. Yet another error source is related to the resolution of the satellite observing system. This null-space error *[Rodgers, 1976]* represents underresolved structure in the observed atmosphere. Consider, for example, a layer of water vapor hundreds of meters deep. While physically realistic, this layer is too thin to be resolved by the broad weighting functions of the AIRS/AMSU/HSB instruments. This inability to resolve fine-scale structure must be reflected in the error estimates of retrieved products. Similar to null-space error is computational noise: uncertainties introduced by modeling a continuous system with discrete numerical elements. An important source of uncertainty in the AIRS products is the errors in the data used to validate those products. The AIRS/AMSU/HSB instrument suite is designed to provide a tro-pospheric retrieval uncertainty of 1.0 K over a 1-km layer for temperature, and 10% over 2-km layers for water vapor. These approach or surpass the combined errors of many *in situ* mea-surements.

AIRS must make use of more conventional measurements, such as standard radiosondes, to obtain a large enough number of comparisons for statistical significance. The error characteristics of all these validation datasets must be known.

All error processes occur in the presence of the large, natural variability of the geophysical system being observed. Natural variability can introduce apparent error in many ways, especially through nonsimultaneous or spatially disjoint observa-tions by the instruments being compared. Some of the effects of natural variability are only subtly distinct from null-space errors. Separating natural variability due to noncoincident sampling—“mismatch error”—from the other error processes described above is one of the great challenges of validating satellite datasets *[Fetzer et al., 2003]*

9.3 Error parameters

In the literature used for the following sections covering microwave sounder measurement uncertainties, various error parametrisations have been used. RMS accuracies have been given where no separation between mean biases and random errors have been reported for both, model and validation studies. For these cases values have been interpreted as precisions according to the definitions used for this study, although it has been not clear if mean biases have been included or not.

Precision have sometimes be estimated using analytical methods or statistics of comparisons with independent measurements. For the latter case it was sometimes not mentioned how/if the error contributions of the reference instruments have been taken into account. Additionally they might contain also remaining contributions from the atmospheric variability depending on the comparison method. If accuracies are mentioned in the overview tables , these are mean biases.

A unique translation of the given error parameters to accuracy and precision has not been possible for most of the cases considered.

9.4 Instruments overview

9.4.1 MSU/AMSU-A / NOAA/EOS-Aqua

The Advanced Microwave Sounding Unit A (AMSU-A) *[Diak et al., 1992]* has been flown on NOAA-15 (May 1998), NOAA-16 (Sept. 2000), and NOAA-17 (June 2002) satellites. The most advanced instrument is stationed on the EOS-Aqua satellite (May 2002). It is also scheduled for operation on the Metop satellite (2005).

AMSU-A is a 15-channel microwave radiometer operating between 23 and 89 GHz and is the successor of the MSU, which had only four channels between 50 and 58 GHz, no clean window channels (transmission loss due to oxygen absorption in the most transparent channel, 50.3 GHz, is around 30%) and no channels at frequencies above 58 GHz *[English, 2002]*. AMSU-A is actually one of two separate radiometers with different frequency complements, the AMSU-A and the Microwave Humidity Sounder (MHS), formerly named AMSU-B *[Diak et al., 1992; Goldberg, 2002]*.

The vertical resolution of the temperature information retrieved from AMSU-A is poor, with only two to three pieces of independent information on temperature in the troposphere. This has not prevented the data being very important for the analysis of large scale flow in NWP models, and having a large impact on the accuracy of NWP forecasts. Those centres using the AMSU radiances have all reported substantial improvements in forecast accuracy compared with use of the older MSU instrument *[English, 2002]*.

9.4.2 SSM/T / DMSP

The SSM/T, first launched in 1978 on a DMSP Block 5D platform, is a seven channel microwave sounder that measures atmospheric emission in the 50 to 60 GHz oxygen band. It has been designed to provide temperature soundings over previously inaccessible regions and at higher altitudes than those attainable with IR sounders. As a cross-track nadir scanning radiometer operating at the nominal 833 km altitude, the subtrack spatial resolution is an approximate circle of 174 km diameter at nadir. There are seven total cross-track scan positions separated by 12 degrees with a maximum cross-track scan angle of 36 degrees. At the far end of each scan, resolution degrades to an ellipse of 213 x 304 km size. The SSM/T data swath is about 1500 km; therefore, there is a data coverage gap between successive orbits over much of the earth *[DMSP Homepage]*.

9.4.3 SSMIS / DMSP

As part of the Defense Meteorological Satellite Program (DMSP) the first of five Special Sensor Microwave Imager/Sounder (SSMIS) successfully launched on 18 October 2003. It is a passive microwave sensor that combines and extends the current imaging and sounding capabilities of three separate DMSP microwave sensors, SSM/T, SSM/T-2 and SSM/I *[NOAA SSMI Website]*. SSMIS will provide the first sounding measurements made with conical-scanning geometry *[Kunkee et al.,*

2002a]. It measures microwave energy from the Earth's surface and atmosphere at 24 discrete frequencies from 19 to 183 GHz. The sensor generates a conical scan pattern at 45 degrees from nadir. This scan pattern, combined with the 144-degree clear field of regard, result in a constant angle of incidence on the Earth of 53.1 degrees and a swath width of 1,707 kilometers *[Aerojet Website]*.

9.4.4 MLS / UARS

The Microwave Limb Sounder (MLS) is one of ten instruments on the Upper Atmosphere Research Satellite (UARS), which was launched from the space shuttle Discovery on 12 September 1991. Observing the Earth's atmosphere in the limb, it measures stratospheric profiles of ozone, water vapor and chlorine monoxide, for which it was designed for. In addition to these data, MLS has produced useful observations of stratospheric and mesospheric temperature, and also additional trace gases *[Livesey et al., 2003]*. MLS measures in the range of the oxygen absorption band around 63GHz, and the water absorption line around 183 and 205GHz.

9.4.5 CMIS / NPOESS

The Conical Microwave Imager/Sounder (CMIS) is a follow-on radiometer of the Special Sensor Microwave/Imager (SSM/I) and the Special Sensor Microwave Imager Sounder (SSMIS) to be launched on-board the National Polar-orbiting Operational Satellite System (NPOESS) in 2009. CMIS utilizes a dual-primary reflector to facilitate measurements across a large frequency range of 6 to 190 GHz. 9 channels centered between 50 GHz to 60 GHz were selected to measure the atmospheric vertical temperature profile below ~20 mb. However, CMIS is also required to measure the temperature profile up to 0.01 mb at reduced spatial resolution. This is primarily achieved by a set of 40 channels within a bandwidth of 20 MHz centered near 60.43476 GHz. The individual channels in this set vary in bandwidth from 1.5 MHz at the edges to 250 kHz at the center of the range *[Kunkee et al., 2002a/b; NPOESS-CMIS-ATBD]*.

9.4.6 ATMS / NPP/NPOESS

The Advanced Technology Microwave Sounder (ATMS) is, besides NPOESS (2009), foreseen as part of the NPOESS Preparatory Project scheduled for launch in 2005. Its primary products are vertical temperature and moisture profiles. ATMS is spectrally similar to AMSU (NOAA-15) with a different scanning geometry providing 96 measurements per scan regardless of frequency with shorter integration times (mean higher noise). However, footprint averaging gives noise similar to AMSU. The nadir footprints are about 32 km in diameter for the temperatur sounding channels *[Goldberg, 2002]*.

9.4.7 EOS-MLS / AURA

EOS-MLS is on the NASA EOS Aura satellite mission launched on July 15, 2004, scheduled for an operational period extending at least until 2009. The Aura orbit is sun-synchronous at 705 km altitude with 98° inclination and 1:45 p.m. ascending equator-crossing time. MLS performs observations with the instrument fields-of-view scanning the limb in the orbit plane to provide 82° N to 82° S latitude coverage on each orbit.

EOS-MLS is a greatly enhanced version of the Upper Atmosphere Research Satellite (UARS) MLS experiment. It is designed for upper tropospheric and lower stratospheric measurements. EOS-MLS provides measurements of several stratospheric chemical species (O_3, H_2O, OH, HO_2, CO, HCN, N_2O, HNO_3, HCl, HOCl, ClO, BrO, volcanically-injected SO_2), temperature and geopotential height. It covers single emission lines at 118 GHz (O_2), 183 GHz (H_2O), 626 GHz (HCl), and 2.5 THz (OH) using 25 spectral channels each with various bandwidth from 6-96 MHz *[EOS-MLS-ATBD].*

MLS nominal operations have 240 limb scans per orbit corresponding to 165 km along-track separation between adjacent limb scans *[EOS-MLS-ATBD].* The horizontal resolution for EOS-MLS data products is 500 km as given on the Aura website (http://aura.gsfc.nasa.gov/instruments/mls/datapro.html).

9.4.8 MASTER/SOPRANO/SMILES

MASTER (Millimetre-wave Acquisitions for Stratosphere-Troposphere Exchange Research) aims at provide valuable data for stratosphere / troposphere exchange research, and also data for research in the areas of radiative forcing, climate feedback, lower stratospheric chemistry, and upper tropospheric chemistry. MASTER has not yet entered phase A. MASTER is proposed to measure in five Bands, namely Bands A, B, C, D and E, respectively: 200.5–209.0, 294.0–305.5, 316.5–325.5, 342.25–348.75 and 497.0–506.0 GHz in limb geometry. It is anticipated that assimilation of high-quality H_2O and O_3 UTLS measurements by forecast models could have potential benefits for numerical weather prediction *[Reburn et al., 1999].*

The main purpose of SOPRANO (Sub-Millimetre Observation of Processes in the Atmosphere noteworthy for Ozone) is to collect data which is needed for stratospheric ozone chemistry research. It measures also in limb, but in six Bands, which are Band A (497.0 - 506.0 GHz), B1 (624.5 - 628.7 GHz), B2 (624.5-628.7 GHz), C2 (648.0-652.0 GHz), F (952.0-955.0 GHz), and G2 (688.5-692.0 GHz) *[Verdes et al., 2000].* SOPRANO has not yet entered phase A.

SMILES (Superconducting Sub-Millimeter Wave Limb Emission) is a heterodyne sub-millimeter receiver which will operate from *The Japanese Experimental Module* (JEM) of *The International Space Station*. In this experiment, it is proposed to use superconductor-insulator-superconductor mixers to achieve ultra-high sensitivity. A system noise temperature of less than 500 K, compared to 4000 K of usual receivers, will be achieved *[Bühler et al., 2004]*.

Characteristics	MASTER	SOPRANO	SMILES
Frequency range, GHz	498.5–505.5	498.5–505.5	624.3–625.5
Platform altitude, km	800	800	400
Antenna size, m	2.2	1	0.4
System noise temperature, K	4743	4743	500

Table 21: Main Characteristics with respect to temperature retrievals of the three proposed limb sounding instruments: MASTER, SOPRANO, SMILES *[Verdes et al., 2002]*.

9.5 Passive systems / microwave spectral region: N_2O

9.5.1.1 EOS- MLS / AURA

Theoretical precision estimates for N_2O profile products as expected from EOS-MLS have been derived using the optimal estimation error analysis method *[Rodgers, 1976].* For a vertical resolution of 3km the precision at 15km is about 50ppbv, about 20ppbv at 25km, and about 40ppbv at 40km (see Table 8-2 of the *EOS-MLS-ATBD, part 1, Waters, 1999).* This can be translated into 20-50ppbv for LS. For EOS-MLS N_2O, the Aura website (http://aura.gsfc.nasa.gov/instruments/mls/datapro.html) gives 10-20% absolute accuracy (accuracy) and 20-50ppbv relative accuracy (precision) for 3km layers in the height range 10-60km. Values refer to daily global coverage.

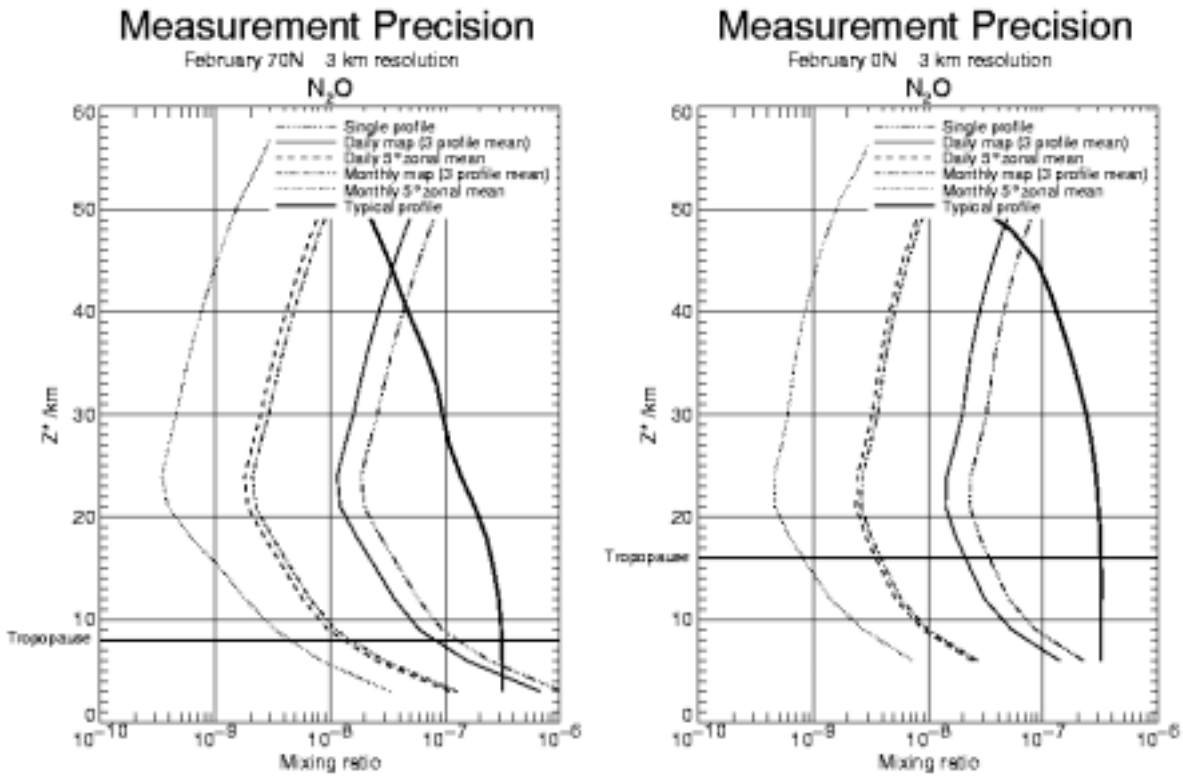

Figure 33: Theoretical precision estimates for EOS-MLS N_2O as given in the *EOS-MLS-ATBD*.

9.5.1.2 MASTER/SOPRANO

For MASTER, useful single-scan precision is obtained on N_2O in different height regions within the stratosphere *[Reburn et al., 1999]*.

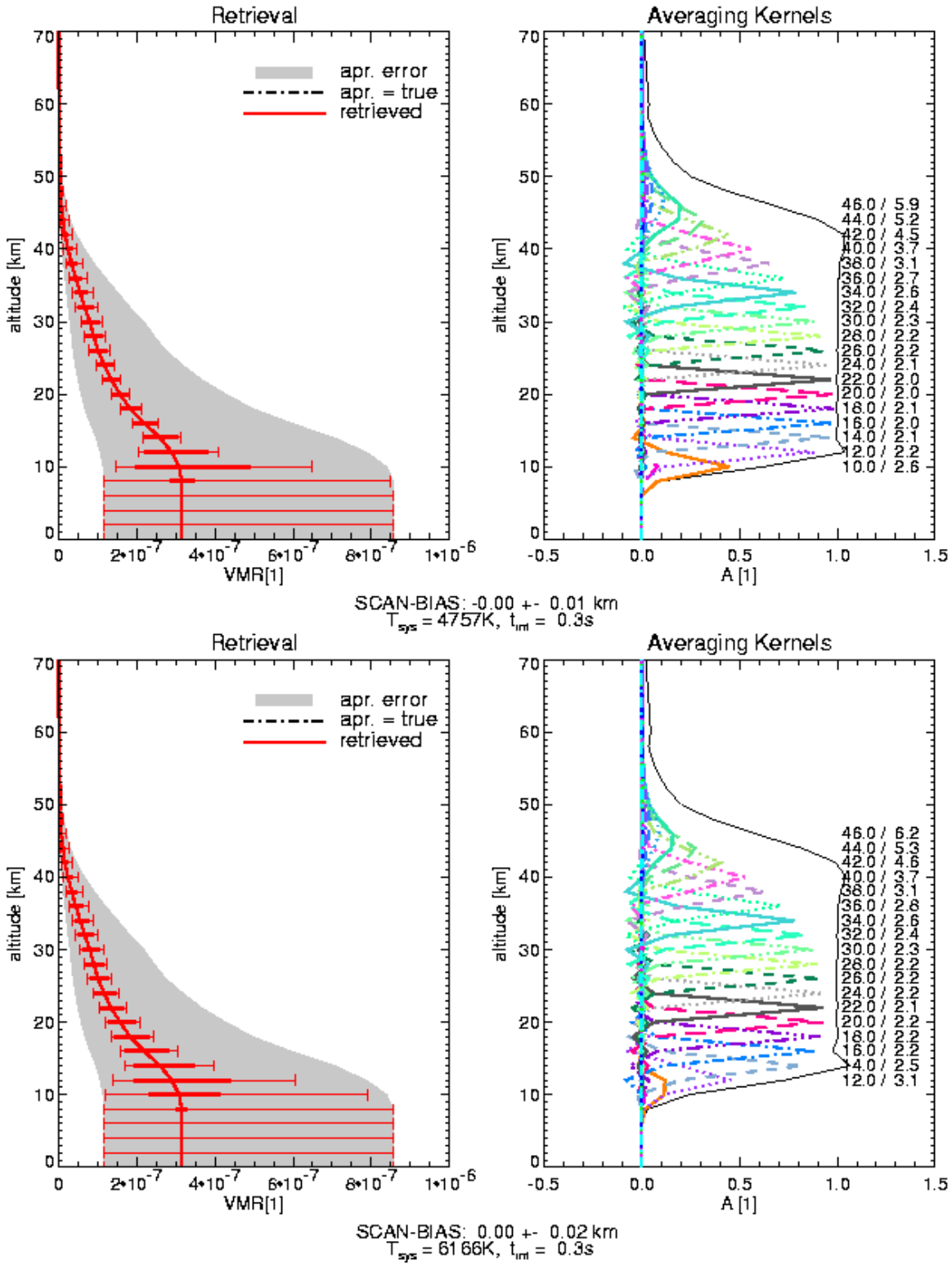

Figure 34: Single scan retrieval errors and corresponding averaging kernels for SOPRANO-A N_2O (top) and SOPRANO-C2 N_2O (bottom). Thin error bars: Total error. Thick error bars: Error due to statistical noise. Shaded area: A priori error *[Verdes et al., 2000].*

9.6 Passive systems / microwave spectral region: Ozone

9.6.1.1 MLS / UARS

Table 6. Estimated Vertical Resolution, Precision, and Accuracy of v5 O3_205

Pressure, hPa	Vertical Resolution,[a] km	Estimated Precision ppmv	Estimated Precision %	Precision Ratio[b]	Estimated Accuracy[c]
0.22	6	0.4	35	0.6	6%
0.32	8	0.35	25	0.6	6%
0.46	5	0.35	20	0.6	6%
0.68	4	0.3	12	0.6	6%
1.0	5	0.3	10	0.6	6%
1.5	5	0.3	7	0.7	6%
2.2	4	0.3	5	0.7	6%
3.2	4	0.3	4	0.8	6%
4.6	4	0.3	4	0.8	6%
6.8	4	0.3	4	0.8	6%
10	3.5	0.3	4	0.8	6%
15	3.5	0.3	4	0.9	6%
22	3.5	0.3	5	0.9	6%
32	3.5	0.3	8	0.9	6%
46	3.5	0.25	10	0.7	6%
68	4	0.25	20	0.6	max. of 0.25 ppmv or 15%
100	4	0.4	>50	0.7	max. of 0.1 ppmv or 15%

[a]As defined in section 6.2.
[b]Data file uncertainties should be multiplied by these numbers to obtain a better value for the "1σ" single profile precision (see text).
[c]Accuracies quoted here represent roughly a 95% confidence level ("2σ" values).

Table 22: UARS/MLS ozone uncertainty parameters *[Livesey, 2003].*

9.6.1.2 EOS- MLS / AURA

Theoretical precision estimates for ozone profile products as expected from EOS-MLS have been derived using the optimal estimation error analysis method *[Rodgers, 1976].* For a vertical resolution of 3km the precision at 3km above the tropopause is about 10%, 2% at 30km, and 10% at 50km (see Table 8-2 of the *EOS-MLS-ATBD, part 1, Waters, 1999).* This can be translated into 2-10% for LS.

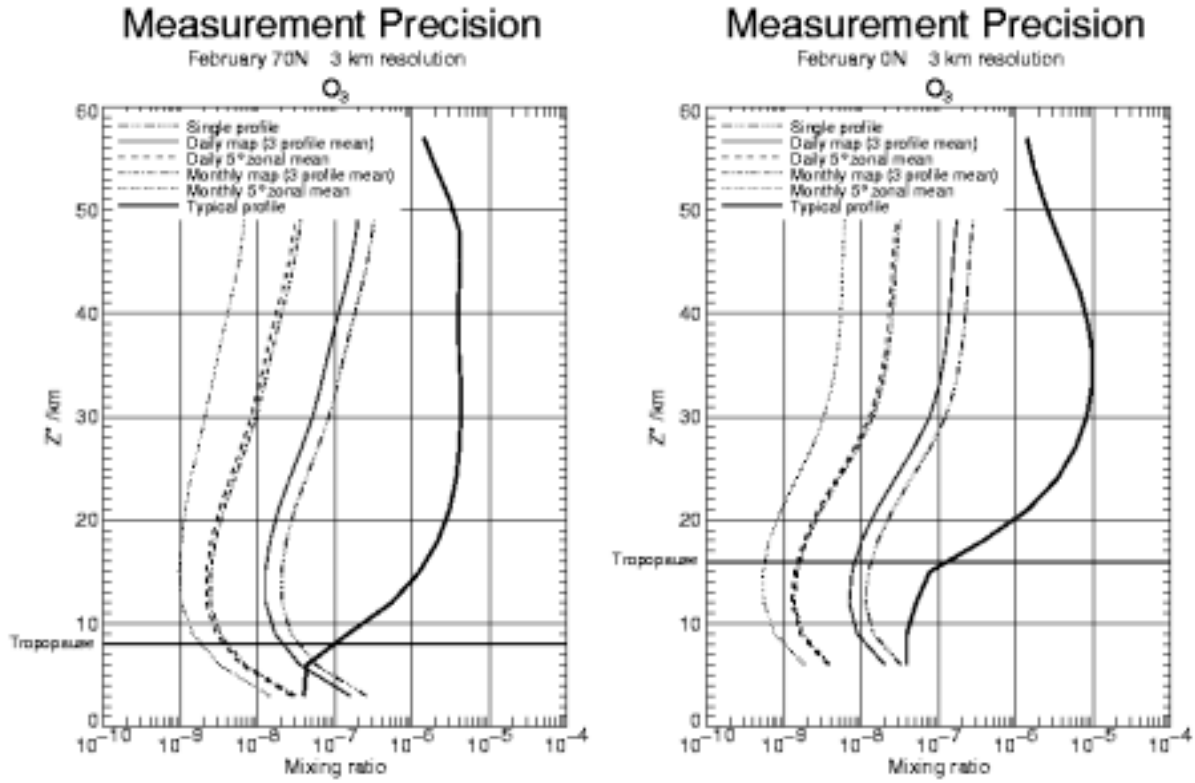

Figure 35: Theoretical precision estimates for EOS-MLS ozone as given in the *EOS-MLS-ATBD.*

9.6.1.3 MASTER/SOPRANO

For MASTER, precision <10% from an individual limb-scan are attainable on O_3 at 2 km resolution in the upper troposphere region from Band. The quality of lower stratospheric O_3 retrievals was demonstrated to be impressively high for Band E: <15% precision at 1km resolution between 18 and 26 km *[Reburn et al., 1999]*. It can be seen that precisions reach from 8% at 15km to up to 100% at 5km, which refers to the HT region. LS precision is between 5% and 9%.

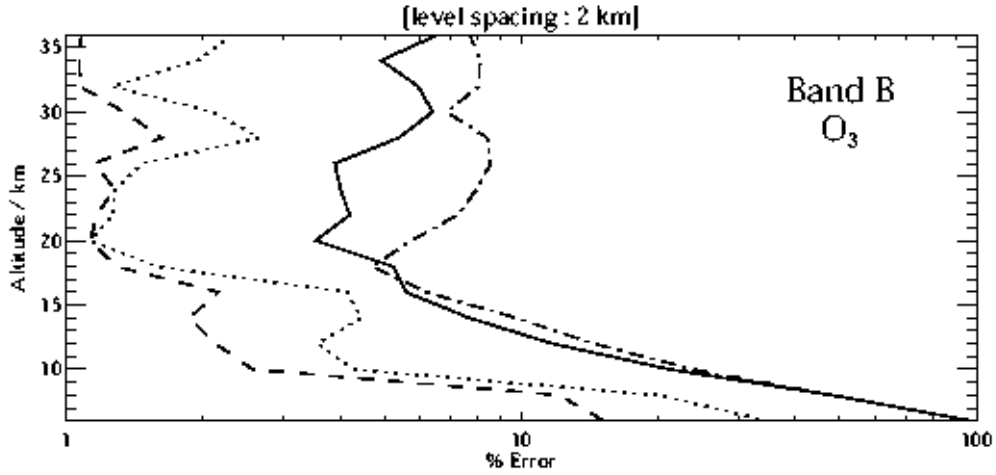

Figure 36: Root-sum-square of random and systematic error budgets for O3 retrieved from MASTER Band B simulations including 2 assumptions for pointing (solid and dashed-dotted) and antenna errors (dashed and dotted) *[Reburn et al., 1999]*.

Estimated precisions of ozone retrievals using simulated SOPRANO measurements have been derived by *Verdes et al., 2000*. The figure shows the ratio of the retrieval precision to the a priori error, which for the case of trace gas retrieval was always taken to be 100%, so this “error ratio” corresponds directly to the retrieval precision.

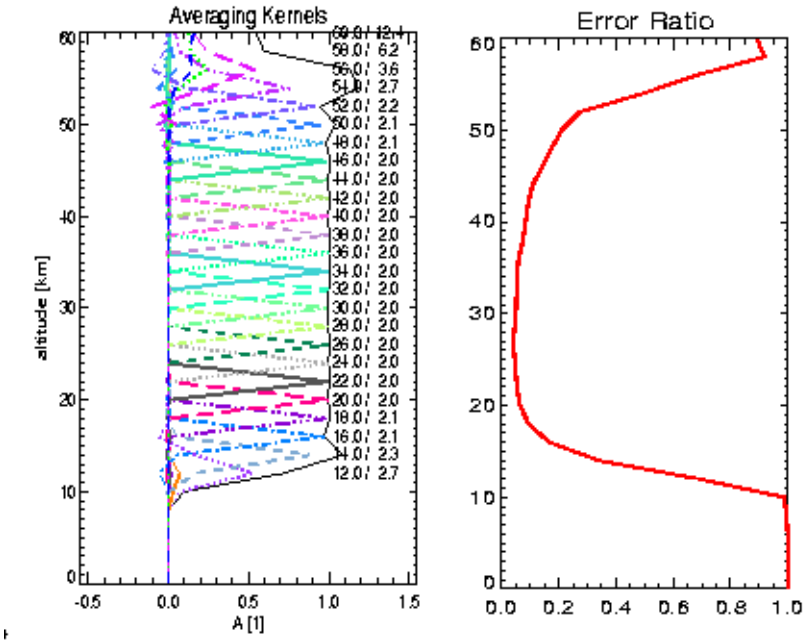

Figure 37: General O_3 retrieval performance of SOPRANO, Band A. Left: averaging kernels, right: error ratio, the ratio of the retrieval precision to the a priori error (100%) *[Verdes et al., 2000]*.

9.7 Passive systems / microwave spectral region: Pressure

9.7.1 Existing systems

9.7.1.1 MLS / AURA

Geopotential height is an operational data product of EOS-MLS *[EOS-MLS-ATBD*]. In addition to microwave radiances, the MLS instrument's knowledge of the altitude of the limb tangent point can be considered as a measurement. Given knowledge of the tangent point pressures, the atmospheric temperature profile as a function of pressure, and the altitude h_0 of a fixed pressure surface p_0, a hydrostatic integration will serve as a forward model for such measurements *[EOS-MLS-ATBD].*

The EOS Level 3 data product "Daily map of geopotential height" has an expected precision < 30 m in the height range 5-30 km (~500-10 hPa) for 3 km vertical resolution *[EOS-MLS Science Objectives]*.

For a standard profile a 100 m increase in altitude corresponds to a 1.2% pressure decrease, i.e., 30 m correspond to a 0.36% pressure change. This conversion factors is used in Table 23 to compare the MLS precisions with the observational requirements of this study. This table shows that the expected EOS precision is worse than the required precision except in the upper part of the lower stratosphere.

Altitude range	**EOS-MLS precision [m]**	**EOS-MLS precision [hPa]**	**Required precision [hPa]**	**Required height assignment [m]**
LS (15-35 km):				
10 hPa	30	0.036	0.1	10
100 hPa	30	0.36	0.1	10
UT (5-15 km):				
100 hPa	30	0.36	0.2	10
500 hPa	30	1.8	0.2	10

Table 23: EOS-MLS geopotential height theoretical precisions compared to the observational requirements for pressure measurements of this study.

The geopotential height product is derived assuming hydrostatic equilibrium. Figure 38 shows precisions of geopotential height retrievals estimated from simulations of the EOS MLS measurement process using an analytical error analysis based on *Rodgers, 1976*. The simulations use a model of the measurement process, making some approximations of geophysical and instrumental effects *[EOS-MLS-ATBD]*.

Table 8-2 of the *EOS-MLS-ATBD (part 1, Waters, 1999)* gives expected precisions(1σ) for some MLS Level 2 profiles produced every 165 km along the measurement track, assuming a vertical resolution of 3 km, derived from the mentioned model study *[EOS-MLS-ATBD (part 4, Filipiak, 1999)]*. The reported precision is about 15 m for the height range 5-30 km, 30 m at 40 km and 70 m at 50 km.

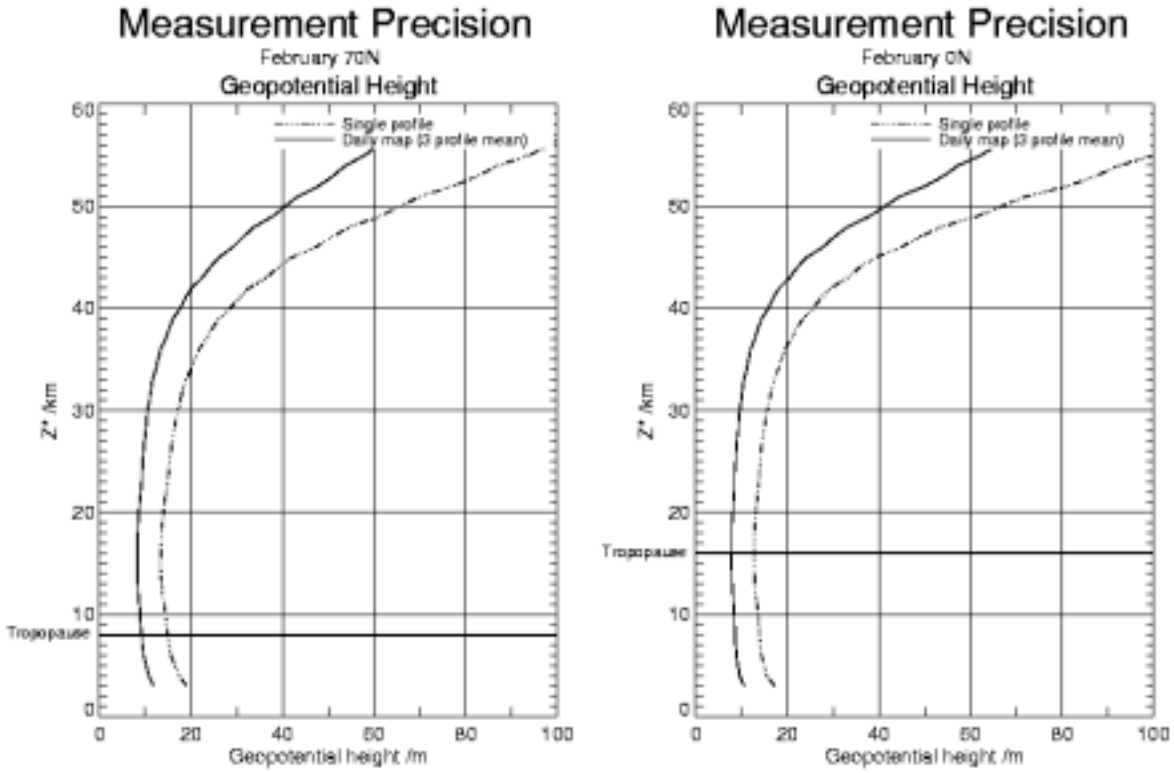

Figure 38: Expected precision of the EOS MLS geopotential height data product *[EOS-MLS-ATBD].*

The estimated EOS-MLS tangent height uncertainties are given in *[EOS-MLS-ATBD].* The 1σ tangent height uncertainties are: absolute tangent height uncertainty = 10 m, tangent height rate uncertainty = 5 ms^{-1}, tangent height jitter = 10 m.

9.8 Passive systems / microwave spectral region: Temperature

Accuracy values given in this section have to be compared with established requirements for global Numerical Weather Prediction (NWP) as described in *[REQ-PT-2004/PM2].*

9.8.1 Existing systems

9.8.1.1 SSM/T / DMSP

The SSM/T contains seven channels, resulting in improved temperature accuracy compared to, e.g. MSU having only four channels. The vertical resolution is about 10 km, the footprint size is175 km diameter in nadir and the accuracy is generally about 2-3 K between 20 and 700 mb pressure levels, as derived from model simulations using radiosonde measurements as input. The computations assumed instrumental noise of 0.3 K and the random effect of a 10% variation in surface emissivity. In detail, from Figure 6.24 on page 295 of *Grody, 1993,* retrieval RMS accuracies are shown to be 2-5 K for LT (1000-500 hPa), 2-3.5 K for HT (500-100 hPa), and 1-3.5 K for LS (100-10 hPa).

9.8.1.2 SSMIS / DMSP

SSMIS as a novel sensor operating since October 2003 on a DMSP Block 5d-3 Platform (F16), also scheduled for launch on F17, has to be illuminated with more care. SSMIS is a conical scanner with a fixed view angle of 53.3°. For the temperature sounding channels, the footprint size is about 38 km *[Goodrum, 2000]* (17.6 km x 27.3 km prior to on-board averaging *[Deblonde and English, 2002]*).

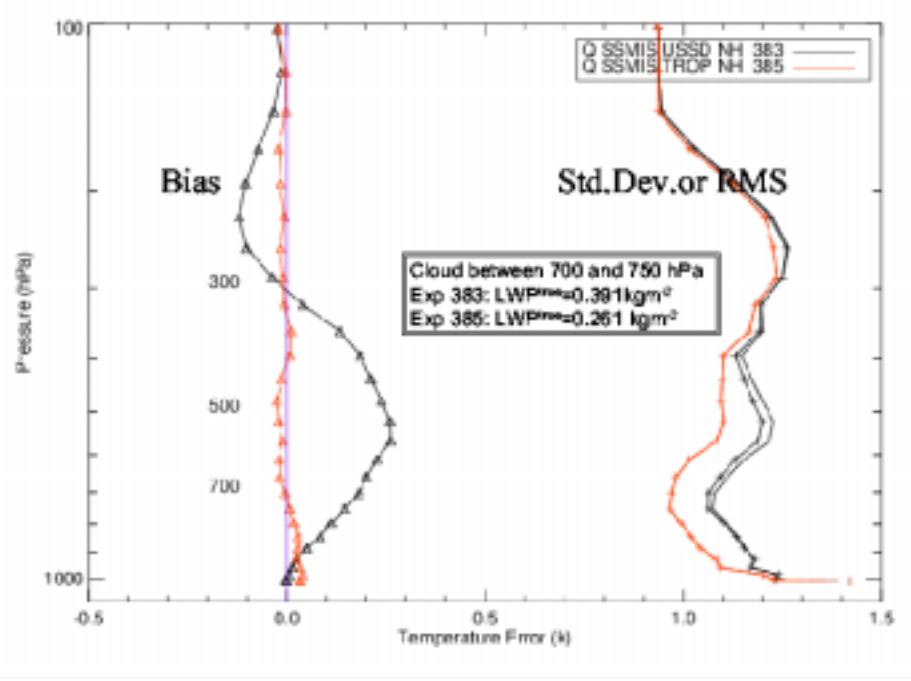

Figure 39: Accuracy estimates for SSMIS temperature profile retrievals from simulated measurements for tropical and US-standard atmospheres *[Deblonde and English, 2002]*.

Deblonde and English, 2002, performed a theoretical error analysis using simulated measurements and a one-dimensional variational assimilation scheme. They estimate a theoretical precison of 0.4 K (most presumably 1σ confidence) including the instrumental, and the representativeness (includes forward modeling errors) error covariance matrices, except for the low frequency window channel (1.5 K). Figure 39 shows the corresponding accuracy (BIAS) of up to 0.3 K for LT and between –0.1 K and 0.3K for HT, estimated for tropical and US-standard atmospheres cloudy scenarios. For the same case RMS precisions between 1K and 1.2K for LT and 0.9K and 1.3K for HT are given. LS has not been assessed. It is assumed that these values refer to the nominal vertical resolution, which can be estimated from the SSMIS-weighting functions to be about 8 to 10 km *[Deblonde and English, 2002]* (see also *[Deblonde and English, 2003]*). These results are below the accuracy goals reported by the manufacturer (RMS accuracies: 4 K (1000 mb), 3 K (850 mb), 1 K (700-10 mb), 5 K (10-.2 mb), 7 K (0.2-.03 mb), 3 K (Tropopause)) *[Aerojet Website]*.

9.8.1.3 AMSU/NOAA

In the error analysis mentioned in the above section 9.8.1.2 also AMSU-A temperature profile uncertainties were investigated *[Deblonde and English, 2002]*. As for SSMIS theoretical precisions on the basis of instrumental and the

representativeness (includes forward modeling errors) error covariance matrices of 0.4 are reported (1.5K for the low frequency window AMSU-A channel 3). Validation of AMSU-A temperature profiles using co-located radiosonde measurements in 1998 resulted in retrieval RMS precisions of about 1-2 K *[Goldberg, 1999]*, which is in good agreement with the theoretical study. For a vertical resolution according to 3 km layers, *Goldberg and Cheng, 2002*, presented an AMSU-A accuracy value of about 1.5 K, which for the nomenclature used here is interpreted as precision.

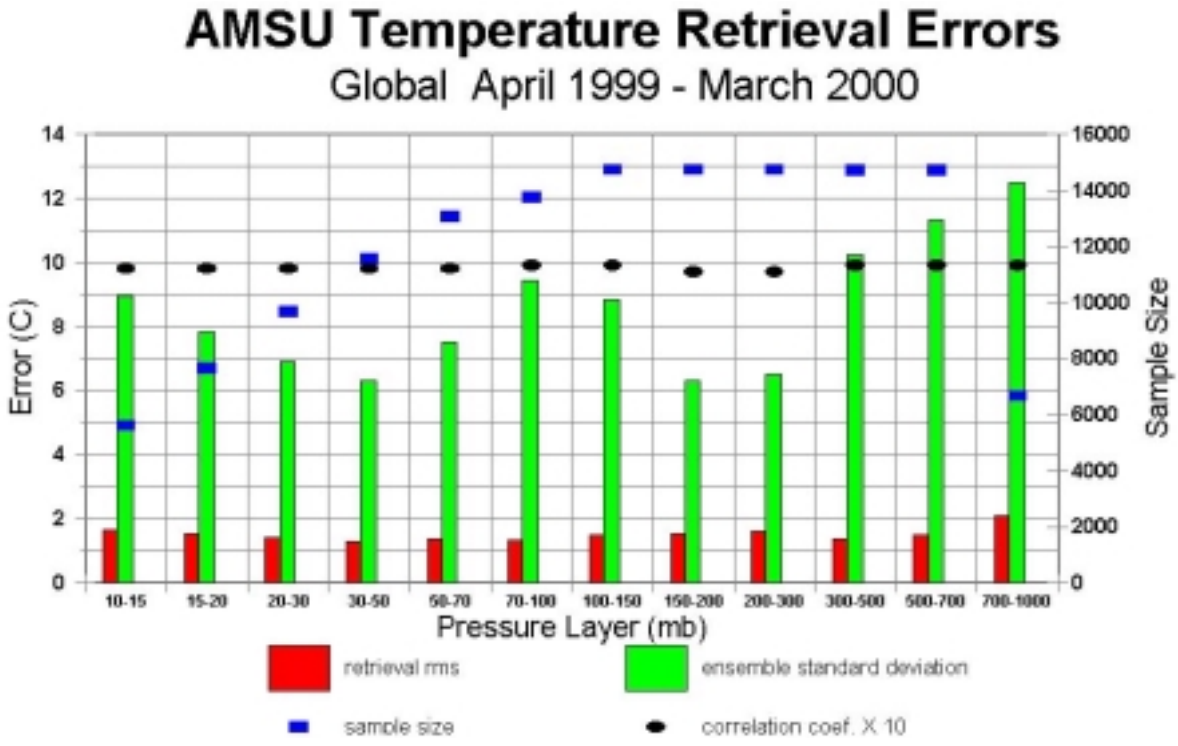

Figure 40: Validation results for AMSU-A temperature profile retrievals as compared to co-located radiosonde measurements *[Goldberg, 1999; Goldberg, 2002]*.

Results of the validation study performed by *Goldberg, 1999*, are shown in Figure 40. Figure 5 of *Goldberg, 1999,* shows bias and standard deviation of differences between AMSU-A temperatures and collocated radiosondes for the period November 1 – December 31, 1999. It is assumed here, that the values given have been interpreted as EOS-MLS accuracies and precision, i.e. either the radiosonde uncertainties are accounted or they are negligible. However, accuracies (mean biases) ranging from –0.1K to 0.3K for LT, -0.5K to 0.3K for HT, and –0.2K to 0.5K for LS. Precisions (standard deviations) are 1.5-2K for LT, 1.5K for HT, and 1.5-2K for LS *[Goldberg, 1999].*

9.8.1.4 MLS / UARS

Livesey et al., 2003, give an overview of the version 5 MLS data products. The data include midstratospheric to lower mesospheric temperature, as well as stratospheric and mesospheric ozone (see Section 9.6.1.1). Table 4 of this paper summarises vertical resolution, precision, and accuracy estimates, the later are interpreted as RMS accuracies with 2σ confidence, which, however, have no relevance with respect to the reference study requirements.

Table 4. Estimated Vertical Resolution, Precision, and Accuracy of v5 Temperature

Pressure, hPa	Vertical Resolution,[a] km	Typical Precision, K	Precision Ratio[b]	Estimated Accuracy,[c] K	v5−NCEP, K
0.46[d]	5	3.3	0.7	5	−1.5
0.68	7	2.1	0.5	5	+5.2
1.0	7	1.8	0.5	5	+8.6
1.5	7	1.7	0.5	5	+6.6
2.2	7	1.5	0.5	4	+4.3
3.2	7	1.5	0.5	4	+1.4
4.6	6	1.4	0.5	5	+0.9
6.8	7	1.4	0.5	4	+0.1
10	7	1.3	0.4	4	+1.1
15	6	1.2	0.4	4	+1.1
22	7	0.8	0.3	4	+1.6
32	7	0.9	0.3	6	+2.0

[a]As defined in section 6.2.

[b]Data file uncertainties should be multiplied by these numbers to obtain a better value for the "1σ" single profile precision (see text).

[c]Accuracies quoted here roughly represent a 95% confidence level ("2σ" values).

[d]The temperature at 0.46 hPa mainly derives from optically thin radiances. These yield information of poorer precision but slightly better resolution than the optically thick radiances that influence the temperature data lower in the atmosphere.

Table 24: UARS/MLS temperature uncertainty parameters *[Livesey, 2003].*

9.8.1.5 EOS-MLS / AURA

Theoretical precision estimates for temperature profile products as expected from EOS-MLS have been derived using the optimal estimation error analysis method *[Rodgers, 1976].* For a vertical resolution of 3km the precision at 5km altitude is about 1K, between 10 and 30km about 0.5K, and at 40km 2K (see Table 8-2 of the *EOS-MLS-ATBD, part 1, Waters, 1999).* This can be translated into 0.5-1K for HT and 0.5-1.5K precision for LS. Estimates on the Aura website (http://aura.gsfc.nasa.gov/instruments/mls/datapro.html) give 1-2K absolute accuracy (accuracy) and 0.5-5K relative accuracy (precision) for the height range 5-60km. Having a vertical resolution of 3km, EOS-MLS would meet the HS requirements, if at least the horizontal sampling would be better (500km).

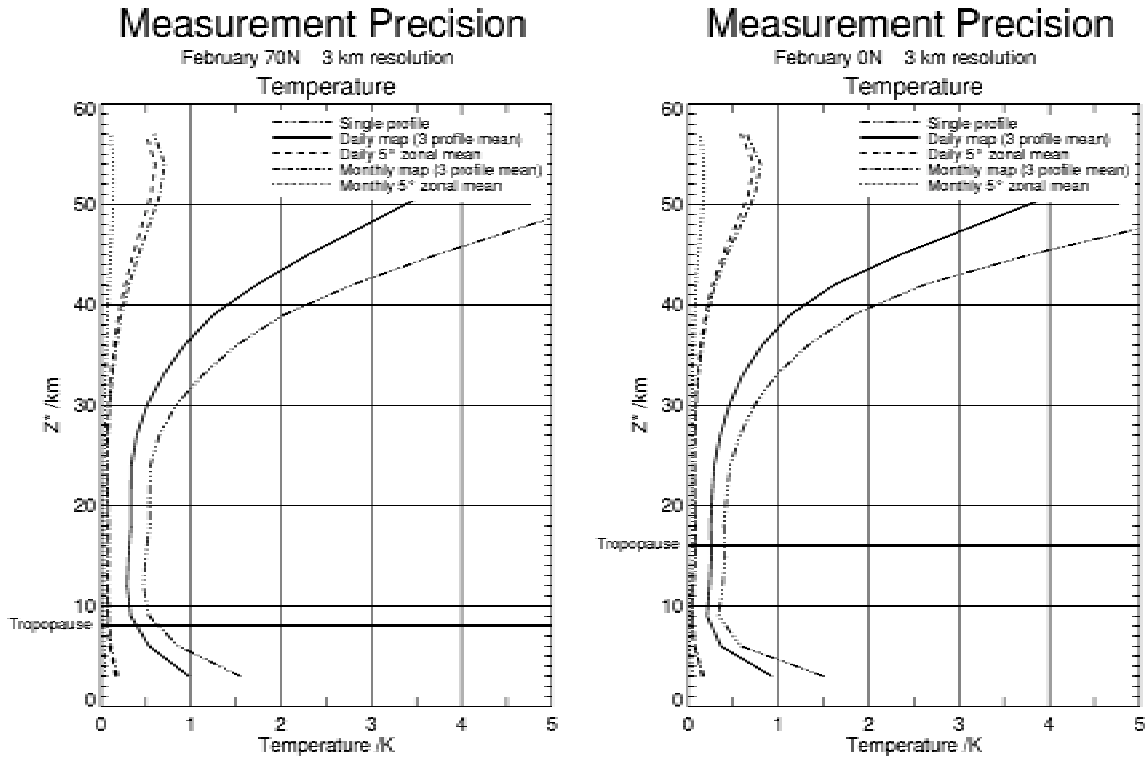

Figure 41: Theoretical precision estimates for EOS-MLS temperature as given in the *EOS-MLS-ATBD.*

9.8.2 Future systems

9.8.2.1 AMSU / METOP

NOAA is providing two copies of the AMSU-A, as flown on NOAA-15 to 17, for flight on the first two Metop spacecraft from 2005 to help ensure data compatibility between the data from the NOAA and EUMETSAT satellites. Temperature profile uncertainties will be therefore similar to the current status (see Section 9.8.1.3).

9.8.2.2 ATMS / NPP/NPOESS

The ATMS draws its heritage directly from AMSU-A/B, but with reduced volume, mass, and power *[Glackin, 2003]*. The footprint size for temperatur sounding is smaller (32 km at nadir instead of about 50 km for AMSU-A). Spectrally the ATMS is similar to AMSU-A *[Goldberg, 2002]* (see Section 9.8.1.3). ATMS shall augment the other NPOESS sensors' capabilities as necessary to meet the Environmental Data Record (EDR) requirements as given in the NPOESS Technical Requirements Document (TRD) *[NPOESS-TRD]*. These are for temperature sounding vertical resolutions of 1 km (surface-300mb), 3 km (300-30mb), and 5 km (30-0.01 mb), and uncertainty treshold values of 2.5 K/km (surface-700 mb), 1.5 K/km (700-300 mb), 1.5K/3km (300-30 mb), 1.5K/5km (30-1 mb), and 3.5K/5km (1-0.01 mb). The reported objective is 0.5K/km for all cells *[NPOESS-TRD].*

9.8.2.3 CMIS / NPOESS

Performance testing for the CMIS temperature profile retrieval has been done using selected test cases, with description of temperature profiles and all other relevant environmental parameters, simulate CMIS brightness temperatures, accounting for sensor design parameters and error characteristics, perform retrievals, and compare retrieved data to the "true" data, which are derived directly from the test case data. The final step involves vertical averaging. A summary of the results is given in Table 25 taken from Table 5-2 of the *[NPOESS-CMIS-ATBD].*

	Performance	Layers
Surface to 700 mb	1.6 K/2.0K (clear/cloudy)	1 km
700 mb to 300 mb	1.4 K	1 km
300 mb to 30 mb	1.3 K	3 km
30 mb to 6 mb	1.5 K	5 km
6 mb to 1 mb	2.4 K	5 km
1 mb to 0.3 mb	3.5 K	5 km
0.3 mb to 0.01 mb	6.5 K	5 km

Table 25: Temperature profile retrieval performance of CMIS *[NPOESS-CMIS-ATBD]*.

Results can be transferred to 1.4-2 K for LT, 1.3-1.4 K for HT, 1.3-1.5 K for LS, and 1.5-2.4 K for HS, in order to be comparable with the requirements tables.

9.8.2.4 MASTER/SOPRANO/SMILES

Temperatur profile retrieval precision estimates have been derived by Verdes et al., 2002, for the three proposed limb instruments MASTER, SOPRANO, and SMILES using simulated measurements. From these results and also from the averaging kernels it is obvious, that, concerning temperature retrievals, non of the instruments meet the performance as required for NWP.

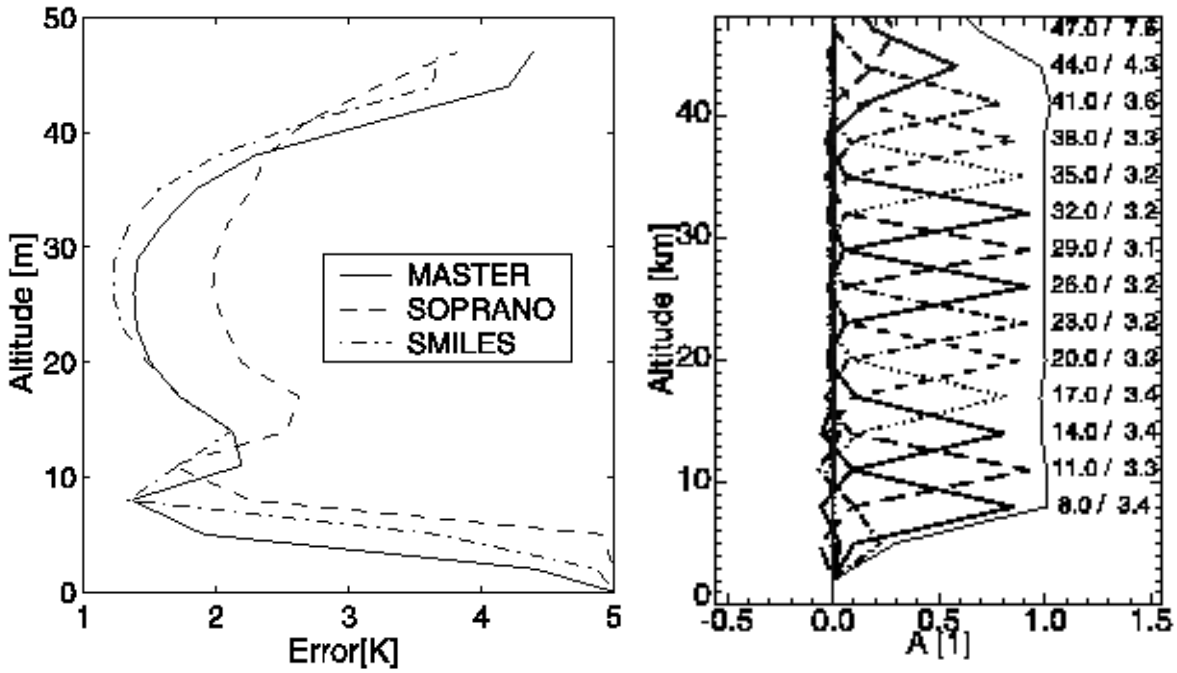

Figure 42: Left: Temperatur profile retrieval precision estimates for the three proposed limb sounding instruments: MASTER, SOPRANO, and SMILES. Simulated measurements at around 500GHz (MASTER, SOPRANO) and 625GHz (SMILES) have been taken, using saturation effects due to ozone absorption as temperature information source. Right: Averaging kernels for the 500GHz temperature retrieval from simulated MASTER measurements *[Verdes et al., 2002]*.

10 Retrievals Using a Combination of Spectral Regions

10.1 Carbon dioxide from combined NIR and TIR measurements

Christi and Stephens, 2004, performed a preliminary theoretical study on the retrieval of CO_2 profiles and columns. They focussed on the retrieval of CO_2 concentration profiles as near the surface as possible. Because thermal infrared (TIR) measurements only have low sensitivity near the surface they investigated the benefit of combining TIR and near-infrared (NIR) measurements. They used high spectral resolution simulated nadir measurements in the NIR around 1.6 µm (6360.1-6389.9 cm^{-1}; resolution 0.025 cm^{-1}; 1193 channels) and moderate resolution simulated measurements from the TIR (500-2500 cm^{-1}; resolution 1 cm^{-1}; 2000 channels) similar as measured by AIRS. They focussed on clear sky soundings but also included scenes with thin clouds.

They discussed typical profile retrieval results obtained using “TIR only”, “NIR only”, and “TIR/NIR combined” measurements (see Figure 43). For TIR only they found that the retrieved profile matches the real profile down to about 2 km, but diverges below that level to the surface as the TIR measurements have difficulty distinguishing between thermal emission from the surface and that of the lower atmosphere and as a result are insensitive to CO_2 in this region. In contrast the profile retrieved from NIR only measurements matches the true profile tightly in the region from the surface to 2 km with “some loosening in the region 2-12 km.” The combined retrieval produces a profile that is better than the “NIR only” profile at mid levels due to the contribution of the TIR measurements and is also closer to the true profile at the surface than the “TIR only” measurements due to the contribution from the NIR.

They also assessed the impact on the retrieved CO_2 column (see Table 26). They found that all errors in column averaged CO_2 were 1 ppmv or less for all cases considered. Retrievals from the NIR alone slightly outperformed those using measurements from the TIR alone provided that atmospheric scatterers were properly constrained. They found that the NIR and TIR measurements complement one another in retrieving column CO_2 and potentially provide better retrievals than using either set of measurements alone.

With respect to CO_2 surface values the preliminary retrieved CO_2 profiles show the NIR measurements “are the clear winner” due to the fact that the NIR obtains its CO_2 information from the lower troposphere as opposed to the TIR measurements which obtains its CO_2 information from the mid and upper troposphere.

They state that measurements in addition to the NIR measurements (such as provided by the O_2 A-band or by lidar) would be required to assist in constraining unwanted scattering although they have not investigated this.

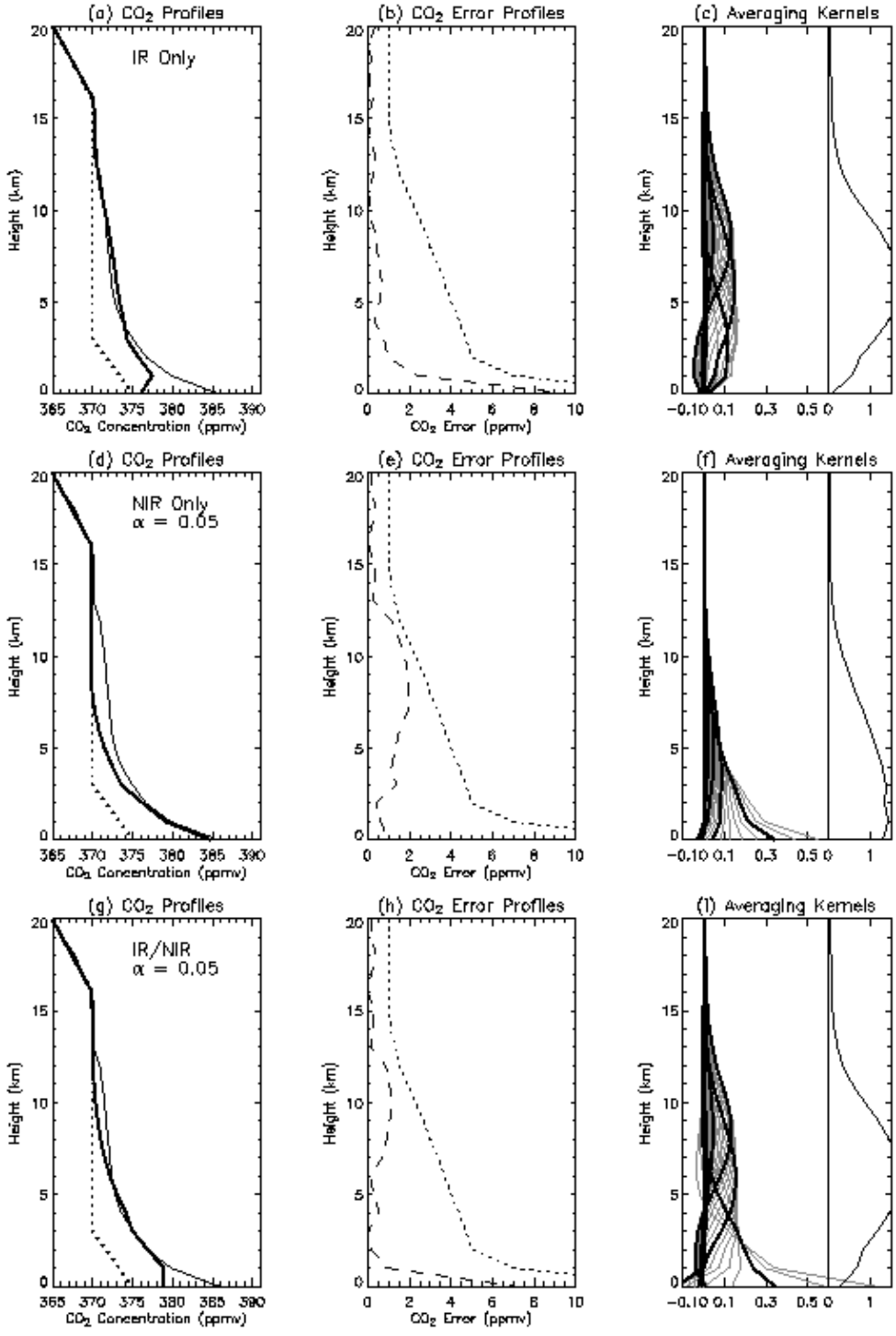

Figure 1. Retrieved source profile of CO_2 in clear sky with associated profiles of error statistics for measurements with $\alpha = 0.05$ and $\theta_{\odot} = 30°$. (a, d, g) Real (thin solid), retrieved (thick solid), and a priori (dashed) CO_2 profiles; (b, e, h) a priori error (dotted), and actual error (dashed); (c, f, i) Averaging kernels for retrieval (left) and their sums at each level (right). See text for details. The retrievals are the result of using only infrared (IR) measurements (upper set), near infrared (NIR) measurements (middle set), and both IR and NIR measurements (lower set).

Figure 43: Figure 1 from *Christi and Stephens, 2004.*

Table 1. Column Average Values of CO_2 Volume Mixing Ratio in ppmv ($\bar{q}$) for Real, a Priori, and Retrieved Profiles Along With Associated Error Expressed in ppmv ($\Delta\bar{q}$) and as a Percentage Error (%)

Profile	Scene	α	$\bar{q}$	$\Delta\bar{q}$	%
Real	–	–	373.43	–	–
a priori	–	–	370.20	−3.23	−0.87
IR only	CLEAR	–	372.67	−0.76	−0.20
NIR only	CLEAR	0.05	372.43	−1.00	−0.27
IR/NIR	CLEAR	0.05	372.76	−0.67	−0.18
NIR only	CLEAR	0.20	372.84	−0.59	−0.16
IR/NIR	CLEAR	0.20	373.05	−0.38	−0.10
IR only	CLOUD	–	372.78	−0.65	−0.17
NIR only	CLOUD	0.05	372.75	−0.68	−0.18
IR/NIR	CLOUD	0.05	373.51	+0.08	+0.02
NIR only	CLOUD	0.20	373.07	−0.36	−0.10
IR/NIR	CLOUD	0.20	373.44	+0.01	+0.00

Retrieved profiles are indicated by the measurements used, the scene (clear or with cirrus cloud), and surface albedo α given in which the profile was retrieved.

Table 26: Table 1 from *Christi and Stephens, 2004.*

10.2 Ozone and methane from combined NIR and TIR measurements

Bovensmann et al. 2004 investigated in a sensitivity studies for O_3, and CH_4 the potential advantage of improving the retrieval of lower tropospheric concentrations by a combined NIR and TIR inversion. For this study the retrieval error on three layers (0 - 2 km, 2 - 7 km, 7 – 15 km) from theTIR retrieval were taken as the a-priori constraints for the NIR retrieval. The results are shown in Table 27: Mean estimated noise induced errors for measurements of the vertical distribution of tropospheric gases from NIR, TIR and the combined NIR/TIR retrieval.. The combined retrieval results in a significantly improved precision in the troposphere, especially in the lowest layer (0-2 km), where the improvement is at least a factor 2 for lower tropospheric O_3 and more than a factor of 3 for lower tropospheric CH_4. This type of synergistic retrieval using solar backscatter and thermal IR sounding was also used recently to derive CO_2 precisions by *Christi and Stephens 2004*.

Species		**Vertical layers boundaries**		
		0–2 km	**2-7 km**	**7-15 km**
O_3	**NIR/TIR**	**5 %**	**< 5 %**	**< 5 %**
TIR		28 %	13 %	6.6 %
NIR		10%	6 %	13 %
CH_4	**NIR/TIR**	**2 %**	**1 %**	**1 %**
TIR		7.1 %	3 %	2.6 %
NIR		13 %	12 %	18 %

Table 27: Mean estimated noise induced errors for measurements of the vertical distribution of tropospheric gases from NIR, TIR and the combined NIR/TIR retrieval.

10.3 Temperature from combined TIR / microwave: AIRS/AMSU/HSB

The AMSU, together with the Atmospheric Infrared Sounder (AIRS), and the Humidity Sounder for Brazil (HSB) form an integrated cross-track scanning temperature and humidity sounding system on the Aqua satellite of the Earth Observing System (EOS). AIRS is an infrared spectrometer/radiometer that covers the 3.7–15.4- μm spectral range with 2378 spectral channels. HSB is a four-channel microwave radiometer that makes measurements between 150 and 190 GHz *[Aumann et al., 2003; Susskind et al., 2003]*.

The limiting effects of cloud contamination in the field of view of the IR sounder has limiting effects, so that only "clear" data from IR sounders are used by ECMWF and NCEP for assimilation into forecast analysis fields. This small fraction of "clear" data from IR sounders has had little impact on the forecast. One way to significantly reduce the effects of clouds is to use microwave data. Unfortunately, the vertical resolution achievable in the troposphere from the microwave region is inferior to that achievable in the 4.3μm CO_2 band, and it is difficult to build microwave instruments with hundreds of temperature sounding channels. In addition, microwave emissivity is strongly frequency and surface dependent, such that even with the best models the residual emissivity uncertainty makes the "microwave-only" solution less attractive. One option to deal with cloud contamination is cloud-clearing IR radiances by analytically combining IR sounder data and 54-GHz band microwave sounder data. The AIRS spectrometer is designed to operate in synchronism with the microwave instruments AMSU-A1, AMSU-A2, and HSB. The simultaneous use of the data from the three instruments provides both new and improved global measurements of cloud properties, atmospheric temperature and humidity, and land and ocean skin temperatures, under clear and cloudy conditions, with the accuracy, resolution, and coverage required by numerical weather prediction and climate models *[Aumann et al., 2003]*.

Using the AIRS Science Team algorithm applied to the integrated cross-track scanning temperature and humidity sounding system AIRS/AMSU/HSB on the Aqua satellite, temperature soundings can be produced under partial cloud cover with RMS errors on the order of, or better than, 1 K in 1-km-thick layers from the surface to 700 mb, 1-km layers from 700–300 mb, 3-km layers from 300–30 mb, and 5-km layers from 30–1 mb *[Aumann et al., 2003; Susskind et al., 2003]*, which is interpreted as RMS accuracies of 1K for 1km layers in the LT and HT, for 3km layers in LS, and for 5km layers in HS.

Fetzer et al., 2003, describe the current status of AIRS/AMSU/HSB validation activities, including procedures for assessing product uncertainties, the sources of "truth" used for these procedures, the sampling and error characteristics of those datasets, and the planned schedule of product uncertainty estimation. An example of validation results can be seen in Figure 44.

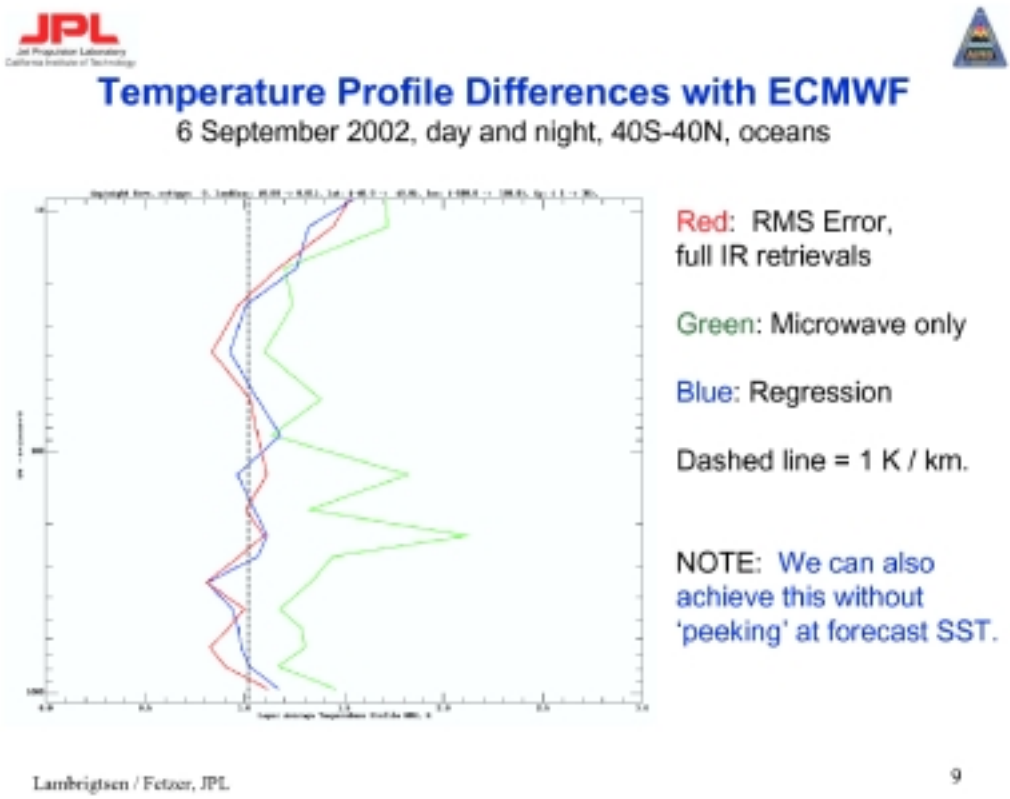

Figure 44: Validation of AIRS/AMSU/HSB retrievals *[Fetzer et al., 2003b]*.

11 Overview by Parameter

An overview about past, current, and future passive space borne sensors, which measure or are supposed to measure at least one of the target parameters relevant for this study, is given in this section.

Abbreviations used in the following tables:

C	Column
P	Profile
p	Pressure
LT	Lower Troposphere (0-5km)
HT	Higher Troposphere (5-15)
LS	Lower Stratosphere (15-35km)
T	Troposphere or Temperature
S	Stratosphere
M	Mesosphere
A	(entire) Atmosphere
Su	Surface
FT	Free Troposphere
B	Boundary layer
U	Upper
L	Lower
Mi	Middle
Cld	Cloud
CldF	Cloud Free
CldFLa	Cloud Free over Land
O	Ocean
La	Land
NA	Not Assessed
TBC	To Be Confirmed
TBD	To Be Determined
SOLAR	Solar spectral region
TIR	Thermal Infra Red
MW	MicroWave
SZA	Solar Zenith Angle

Precision:

The retrieval precisions given in the following tables are a measure of the random error of the considered parameter. Random errors are those error components that will improve (get smaller) upon averaging of several measurements. The values given in the tables are 1-sigma values if not stated otherwise and refer to the spatial/time resolution as given in the corresponding row of the table.

Most precision values as given in the tables have been determined by simulated retrievals or other theoretical approaches taking into account (mainly) the instrument signal-to-noise performance and (partially) effects due to (quasi random components of) atmospheric variability. The precision can be estimated relatively easily using simulations. In orbit measurements of the precision are difficult and require, for example, many atmospheric observations under similar conditions in regions where atmospheric variability is sufficiently low.

The precision is a more fundamental quantity than accuracy (which typically depends significantly on the details of the algorithm used).

Accuracy:

The reliable estimation of biases is difficult for many reasons. Biases are a problem (only) if they are essentially unknown (despite validation) for example because they depend in a complex and difficult to characterise way on many parameters (e.g., location (via albedo) and/or time (via solar zenith angle)). If a bias exists but is well characterised it simply can be “subtracted”. There still will be a residual bias which also can be corrected for if well characterized, etc. Typically, biases gets smaller with improved version of the retrieval algorithms. For example, the accuracies given in this document for the SCIAMACHY greenhouse gas column measurements are poor (i.e., the biases are large) because currently only an initial version of the retrieval algorithm exists (WFM-DOAS Version 0.4 from the University of Bremen).

The retrieval accuracies given in the following tables are a measure of systematic error components (biases). They have been (mainly) estimated by comparison of the retrieved quantities with independent measurements (partially also from simulated retrievals). For future systems or (new) systems where detailed validation results are not (yet) available no reliable accuracy values can be given. For some future systems certain error sources that are supposed to result in biases have been estimated. If these estimates are available they are given in the following tables. If no bias estimates were available the entry NA (= not assessed) has been included in the following tables.

CO_2:

Para-meter	Entity	Sensor	View	Spec. region	Vertic. range	Vertic resol. [km]	Horizontal resol. [km^2] [Time resol.]	Precision	Accuracy	References
CO2	C	SCIAMACHY	Nadir	SOLAR	-	-	30 x 60 [0.25 s]	1% theoret.; WFMD V0.4 estimate: ~1-4% (land) (Lv1+Lv2 issues; to be improved)	WFMD V0.4 estimate: ~2-5% (land) (Lv1+Lv2 issues; to be improved)	Bovensmann et al., 1999; Buchwitz et al, 2000a; Buchwitz and Burrows, 2004; Warneke et al., 2004; Buchwitz et al., 2004c; Buchwitz et al., 2004d
CO2	C	OCO	Nadir	SOLAR	-	-	4 deg x 5 deg [16 days]	requirement: 0.3 % (1 ppm)	requirement: < 1-2 ppm (bias reduction by cal/val program)	Kuang et al., 2002; Crisp et al., 2004; Crisp et al., 2004b
CO2	P	SCIAMACHY	Limb	SOLAR	UT, LS	~3	~250 [~60 s]	<10% (theoret.)	NA	Bovensmann et al., 1999; Kaiser et al., 2002
CO2	P	SOFIS (cancelled)	Solar occ.	SOLAR	MT, UT	4-6 layers in tropos.	~250	requirement: ~1.4 ppm	NA	Kuze et al., 2000; Patra et al., 2003
CO2	C(P)	GOSAT	Nadir	SOLAR +TIR	BL, FT	2 points in tropos.	TBD	TBD	TBD	Ogawa et al., 2004; Shimoda, 2003
CO2	Mid. tropos. VMR	HIRS (+ AMSU)	Nadir	TIR (+ MW)	FT-S	-	15°x15° [1 month]	1% (rough estimate) (20N-20S)	NA	Chedin et al., 2003a
CO2	C	IMG	Nadir	TIR	FT-S	-	8 x 8	NA	NA	Chedin et al, 2003b
CO2	C	AIRS	Nadir	TIR	FT-S	-	14 x 14	< 1% (theoretic.)	NA	Engelen and Stephens, 2004
CO2	C	IASI	Nadir	TIR	FT-S	-	500 x 500 [14 days]	1% (theoretic.)	NA	Chedin et al., 2003b

Table 28: Overview about passive systems which measure CO_2.

CH_4:

Para-meter	Entity	Sensor	View	Spec. region	Vertic. range	Vertic resol. [km]	Horizontal resol. [km^2] [Time resol.]	Precision	Accuracy	References
CH4	C	MOPITT	Nadir	SOLAR	A	-	22 x 22	~1% (theoret.)	NA (large errors; no products released)	Pan et al., 1998; Deeter et al., SPIE
CH4	C	SCIAMACHY	Nadir	SOLAR	A	-	30 x 120 [0.5 s]	1% theoretic.; WFMD V0.4 estimate: ~1-6% (land) (Lv1+Lv2 issues; to be improved)	WFMD V0.4 estimate: ~2-15% (land) (Lv1+Lv2 issues; large bias due to ice issue; to be improved)	Schrijver et al., 1998; Bovensmann et al., 1999; Buchwitz et al, 2000a; Buchwitz and Burrows, 2004; Warneke et al., 2004; Buchwitz et al., 2004c; de Maziere et al., 2004; Buchwitz et al., 2004d
CH4	P	HALOE	Solar occ.	SOLAR	S, M	~2.5	~250	TBD	15% (10-50km) (Version 19)	Camy-Peyret et al., 2004
CH4	P	SCIAMACHY	Limb	SOLAR	UT, LS	~3	~250 [~60 s]	<10% (theoret.)	NA	Bovensmann et al., 1999; Kaiser et al., 2002

Para-meter	Entity	Sensor	View	Spec. region	Vertic. range	Vertic resol. [km]	Horizontal resol. [km^2] [Time resol.]	Precision	Accuracy	References
CH4	C	IMG	Nadir	TIR	FT-S	-	8 x 8	TBD	4% (rough estimate)	Clerbaux et al., 2003 Chazette et al., 1998
CH4	C	TES	Nadir	TIR	FT-S	-	5 x 8	3%	NA	Worden et al. 2004
CH4	P	TES	Limb	TIR	0-34 (scan range)	2-6 km	55 x 170	3% (req.)	NA	TES web page
CH4	C	IASI	Nadir	TIR	FT-S	-	12 x 12	5 - 10% (req.)	NA	CNES IASI web page

Table 29: Overview about passive systems which measure CH_4.

N_2O:

Para-meter	Entity	Sensor	View	Spec. region	Vertic. range	Vertic resol. [km]	Horizontal resol. [km^2] [Time resol.]	Precision	Accuracy	References
N2O	C	SCIAMACHY	Nadir	SOLAR	A	-	30 x 120 [0.5 s]	10% theoretic.; WFMD V0.4 estimate: ~10-20% (land) (L1 issues)	WFMD V0.4 estimate: ~30% (land) (L1 issues)	Schrijver et al., 1998; Bovensmann et al., 1999; Buchwitz et al, 2000a; Buchwitz and Burrows, 2004; Warneke et al., 2004; de Maziere et al., 2004; Buchwitz et al., 2004d
N2O	P	SCIAMACHY	Limb	SOLAR	UT	~3	~250 [~60 s]	<50% (theoret.)	NA	Bovensmann et al., 1999; Kaiser et al., 2002

Para-meter	Entity	Sensor	View	Spec. region	Vertic. range	Vertic resol. [km]	Horizontal resol. [km^2] [Time resol.]	Precision	Accuracy	References
N2O	C	IMG	Nadir	TIR	300-700 hPa	-	8 x 8 [10 s]	1-3% (theoretic.)	NA	Lubrano et al., 2003
N2O	C	IASI	Nadir	TIR	300-700 hPa	-	12 x 12	1-3% (theoretic.)	NA	Lubrano et al., 2003

Para-meter	Entity	Sensor	View	Spec. region	Vertic. range	Vertic resol. [km]	Horizontal resol. [km^2] [Time resol.]	Precision	Accuracy	References
N2O	P	EOS-MLS	Limb	MW	LS	3	500 [24.7 s]	LS: 20-50 ppbv (~6-30%)	NA	EOS-MLS-ATBD EOS MLS web site

Table 30: Overview about passive systems which measure N_2O.

Ozone:

Para-meter	Entity	Sensor	View	Spec. region	Vertic. range	Vertic resol. [km]	Horizontal resol. [km^2] [Time resol.]	Precision	Accuracy	References
O3	C	TOMS/ Nimbus-7	Nadir	SOLAR	A	-	1x1 deg gridded [monthly avg.]	2% (-5%) (TOMS EP)	2-5% (V 7)	TOMS V7 web page
O3	C	TOMS/EP	Nadir	SOLAR	A	-	39 x 39	2 % (SZA>80: 5%)	3 % (SZA>80: 4%)	TOMS EP web page
O3	C	GOME	Nadir	SOLAR	A	-	40 x 320 [1.5 s]	~1% (theoret.)	SZA < 70: 2-4% SZA > 70: 5-8% O_3 hole: <10% (GDP 3.0)	Diebel et al., 1995; Burrows et al., 1999; Lambert et al., 2003; GDP3ESA, 2002
O3	C	GOME	Nadir	SOLAR	A	-	40 x 320 [1.5 s]	~3% (SZA > 80: <5%)	Mid.Lat.: ~1-3% High Lat.: <5% O_3 hole: < 8% (WF-DOAS)	Weber et al., 2004a; Weber et al., 2004b
O3	C	SCIAMACHY	Nadir	SOLAR	A	-	30 x 60 [0.25 s]	~1%	see GOME	Bovensmann et al., 1999
O3	C	OMI	Nadir	SOLAR	A	-	13 x 24	see GOME	NA (see GOME)	OMI/AURA web page
O3	C	GOME-2	Nadir	SOLAR	A	-	40 x 80	see GOME	NA (see GOME)	EUMETSAT web page
O3	TC	TOMS/SBUV	Nadir	SOLAR	T	1 point in tropos.	1 deg x 1.25 deg [daily maps]	NA	~20% (monthly avg.)	Fishman et al., 2003
O3	TC	GOME	Nadir	SOLAR	T	1 point in tropos.	40 x 320 [1.5 s]	< ~40%	< ~30%	Siddans et al., 1997; Siddans et al., 1998; Munro et al., 1998
O3	TC	SCIAMACHY	Limb/ Nadir	SOLAR	T	1 point in tropos.	30 x 60 (TBC) [0.25 s]	~10% (theoretic.)	NA	Bovensmann et al., 1999
O3	P	SBUV/2	Nadir	SOLAR	S (0.5-100 hPa)	~6 km (9 Umkehr layers)	183 x 183 [32 s]	~5-15%	~5-15%	Bhartia et al., 1996; SPARC web page
O3	P	SAGE III	Occult. (solar)	SOLAR	MT, UT, S, M (6-85 km)	0.5-2	~250 (TBC) [~60 s]	requirement: 5%	requirement: 6%	SAGE3-Val-Summary, 2001
O3	P	GOME	Nadir	SOLAR	S	~6	40 x 320 [1.5 s]	~10%	~10%	Diebel et al., 1995; Munro et al., 1998; Hoogen et al., 1999
O3	P	SCIAMACHY	Nadir	SOLAR	S	~6	30 x 60 [0.25 s]	see GOME	NA (see GOME)	Bovensmann et al., 1999; GOME references
O3	P	SCIAMACHY	Limb	SOLAR	S (M, UT)	~3	~250 [~60 s]	~1%	~10%	Bovensmann et al., 1999; Kaiser et al., 2002; van Savigny et al., 2004
O3	P	SCIAMACHY	Occult. (solar)	SOLAR	S (M, UT)	~3	~250 [~60 s]	~5%	~10%	Meyer, 2004
O3	P	POAM III	Occult. (solar)	SOLAR	S, M	~3	~250 [~60 s]	5-10% (13-60 km)	5-10% (13-60 km)	POAM III validation web page
O3	P	GOMOS	Occult. (stars)	SOLAR	S	~3	~250 [~60 s]	Prelim.valid.: ~5-15% (18-50km)	Prelim.valid.: bias <~5% (18-50km)	ACVE-2/GOMOS, 2004
O3	P	OMI	Nadir	SOLAR	S	~6 (GOME)	13 x 24	see GOME	NA (see GOME)	(GOME estimate)
O3	P	GOME-2	Nadir	SOLAR	S	~6 (GOME)	5 x 40	see GOME	NA (see GOME)	(GOME estimate)

Para-meter	Entity	Sensor	View	Spec. region	Vertic. range	Vertic resol. [km]	Horizontal resol. [km^2] [Time resol.]	Precision	Accuracy	References
O3	C	HIRS	Nadir	TIR	UT-S	-	10 x 10	TBD	10%	Drouin et al. 2003
O3	C	IMG	Nadir	TIR	FT - S	-	8 x 8	6%	10%	Turquety et al. 2002
O3	C	IMG	Nadir	TIR	FT - S	-	8 x 8	TBD	3%	Clerbaux et al. 2003
O3	C	AIRS	Nadir	TIR	FT - S	-	14 x 14	20%	TBD	Aumann et al. IEEE 2003
O3	C	AIRS	Nadir	TIR	FT - S	-	14 x 14	5%	5%	AIRS Validation Report 2003
O3	P	TES	Nadir	TIR	FT-S	5 - 10	5 x 8	20-30% (FT-LS) 10% (S)	NA	Worden et al. 2004
O3	C	IASI	Nadir	TIR	FT - S	-	12 x 12	3%	NA	CNES IASI web page
O3	TC	IMG	Nadir	TIR	T	-	8 x 8	NA	13% (rough estimate)	Clerbaux et al. 2003
O3	TC	IASI	Nadir	TIR	T	-	12 x 12	9-28 %	NA	CNES IASI web page
O3	P	TES	Limb	TIR	0-34 (scan range)	2 - 6	55 x 170	3% (req.)	NA	TES web page

Para-meter	Entity	Sensor	View	Spec. region	Vertic. range	Vertic resol. [km]	Horizontal resol. [km^2] [Time resol.]	Precision	Accuracy	References
O3	P	MLS	Limb	MW	S (>20km)	4	~250	4-10%	6%	Livesey et al., 2003
O3	P	EOS-MLS	Limb	MW	LS	4	500 [24.7 s]	2-10%	5-10 %	EOS-MLS-ATBD; EOS MLS web site
O3	P	MASTER	Limb	MW	UT, LS	2	~250	UT: >20% LS: 5-9% (>15km) 8-20% (10-15km)	NA	Reburn et al., 1999
O3	P	SOPRANO	Limb	MW	LS	3	~250	LS: 5-10% (20-40km) 10-30% (15-20km)	NA	Verdes et al., 2000

Table 31: Overview about passive systems which measure ozone.

Pressure:

Para-meter	Entity	Sensor	View	Spec. region	Vertic. range	Vertic resol. [km]	Horizontal resol. [km^2] [Time resol.]	Precision	Accuracy	References
p	P	SAGE III	Occ. (solar)	SOLAR	MT,UT,S, M (6-85 km)	0.5-2	~250 [~60 s]	requirement: 2%	requirement: 2%	Pitts et al.; SAGE3-Val-Summary, 2001
p	P	SCIAMACHY	Limb	SOLAR	S (M)	3	~250 [~60 s]	NA	NA	ATBD SCIA Lv1-2

Para-meter	Entity	Sensor	View	Spec. region	Vertic. range	Vertic resol. [km]	Horizontal resol. [km^2] [Time resol.]	Precision	Accuracy	References
p Geopot. Height	P	EOS-MLS	Limb	MW	UT, LS	3	500 [24.7 s]	< 30 m (5-30 km): at 10 hPa: 0.036hPa; at 100 hPa: 0.36 hPa; at 500 hPa: 1.8 hPa	30-100m (absolute accuracy)	EOS MLS Science Objectives; EOS MLS ATBD; EOS MLS web site

Table 32: Overview about passive systems which measure pressure.

Temperature:

Para-meter	Entity	Sensor	View	Spec. region	Vertic. range	Vertic resol. [km]	Horizontal resol. [km^2] [Time resol.]	Precision	Accuracy	References
T	P	SAGE III	Solar occ.	SOLAR	MT,UT,S, M (6-85 km)	~1.0	~250 [~60 s]	requirement: 2K	requirement: 2K	Pitts et al.; SAGE3-Val-Summary, 2001
T	P	SCIAMACHY	Limb	SOLAR	S (M)	~3	~250 [~60 s]	NA	NA	ATBD SCIA Lv1-2
T	P	GOMOS	Stellar occ.	SOLAR	S, M	~3	~250 [~60 s]	requirement: 1K	prelim. valid.: few K	ACVE-2/GOMOS, 2004

Para-meter	Entity	Sensor	View	Spec. region	Vertic. range	Vertic resol. [km]	Horizontal resol. [km^2] [Time resol.]	Precision	Accuracy	References
T	P	AIRS	Nadir	TIR	T, UTLS	1 km	14	1 K	1 K	Aumann et al., 2003; Susskind et al., 2003; Fetzer et al., 2003
T	P	TES	Limb	TIR	0-34 km (scan range)	2-6 km	55 x 170	1 K (req.)	2 K (req.)	TES web page
T	P	TES	Nadir	TIR	Surface - S	3 - 10	5 x 8	1 K	NA	Worden et al. 2004
T	P	TES	Nadir	TIR	0-34 km (scan range)	2-6 km	5 x 8	1 K (req.)	2 K (req.)	TES web page
T	P	IASI	Nadir	TIR	T, S	1 km	12 x 12	1 K	NA	Aires et al., 2002
T	P	GIFTS	Nadir	TIR	T,S	1 km	4 x 4	1 K	NA	GIFTS web page

Para-meter	Entity	Sensor	View	Spec. region	Vertic. range	Vertic resol. [km]	Horizontal resol. (diam.) [km] [Time resol]	Precision	Accuracy	References
T	P	SSM/T	Nadir	MW	LT,UT,LS (0-30km)	~8-10	175 - ~260 [2.7s]	LT: 2-5 K UT: 2-3.5 K LS: 1-3.5 K	NA	Grody, 1993; Goodrum, 2000; Redmann, 1992
T	P	AMSU-A	Nadir	MW	LT,UT,LS (0-48km)	3	50 - 150 (NOAA)	LT: 1.5 - 2 K UT: 1.5 K LS: 1.5 - 2 K	LT: -0.1 - +0.3 K UT: -0.5 - +0.3 K LS: -0.2 - +0.5 K	Grody, 1993; Diak et al., 1992; Kidder et al., 2000; Goodrum, 2000; Goldberg, 1999; Goldberg, 2002; Deblonde and English, 2002
T	P	AIRS/AMSU	Nadir	TIR + MW	T, LS	T: 1 km; LS: 3km	14	1 K	< 0.5 K	Aumann et al., 2003; Susskind et al., 2003; Fetzer et al., 2003; Fetzer et al., 2003c
T	P	SSMIS	Nadir	MW	LT, UT, LS	~8-10	38 [0.02s]	LT: 1 - 1.2 K UT: 0.9 - 1.3K LS: NA	LT: < +0.3 K UT: -0.1 - +0.3 K LS: NA	Goodrum, 2000; Redmann, 1992 Deblonde and English, 2002
T	P	UARS-MLS	Limb	MW	LS (>20km)	7	~250	1-2 K	4-5 K	Livesey et al., 2003
T	P	EOS-MLS	Limb	MW	UT, LS (5-60km)	3	165 km (500) [24.7 s]	UT: 0.5 - 1 K LS: 0.5 - 1.5 K	1 -2 K	EOS-MLS-ATBD
T	P	ATMS	Nadir	MW	LT, UT, LS (0-48km)	TBD	approx. as AMSU-A/B	TBD	NA	Goldberg, 2002
T	P	CMIS	Nadir	MW	LT, UT, LS	1-5: 1: > 300hPa 3: > 30hPa 5: > 0.01hPa	40	LT: 1.4 - 2 K HT: 1.3 - 1.4 K LS: 1.3 - 1.5 K	Required: 0.5K/km	Kunkee, 2002a/b; NPOESS-CMIS-ATBD; NPOESS TRD

Table 33: Overview about passive systems which measure temperature.

12 Summary including Comparison with Observational Requirements

12.1 Carbon dioxide (CO_2)

Remote sensing of the CO_2 concentration from space is a new area. So far CO_2 absorption bands have mainly been used (and are still used) to derive information on the temperature profile. Only first attempts have been made to retrieve CO_2 concentrations from satellites.

Extremely high accuracy and precision is required to achieve a data quality useful for the main application of such measurements, namely the quantification of CO_2 surface sources and sinks. For this very interesting and important but challenging application only small variations on top of a large CO_2 background are relevant. The concentration signal of local CO_2 surface sources and sinks is located primarily in the lower troposphere. This adds to the complexity of the retrieval as the troposphere is highly variable (e.g., with respect to humidity, temperature, clouds, and aerosols) and also the (varying) surface spectral reflectance influences the retrieval. Tropospheric measurements of atmospheric trace gas constituents, in general, is a relatively new area.

Currently no passive satellite systems exist for which it has been demonstrated that the requirements for column and range resolved CO_2 measurements as given in *[REQ-GHG-2004]* can be met but some sensors have the potential to meet the threshold requirement for the column measurements.

For columns the requirements are: target precision: 0.8 ppmv or 0.2% (1 day average for 50 km horizontal resolution), threshold precision: 3.5 ppmv or 1% (6 days average for 500 km resolution). The precisions are relaxed by about a factor of two for the range resolved measurements which are required to provide independent information on three regions (boundary layer, free troposphere, stratosphere).

According to the latest requirement update given in *[REQ-GHG-2004Update1]* the following target requirements for the columns of CO_2 should be used: Temporal resolution: 6 days (instead of 1 day), horizontal resolution: 500 km (instead of 50 km)

The only instrument operating in the solar spectral region that currently measures CO_2 columns is SCIAMACHY onboard ENVISAT (launched in 2002). The SCIAMACHY averaging kernels indicate that SCIAMACHY nadir observations are highly sensitive to CO_2 concentration changes in the entire troposphere including the boundary layer *[Buchwitz and Burrows, 2004; Buchwitz et al., 2004c]*. Via simultaneous O_2 column measurements (e.g., using the O_2 A band) SCIAMACHY is able to measure the required dry air column averaged mixing ratio of CO_2 denoted XCO_2.

The feasibility of range resolved SCIAMACHY CO_2 measurements in the troposphere has not yet been investigated. Therefore, the following discussion is restricted to column measurements.

For single measurements the theoretical retrieval precision has been estimated to ~1% (1-sigma) *[Buchwitz et al., 2000a]* using SCIAMACHY's entire channel 7 for retrieval (for an integration time of 1 s) and taking into account a pre-flight estimate of the instrument in-orbit performance (mainly in terms of signal-to-noise performance and detector pixel characteristics including dead pixels).

For various reasons (e.g., reversible ice build up in channel 7, a possible light leak in channel 7, calibration issues, strong interference with atmospheric water vapor absorption bands) analysis of the real flight data has so far mainly been limited to a (rather weak) CO_2 absorption band in channel 6 *[Buchwitz and Burrows, 2004; Buchwitz et al., 2004c]*.

The theoretical CO_2 total column retrieval precision (defined has column retrieval random error due to instrument noise) for the channel 6 band currently used has been estimated to ~1% (1-sigma) for an albedo of 0.1 and a solar zenith angle of 50^o *[Buchwitz and Burrows, 2004]*. This precision refers to an integration time of 0.25 s for a single spectrum (as currently used by SCIAMACHY for orbital positions corresponding to low to moderate solar zenith angles, i.e., relatively high solar elevation).

On the illuminated part of the Earth SCIAMACHY performs alternating limb and nadir observations. A SCIAMACHY nadir state (which is followed by a limb state) lasts about one minute (~240 spectra, 0.25 s integration time per spectrum) and covers a region of about 960 x 390 km^2 with single pixels having a footprint size of 60 x 30 km^2. Every six days approximately the same area is observed again. At low and mid latitudes an area of about 960 x 780 km^2 is observed by approximately two nadir states within a six days time periode. This corresponds to approximately 480 individual spectra. Assuming that only 20% of these pixels are useful (strictly cloud free etc.) this results in approximately 96 individual measurements for a time periode of six days and an area of 960 x 780 km^2 or 32 individual measurements for an area of 500 x 500 km^2 Assuming that the precision improves upon averaging with the square root of the number of measurements added, the precision of 32 averaged measurements is approximately a factor of 6 better than the precision of a single measurement. For an averaging time periode of one day and an area of 50 x 50 km^2 not more than two measurements can be averaged leading to an improvement factor of 1.4.

Using simulated retrievals additional error sources (i.e., errors that need to be considered in addition to instrument noise) have been investigated by *Buchwitz and Burrows, 2004,* which are expected to result in biases but also have random components not included in the precision value of ~1% given above. These error sources comprise, e.g., the variability of temperature and water vapour profiles, undetected sub-visual cirrus clouds, aerosols, and albedo effects. For the current version of the University of Bremen WFM-DOAS retrieval algorithm (Version 0.4) these effects might result in column retrieval errors on the order of several percent being partially random partially systematic *[Buchwitz and Burrows, 2004; Buchwitz et al., 2004c; Buchwitz et al., 2004d]*.

Due to the limited validation it is currently not possible to reliably quantify the overall error of the current SCIAMACHY / WFM-DOAS Version 0.4 CO_2 data product and

the quantification of its random and systematic components. A rough estimate of the measurement errors from what is currently known *[Buchwitz et al., 2004c; Buchwitz et al., 2004d]* mainly from analysing cloud free measurements over land at mid and low latitudes is: precision: ~1-4% (1-sigma), bias: 2-5%.

Applying the precision improvement factor of 6 for six days / 500 x 500 km^2 time and space averages indicates that a precision of 0.2-0.7% can be achieved for SCIAMACHY measurements over land (the threshold requirement is 1%).

For a one day average the improvement factor is 1.4 resulting in a precision of 0.7-3% (target requirement: 0.2%). For the updated requirements given in *[REQ-GHG-2004Update1]* six days / 500 x 500 km^2 time and space averaging is relevant and, therefore, the improvement factor is 6. The resulting precision is 0.2-0.7% (target requirement 0.2%).

These rough estimates indicate that SCIAMACHY has the potential to provide measurements (over land) with a precision better than the threshold requirement but probably worse than the target requirement. This needs to be confirmed by more studies including validation. Also the biases need to be considered. So far retrieval studies have only focussed on total column measurements. It has not yet been investigated if it is possible to discriminate between, e.g., the boundary layer and the free troposphere.

CO_2 has also recently been retrieved from TOVS/NOAA-10 measurements in the thermal infrared spectral region *[Chedin et al., 2003a]* including the microwave spectral region to get simultaneous information on temperature. The quantity retrieved is the average CO_2 mixing ratio in the middle troposphere in the tropical region. The algorithm used requires low variability of atmospheric temperature. If it will be possible to extend the methode developed by *Chedin et al., 2003a,* to extra tropical regions needs to be investigated. The retrieved annual variability of the CO_2 mixing ratio is similar to what is know from in-situ ground based measurements and model simulations. The precision is roughly estimated to ~3.6 ppmv (~1%). *Chedin et al., 2003a,* also investigated by simulation the potential of (current and future) high resolution thermal infrared instruments such as AIRS/AQUA (launch 2002) and IASI/METOP (launch 2005) and concluded in line with other studies (e.g., *Engelen et al., 2001*) that using these data 1-2 ppmv (~0.3-0.5%) might be achievable.

The thermal infrared measurements, however, have their maximum sensitivity in the middle troposphere. They lack sensitvity in the lower troposphere (boundary layer) where the variation of the CO_2 concentration due to local sources and sinks is largest.

Measurements of CO_2 in the microwave spectral region are not possible due to lack of CO_2 absorption lines.

A promising near future high spectral / high spatial resolution satellite system is NASA/JPLs Orbiting Carbon Observatory (OCO) mission. OCO will operate in the near-infrared and visible spectral regions. The launch is planned for 2007. The goal is to deliver XCO_2 measurements accurate and precise enough for CO_2 surface source/sink detection. The objective of OCO is to measure XCO_2 with an

accuracy/precision of 1 ppmv (0.3%) in 16 day intervals with a spatial resolution corresponding to regional scales (4^o x 5^o) *[Crisp et al., 2004]*. Current studies indicate that this might be possible (see *Crisp et al., 2004*, *Crisp et al., 2004b*, and references given therein).

The Japanese space agency also plans to build a satellite for CO_2 measurements accurate enough for source/sink quantification, namely GOSAT which is due for launch in 2007 *[Ogawa et al., 2004; Shimoda, 2003]*. GOSAT shall make high spectral resolution Fourier transform nadir measurements in the NIR and TIR spectral regions. These measurements shall allow a discrimination between boundary layer and free tropospheric CO_2 concentrations.

12.2 Methane (CH_4)

Remote sensing of the CH_4 concentration from space is a new area. Only first attempts have been made to retrieve CH_4 concentrations from satellites.

High accuracy and precision is required to achieve a data quality useful for a main application of such measurements, namely the quantification of CH_4 surface sources and sinks. For this very interesting and important but challenging application only small variations on top of the large CH_4 background column are relevant. The concentration signal of local CH_4 surface sources and sinks is located primarily in the lower troposphere. This adds to the complexity of the retrieval as the troposphere is highly variable (e.g., with respect to humidity, temperature, clouds, aerosols) and also the surface spectral reflectance influences the retrieval. Tropospheric measurements of atmospheric trace gas constituents, in general, is a relatively new area.

Currently no passive satellite systems exist for which it has been demonstrated that the requirements for column and range resolved CH_4 measurements as given in *[REQ-GHG-2004]* can be met but some sensors have the potential to meet the threshold requirement for the column measurements.

For columns the requirements are: target precision: 10 ppbv or 0.6% (1 day average for 50 km horizontal resolution), threshold precision: 35 ppbv or 2% (6 days average for 500 km resolution). The precisions are relaxed by about a factor of two for the range resolved measurements which are required to provide independent information on three regions (boundary layer, free troposphere, stratosphere).

According to the latest requirement update given in *[REQ-GHG-2004Update1]* the following target requirements for the columns of CH_4 should be used: Temporal resolution: 6 days (instead of 1 day), horizontal resolution: 500 km (instead of 50 km)

The first global maps of measured methane distributions from satellite have been generated from IMG/ADEOS-1 measurements (see, e.g., *Kobayashi et al., 1999; Clerbaux et al., 2003*). The data show qualitatively the expected variability, for example a strength North-South gradient, but also some problems which migh be related to the algorithm (e.g., treatement of surface emissivity).

Methane total columns can also be retrieved from AIRS/AQUA. CH_4 total columns from AIRS are not an operational Level 2 core product of AIRS but a scientific data product under development by members of the AIRS science team (we are not aware of any published results based on in-flight data).

Currently, there are two instruments in space which measure reflected sun light in spectral regions which correspond to the near-infrared (NIR) absorption bands of CH_4, namely MOPITT onboard TERRA and SCIAMACHY on ENVISAT. These NIR nadir measurements are sensitive to CH_4 concentration changes at all altitude levels, including the boundary layer (see, e.g., *Buchwitz and Burrows, 2004; Buchwitz et al., 2004c*). Both instruments have a theoretical single pixel CH_4 column retrieval

precision of ~1% *[Deeter et al., SPIE; Buchwitz et al., 2000a]*. Due to problems with the near-infrared channels MOPITT has not delivered any CH_4 column data products.

The SCIAMACHY averaging kernels indicate that SCIAMACHY nadir observations are highly sensitive to CH_4 concentration changes in the entire troposphere including the boundary layer *[Buchwitz and Burrows, 2004; Buchwitz et al., 2004c]*. Via simultaneous O_2 column measurements (e.g., using the O_2 A band) SCIAMACHY is able to measure the required dry air column averaged mixing ratio of CH_4 denoted XCH_4.

The feasibility of range resolved SCIAMACHY CH_4 measurements in the troposphere has not yet been investigated. Therefore, the following discussion is restricted to column measurements.

For single measurements the theoretical retrieval precision has been estimated to ~1% (1-sigma) *[Buchwitz et al., 2000a]* using SCIAMACHY's entire channel 8 for retrieval (for an integration time of 1 s) and taking into account a pre-flight estimate of the instrument in-orbit performance (mainly in terms of signal-to-noise performance and detector pixel characteristics including dead pixels).

For various reasons (e.g., calibration issues, strong interference with atmospheric water vapor absorption bands) analysis of the real flight data has so far mainly been limited to a small spectral fitting window in channel 8 *[Buchwitz and Burrows, 2004; Buchwitz et al., 2004c]*.

The theoretical CH_4 total column retrieval precision (defined here as column retrieval random error due to instrument noise) for the channel 8 fitting window currently used has been estimated to ~1.1% (1-sigma) for an albedo of 0.1 and a solar zenith angle of 50^o *[Buchwitz and Burrows, 2004]*. This precision refers to an integration time of 0.5 s for a single spectrum (as currently used by SCIAMACHY for orbital positions corresponding to low to moderate solar zenith angles, i.e., relatively high solar elevation).

On the illuminated part of the Earth SCIAMACHY performs alternating limb and nadir observations. A SCIAMACHY nadir state (which is followed by a limb state) lasts about one minute (~120 spectra, 0.5 s integration time per spectrum) and covers a region of about 960 x 390 km^2 with single pixels having a footprint size of 120 x 30 km^2. Every six days approximately the same area is observed again. At low and mid latitudes an area of about 960 x 780 km^2 is observed by approximately two nadir states within a six days time periode. This corresponds to approximately 240 individual spectra. Assuming that only 20% of these pixels are useful (strictly cloud free etc.) this results in approximately 48 individual measurements for a time periode of six days and an area of 960 x 780 km^2 km^2 or 16 individual measurements for an area of 500 x 500 km^2. Assuming that the precision improves upon averaging with the square root of the number of measurements added, the precision of 16 averaged measurements is approximately a factor of 4 better than the precision of a single measurement. For an averaging time periode of one day and a horizontal resolution of 50 x 50 km^2 no averaging can be performed.

Using simulated retrievals additional error sources (i.e., errors that need to be considered in addition to instrument noise) have been investigated by *Buchwitz and Burrows, 2004,* which are expected to result in biases but also have random components not included in the precision value of ~1.1% given above. These error sources comprise, e.g., the variability of temperature and water vapour profiles, undetected sub-visual cirrus clouds, aerosols, and albedo effects. For the current version of the University of Bremen WFM-DOAS retrieval algorithm (Version 0.4) these effects might result in column retrieval errors on the order of several percent being partially random partially systematic *[Buchwitz and Burrows, 2004]*.

So far only a limited amount of (real) SCIAMACHY CH_4 data have been compared with independent measurements. A first comparison with ground based (ship borne) solar occultation FTIR measurements showed agreement with ~5% *[Warneke et al., 2004]*.

An initial comparison of the WFM-DOAS (Version 0.4) methane column data products with various ground based FTIR measurements has been performed. First results have been presented at the second ENVISAT validation workshop (ACVE-2) beginning of May, 2004, in ESRIN, Italy *[ACVE-2/SCIAMACHY, 2004]*. Agreement with the FTIR measurements was typically within 15%. This value however has to be interpreted with care for many reasons. For example, many stations are located at high altitudes and measure the column above the station whereas SCIAMACHY measures the entire column for a large ground pixel. Other issues are related to clouds and SCIAMACHY ground pixels over water which were included in the comparison with stations located near the coast.

Because of the limited number of ground stations that measure CH_4 columns it is also planned to extensively compare the SCIAMACHY data with global models of atmospheric transport and chemistry. If it turned out that the quality of the data is sufficiently high the data will be used in combination with inverse modelling to constrain the surface sources and sinks of CH_4 (see http://www.kmni.nl/evergreen).

Due to the limited validation it is currently not possible to reliably quantify the overall error of the current SCIAMACHY / WFM-DOAS Version 0.4 CH_4 data product and the quantification of its random and systematic components. A rough estimate of the measurement errors from what is currently known *[Buchwitz et al., 2004c; Buchwitz et al., 2004d]* mainly from analysing cloud free measurements over land at mid and low latitudes is: precision: ~1-6% (1-sigma), bias: 2-15% (time dependent bias due to ice issue; to be improved).

Assuming a single measurement precision of 1-6% and applying the precision improvement factor of 4 for six days / 500 x 500 km^2 time and space averages indicates that a precision of 0.25-1.5% might be achievable for SCIAMACHY over land (threshold requirement: 2%).

For one day no averaging is possible and the estimated SCIAMACHY precision is in the range 1-6% (target requirement: 0.6%). For the updated requirements given in *[REQ-GHG-2004Update1]* six days / 500 x 500 km^2 time and space averaging is relevant and, therefore, the improvement factor is 4. The resulting precision is 0.25-1.5% (target requirement 0.6%).

These rough estimates indicate that SCIAMACHY has the potential to provide measurements (over land) with a precision better than the threshold requirement but probably not better than the target requirement. This needs to be confirmed by more studies including validation. Also the biases need to be considered. So far retrieval studies have only focussed on total column measurements. It has not yet been investigated if it is possible to discreminate between boundary layer and free troposphere.

TES/AURA: The required precision for methane total columns and vertical profiles (vertical resolution: 2-6 km) to be retrieved from TES is ~3% for single measurements.

IASI/METOP: The required measurement accuracy for methane total columns to be retrieved from IASI is < 5-10% for single measurements *[Diebel et al., 1996; Clerbaux et al., 1998; Hadji-Lazaro et al., 2003]*.

The thermal infrared measurements, however, have their maximum sensitivity in the middle troposphere and lack sensitvity in the lower troposphere (boundary layer) where the variation of the CH_4 concentration due to local sources and sinks is largest.

Measurements of CH_4 in the microwave spectral region are not possible with reasonable accuracy and precision because of the CH_4 absorption lines are very weak.

12.3 Nitrous oxide (N_2O)

Remote sensing of the N_2O concentration from space is a new area. Only first attempts have been made to retrieve N_2O concentrations from satellites.

Extremely high accuracy and precision is required to achieve a data quality useful for a main application of such measurements, namely the quantification of N_2O surface sources. For this very interesting and important but challenging application only small variations of the N_2O background concentration are relevant. The concentration signal of local N_2O surface sources is located primarily in the lower troposphere. This adds to the complexity of the retrieval methods as the troposphere is highly variable (e.g., with respect to humidity, temperature, clouds, aerosols) and also the surface spectral reflectance strongly influences the retrieval. Tropospheric measurements of atmospheric trace gas constituents, in general, is a relatively new area.

Currently no passive satellite systems exist for which it has been demonstrated that the requirements for column and range resolved N_2O measurements as given in *[REQ-GHG-2004]* can be met.

For columns the requirements are: target precision: 0.1 ppbv or 0.03% (1 day average for 50 km horizontal resolution), threshold precision: 1 ppbv or 0.3% (6 days average for 500 km resolution). The precisions are relaxed by about a factor of three for the range resolved measurements which are required to provide independent information on three regions (boundary layer, free troposphere, stratosphere).

According to the latest requirement update given in *[REQ-GHG-2004Update1]* the following target requirements for the columns of N_2O should be used: Temporal resolution: 6 days (instead of 1 day), horizontal resolution: 500 km (instead of 50 km)

IMG/ADEOS-1 was the first high resolution TIR nadir sounder representing a new generation of satellite instruments. Until now only a limited amount of IMG data have been processed to retrieve N_2O columns *[Lubrano et al., 2003]*. Based on simulated IMG retrievals *Lubrano et al., 2003*, conclude that a measurement precision of 1-3% should be possible (single 10 s measurements, 8 x 8 km^2). The sensitivity maximum is between 300 – 700 hPa with no information from the boundary layer. *Lubrano et al., 2003*, estimate that the single pixel retrieval precision for AIRS/AQUA and IASI/METOP should be similar as for IMG.

Chedin et al., 2002, present first results concerning the retrieval of N_2O atmospheric mixing ratios from space. Their method relies on the analysis of the difference between NOAA/TOVS observations (radiances) and simulations using collocated radiosonde data. Collocated radiosondes had to be used as not all the necessary informations can be derived from TOVS. No precision/accuracy values are given in *Chedin et al., 2002.*

The only instrument operating in the solar spectral region that currently measures N_2O columns is SCIAMACHY onboard ENVISAT (launched in 2002). SCIAMACHY nadir observations are highly sensitive to N_2O concentration changes in the entire troposphere including the boundary layer. This can indirectly be concluded from the

averaging kernels of SCIAMACHY's CO measurements *[Buchwitz and Burrows, 2004]*. CO absorbs in a similar spectral region as N_2O and has absorption lines of similar strength. Via simultaneous O_2 column measurements (e.g., using the O_2 A band) SCIAMACHY is able to measure the required dry air column averaged mixing ratio of N_2O denoted XN_2O.

For single measurements the theoretical retrieval precision has been estimated to ~10% (1-sigma) *[Buchwitz et al., 2000a]* using SCIAMACHY's entire channel 8 for retrieval (for an integration time of 1 s) and taking into account a pre-flight estimate of the instrument in-orbit performance (mainly in terms of signal-to-noise performance and detector pixel characteristics including dead pixels).

For various reasons (e.g., calibration issues, interference with atmospheric water vapor absorption bands) analysis of the real flight data has so far mainly been limited to a small spectral fitting window in channel 8 covering not all N_2O lines detected by SCIAMACHY (but most of them) *[Buchwitz and Burrows, 2004]*. Taking into account that not all lines are covered and that the integration time for SCIAMACHY channel 8 nadir measurements is 0.5 s for most of the orbit we might assume a theoretical retrieval precision of ~15-20% (1-sigma), i.e., up to about a factor of two worse than the value given in *[Buchwitz et al., 2000a]*. This is also consistent with the analyis of CO reported in *Buchwitz et al., 2000a,* and *Buchwitz and Burrows, 2004*.

On the illuminated part of the Earth SCIAMACHY performs alternating limb and nadir observations. A SCIAMACHY nadir state (which is followed by a limb state) lasts about one minute (~120 spectra, 0.5 s integration time per spectrum) and covers a region of about 960 x 390 km^2 with single pixels having a footprint size of 120 x 30 km^2. Every six days approximately the same area is observed again. At low latitudes (e.g., tropics) an area of about 960 x 780 km^2 is observed by approximately two nadir states within a six days time periode. This corresponds to approximately 240 individual spectra. Assuming that only 20% of these pixels are useful (strictly cloud free etc.) this results in approximately 48 individual measurements for a time periode of six days and an area of 960 x 780 km^2 km^2 or 16 individual measurements for an area of 500 x 500 km^2. Assuming that the precision improves upon averaging with the square root of the number of measurements added, the precision of 16 averaged measurements is approximately a factor of 4 better than the precision of a single measurement. For an averaging time periode of one day and a horizontal resolution of 50 x 50 km^2 no averaging can be performed.

So far the analysis of the SCIAMACHY data focussed on single measurements *[Buchwitz and Burrows, 2004]*. For SCIAMACHY the precision and accuracy of time and space averaged XN_2O (e.g., for a spatial resolution of 1000 x 1000 km^2 and one day or six day time periodes) has not yet been established. Current best estimates for precision and accuracy are *[Buchwitz et al., 2004d]*: precision: 10-20%, bias: +/- 30%. More studies are needed to confirm this.

Assuming a single measurement precision of 10-20% and applying the precision improvement factor of 4 for six days / 500 x 500 km^2 time and space averages indicates that a precision of 2.5-5% might be achievable for SCIAMACHY over land (threshold requirement: 0.3%).

For one day no averaging is possible and the estimated SCIAMACHY precision is in the range 10-20% (target requirement: 0.03%). For the updated requirements given in *[REQ-GHG-2004Update1]* six days / 500 x 500 km^2 time and space averaging is relevant and, therefore, the improvement factor is 4. The resulting precision is 2.5-5% (target requirement 0.03%).

These rough estimates indicate that SCIAMACHY probably not meets the threshold or target requirements for the column measurements.

Measurements of N_2O in the microwave spectral region so far have been limited to the limb viewing geometry (e.g., MLS/UARS) yielding stratospheric profiles of N_2O. We are not aware of any studies investigating the retrieval of N_2O from microwave nadir observations.

12.4 Ozone (O_3)

The target observational requirement according to *[REQ-O3-2004]* for vertical profiles of the dry air O_3 volume mixing ratio are: precision < 10%, accuracy < 5%, vertical resoution 1 km; horizontal resolution 10 km. The threshold requirements are: troposphere: precision < 20%; accuracy < 10%, vertical resolution 3 km; horizontal resolution: 20 km; UTLS: precision < 20%; accuracy < 10%, vertical resolution 2 km; horizontal resolution: 50 km; stratosphere: precision < 20%; accuracy < 10%, vertical resolution 2 km; horizontal resolution: 100 km.

Ozone vertical profiles are retrieved from nadir looking instruments measuring in the UV/visible such as SBUV/2 and GOME. The vertical resolution is about 6 km in the middle stratosphere (20-25 km) and worse (~10-12 km resolution) above and below. The precision and accuray of the stratospheric profiles is in the range 5-15%. Tropospheric information is, however, limited. According to *Bhartia et al., 1996,* SBUV profiles are strongly influenced by a-priori assumptions outside the range 1-20 hPa (~26-50 km). For the GOME instrument more information is available as (continuous) spectra are recorded *[Munro et al., 1998; Hoogen et al., 1999]*. Nevertheless, the errors on the retrieved tropospheric ozone columns are quite large. According to *Siddans et al., 1997,* agreement with ozone sonde measurements is within 30-40%.

Similar results can be expected from their successors instruments SCIAMACHY (nadir mode) OMI/AURA and GOME-2/METOP but with faster global coverage (one day for OMI and GOME-2) and smaller ground pixel size (e.g., 13 x 24 km^2 for OMI).

Tropospheric ozone has also been determined using a combination of sensors (e.g., TOMS / SAGE or TOMS / SBUV). *Fishman et al., 2003*, used a methode which essentially subtracts the stratospheric column measured by SBUV from the total column as measured by TOMS. *Fishman et al., 2003*, report on agreement with ozone sonde measurements within 13-20%. *de Laat and Aben, 2003,* however, point out that the method used *by Fishman et al., 2003*, is not unproblematic. *de Laat and Aben, 2003*, report that they can produce similar maps of tropospheric ozone using (mainly) tropopause height information.

Tropospheric information can also be derived from SCIAMACHY due to its quasi simultaneous limb and nadir observation of the same air mass. The theoretical retrieval precision has been estimated to ~10% *[Bovensmann et al., 1999]*. At present, however, no detailed information based on comprehensive theoretical analysis or validation of real data is available.

In summary, retrieval of tropospheric ozone information from space is still in its initial stages and uncertainties are large. The best that has been obtained so far is one point for the troposphere (i.e., no vertical resolution within the troposphere) with a large error.

Many limb viewing instruments exist that measure vertical profiles of ozone in the stratosphere and mesosphere by solar, lunar or stellar occultation (e.g., SAGE, POAM, SCIAMACHY, GOMOS), measurements of scattered limb radiance (e.g.,

SCIAMACHY) or limb thermal emission (e.g., MLS/UARS). Occultation measurements may have high precision and vertical resolution (SAGE III: ~6% precision, ~1 km vertical resolution) but cannot provide global coverage. Using SCIAMACHY limb observations of scattered light stratospheric (and mesospheric) ozone profiles have been retrieved with a vertical resolution of 3 km and an accuracy of ~10% *[von Savigny et al., 2004]*. The lowest altitude that can be observed is mainly determined by clouds.

TES/AURA: TES operates in nadir and limb mode. For the nadir measurements *Clough et al., 1995*, estimate the ozone profile retrieval precision to approximately 5% (1 sigma) for a vertical resolution of 5 km in the middle and upper troposphere (corresponding to 2-3 independent pieces of information, see also *Luo et al., 2002*). If boundary layer ozone can be retrieved depends on the (thermal) contrast between the boundary layer and the surface. The vertical resolution in limb mode is about 2-6 km. For OMI/AURA and GOME-2/METOP: see GOME/ERS-2 discussion given above. IASI/METOP: The required ozone total column precision is < 5-10% *[Clerbaux et al., 1998]*.

No passive satellite system has been identified for which it has been demonstrated that the target requirements given in *[REQ-O3-2004]* can be met (especially 1 km vertical resolution with global coverage and a horizontal resolution of 10 km).

No passive satellite system has been identified for which it has been demonstrated that the tropospheric threshold requirements given in *[REQ-O3-2004]* can be met (especially 3 km vertical resolution with global coverage and a horizontal resolution of 20 km).

No passive satellite system has been identified for which it has been demonstrated that the UTLS threshold requirements given in *[REQ-O3-2004]* can be met (especially 2 km vertical resolution with global coverage and a horizontal resolution of 50 km).

No passive satellite system has been identified for which it has been demonstrated that the stratospheric threshold requirements given in *[REQ-O3-2004]* can be met (especially 2 km vertical resolution with global coverage and a horizontal resolution of 100 km).

12.5 Pressure

The threshold observational requirements for pressure are *[REQ-PT-2004]:* Surface pressure: precision < 1 hPa, accuracy < 0.5 hPa, horizontal sampling 50 km; lower troposphere: precision 0.6 hPa, accuracy < 0.5 hPa, horizontal sampling 50 km, vertical sampling 1 km; upper troposphere: precision 0.2 hPa, accuracy < 0.2 hPa, horizontal sampling 100 km, vertical sampling 1 km; lower stratosphere: precision 0.1 hPa, accuracy < 0.1 hPa, horizontal sampling 200 km, vertical sampling 2 km. The height assignment requirement is 10 m. The target requirements are even more stringent, e.g., horizontal sampling 15 km, precision surface pressure 0.5 hPa. In addition, there are near-real time data delivery requirements of 1 or 3 hours.

Surface pressure: In principle, the (dry air) surface pressure can be determined by measuring the total column of a well mixed gas, for example O_2 or CO_2, from which the (dry) air column can be computed and hence surface pressure.

O'Brian, 2002, has reviewed recent and past attempts to measure surface pressure (or, basically equivalent, the geopotential height of pressure levels in the troposphere, e.g., the 500 hPa level) from space. He summarizes his findings as follows: *"While satellites now provide routine measurements of many important meteorological and geophysical parameters, measurements of surface pressure has remained elusive, despite its importance for … NWP. The difficulty is principally one of accuracy …"*. The review of *O'Brian, 2002*, covers various techniques, including microwave, thermal infrared, and visible/near-infrared passive sensors as well as active sensors (GPS occultations, DIAL, milimeter radar). The main part of his study is devoted to surface pressure retrieval using oxygen A band measurements from a geostationary orbit.

As discussed in, e.g., *O'Brian, 2002*, the O_2 column can be determined, for example, from nadir radiance measurements in spectral regions corresponding to its visible/near-infrared absorption bands. The band that has been investigated in most studies is the O_2 A band located at 760 nm. The problem in retrieving the O_2 column is not a principal one but one of accuracy due to the demanding accuracy requirements for NWP applications. A 1 hPa surface pressure change corresponds to a 0.1% air column change which corresponds to a 0.1% O_2 column change. This means that the O_2 column (or the column of any other well mixed gas) needs to be determined with an accuracy of better than 0.1%. This is (at least) one order of magnitude better than what has been achieved for other gases which have been extensively studied over many years (e.g., ozone). The main problem in accurately determining the O_2 column using, for example, the O_2 A band, are uncertainties resulting from highly variable atmospheric scatterers (aerosols and clouds) which influence the path length of solar photons in the atmosphere. In addition, there are many other radiative transfer effects that affect accuracy such as the dependence of the retrieved column on surface reflectivity. There are also demanding requirements on the instrument: high stability, high signal to noise ratio, high spectral resolution, high spatial resolution, to mention the most important ones.

3-D pressure field: There are a number of limb viewing instruments that measure or aim at measuring pressure as a function of altitude in the stratosphere and above. For all these systems the horizontal resolution (in the line-of-sight direction) is ~200-250 km basically for geometrical reasons. SAGE III, for example, aims at measuring pressure with a with a precision and accuracy of 2% (vertical resolution ~1 km) but these are solar occultation measurements with no global coverage. MIPAS/ENVISAT determines pressure levels from its CO_2 measurements with a precision of ~2% (vertical resolution ~3 km). Pressure as a function of altitude is a planned operational data product from SCIAMACHY (vertical resolution ~3 km). The operational algorithm is, however, currently only in its initial stage. In addition, the (platform) pointing knowledge uncertainties are quite large (currently < 3 km, to be improved to ~1 km) which affects both MIPAS and SCIAMACHY.

EOS-MLS has a Level 3 data product “Daily map of geopotential height”. The expected precision (for 3 km vertical resolution) is < 30 m in the height range 5-30 km (~ 500-10 hPa) *[EOS MLS Science Objectives]*. The EOS-MLS geopotential height retrieval is based on the assumption of hydrostatic equilibrium (i.e., pressure and temperature are not retrieved independently). For a standard profile a 100 m increase in altitude corresponds to a 1.2% pressure decrease, i.e., 30 m correspond to a 0.36% pressure change. This means that the expected EOS-MLS retrieval precision is 1.8 hPa at 500 hPa (required 0.2 hPa), 0.36 hPa at 100 hPa hPa (required 0.1/0.2 hPa), and 0.036 hPa at 10 hPa hPa (required 0.1 hPa). If EOS-MLS reaches its expected performance it might be able to provide data in the middle stratosphere (30 km, 10 hPa) close to the required values.

Concerning the troposphere: We are not aware of any passive satellite system that measures pressure as a function of altitude or of systems that measure the geopotential height of pressure levels in the troposphere (*O’Brian, 2002*). The troposphere is, however, the most important region for NWP.

In summary, no passive satellite systems exist for which it has been demonstrated that the target or threshold requirements given in *[REQ-PT-2004]* can be met. Furthermore, we are not aware of any such systems planned for the future (see also *Eyre et al., 2002, and O’Brian, 2002*).

12.6 Temperature

The threshold observational requirements for temperature are *[REQ-PT-2004]:* troposphere: precision 1 K, accuracy < 0.5 K, vertical sampling 1 km, horizontal sampling 50-100 km; stratosphere: precision 2 K, accuracy < 0.5 K, vertical sampling 2-3 km, horizontal sampling 200-250 km. The target requirements are even more stringent, e.g., horizontal sampling 15 km, vertical sampling 0.5 km, precision 0.5 K. In addition, there are near-real time data delivery requirements of 1 or 3 hours.

The sensors that measure temperature profiles in the troposphere and stratosphere are nadir sounders operating in the microwave and thermal infrared spectral region. Temperature sounding from space has a relatively long history for NWP and other applications (e.g., the microwave instrument series MSU/AMSU on NOAA satellites and SSM/T / SSMIS series on DMSP satellites). SSM/T has a precision of 0.3 K, an accuracy of 2-3 K, a vertical resolution of 6-10 km, and a horizontal resolution of 175 km at direct nadir (~260 km at extreme swath) *[Grody, 1993; Goodrum, 2000; Redmann, 1992; Deblonde and English, 2002]*. AMSU-A/NOAA has a better performance, namely a precision better than 0.27 K, an accuracy of 1.5 K, a vertical resolution of 3 km in the height range 0-48 km and a horizontal resolution of 50 km at direct nadir (85x172 km^2 at extreme swath) *[Grody, 1993; Diak et al., 1992; Kidder et al., 2000; Goodrum, 2000; Goldberg, 2002; Goldberg, 2002b; Goldberg 1999; Deblonde and English, 2002]*. An advantage of the microwave sounders is that they are quite insensitive to clouds and measure during day and night. The new generation of high resolution thermal infrared (TIR) nadir sounds such as AIRS/AQUA and IASI/METOP have a vertical resolution of 1 km and a (required) precision of 1 K, and a ground pixel size of 14 x 14 km^2 (AIRS) or 12 x 12 km^2 (IASI) *[Aumann et al., 2003; Susskind et al., 2003; Fetzer et al., 2003; Aires et al., 2002]*. The TIR measurements are also performed during day and night but are affected by clouds which reduces the number of useful measurements. 1 km / 1 K is also the performance of the sensor combination AIRS/AMSU-A onboard AQUA *[Grody, 1993; Diak et al., 1992; Kidder et al., 2000; Goodrum, 2000; Goldberg, 2002; Goldberg, 2002b; Goldberg 1999; Deblonde and English, 2002]*. The predicted performance of the nadir/limb sounder TES/AURA is 1-2 K with a vertical resolution of 2-6 km in the height range 0-34 km (horizontal resolution 5 x 8 km^2, no scan) *[TES web page]*.

Main conclusion: In summary, there are several satellite sensors with global coverage with a performance or predicted performance close to or better than the required threshold performance (e.g., AIRS/AMSU-A/HSB on AQUA and IASI on METOP both with 1 K accuracy, 1 km vertical resolution, < 50 km horizontal resolution). The target performance of 0.5 K accuracy and precision, 0.5 km vertical resolution, and 15 km horizontal resolution is, however, not achieved.

13 References

1. **[ACVE-2/GOMOS, 2004]** Fussen, D., et al., GOMOS validation summary presentation, Atmospheric Chemistry Validation of ENVISAT (ACVE-2), ESA/ESRIN, Frascati, Italy, 3-7 May 2004 (http://envisat.esa.int/workshops/acve2/)
2. **[ACVE-2/MIPAS, 2004]** Fischer, H., et al., MIPAS validation summary presentation, Atmospheric Chemistry Validation of ENVISAT (ACVE-2), ESA/ESRIN, Frascati, Italy, 3-7 May 2004 (http://envisat.esa.int/workshops/acve2/)
3. **[ACVE-2/SCIAMACHY, 2004]** Kelder, H., et al., SCIAMACHY validation summary presentation, Atmospheric Chemistry Validation of ENVISAT (ACVE-2), ESA/ESRIN, Frascati, Italy, 3-7 May 2004 (http://envisat.esa.int/workshops/acve2/
4. **[Aerojet Website]** http://www.aerojet.com/program/detail/about_ssmis.htm (Former a project of Aerojet, SSMIS has now been taken over by Northrop Grumman).
5. **[Aires et al., 2002a]** Aires, F., A. Chedin, N. A. Scott, W. B. Rossow, A regularized neuronal net approach for retrieval of atmospheric and surface temperatures with the IASI instrument, Journal of Applied Meteorology, Vol. 41, 144-159, 2002.
6. **[Aires et al., 2002b]** Aires, F., W. B. Rossow, N. A. Scott, A. Chedin, Remote sensing from the infrared atmospheric sounding interferometer instrument 1. Compression, denoising, and first guess retrieval algorithm, J. Geophys. Res., 107 (D22), 4619, doi:10.1029/2001JD000955, 2002.
7. **[Aires et al., 2002c]** Aires, F., W. B. Rossow, N. A. Scott, A. Chedin, Remote sensing from the infrared atmospheric sounding interferometer instrument 2. Simultaneous retrieval of temperature, water vapor, and ozone atmospheric profiles, J. Geophys. Res., 107 (D22), 4620, doi:10.1029/2001JD001591, 2002.
8. **[AIRS web page]** http://www-airs.jpl.nasa.gov
9. **[AIRS Validation Report 2003]** Validation of AIRS/AMSU/HSB Core products for Data Release Version 3.0, edited by E. Fetzer, JPL publication JPL D-26538, August 13, 2003
10. **[ATBD SCIA Lv1-2]** Spurr et al., ENVISAT-1 SCIAMACHY Level 1c to 2 Off-line Processing Algorithm Theoretical Basis Document, DLR, Germany, December 21, 2000.
11. **[Aumann et al., 2003]** Hartmut H. Aumann, Moustafa T. Chahine, Catherine Gautier, Mitchell D. Goldberg, Eugenia Kalnay, Larry M. McMillin, Hank Revercomb, Philip W. Rosenkranz, William L. Smith, David H. Staelin, L. Larrabee Strow, and Joel Susskind, AIRS/AMSU/HSB on the Aqua mission: design, science objectives, data products, and processing systems, IEEE Transactions on Geoscience and Remote Sensing, Vol. 41, No. 2, Feb. 2003.
12. **[Beer et al., 2003]** Beer, R., et al., TES project overview, presentation given at ASSFTS 11 workshop (Atmospheric Science from Space using Fourier Transform Spectroscopy) (http://www-imk.fzk.de/asf/ame/assfts/), Bad Wildbad, Germany, 8-10 October 2003.
13. **[Bhartia et al., 1996]** Bhartia, P. K., R. D. McPeters, C. L. Mateer, L. E. Flynn, C. Wellemeyer, Algorithm for the estimation of vertical ozone profiles from the backscatter ultraviolet technique, J. Geophys. Res., 101 (D13), 18793-18808, 1996.
14. **[Bogumil et al., 2000]** Bogumil, K., J. Orphal und J. P. Burrows, "Temperature dependent absorption cross sections of O_3, NO_2, and other

atmospheric trace gases measured with the SCIAMACHY spectrometer", Proceedings of the ERS - Envisat - Symposium, Goteborg, Schweden, 2000.
15. **[Bovensmann et al., 2002a]** Bovensmann, H., B., B. Ahlers, M. Buchwitz, J. Frerick, M. Gottwald, R. Hoogeveen, J. W. Kaiser, Q. Kleipool, E. Krieg, G. Lichtenberg, R. Mager, J. Meyer, S. Noël, A. Schlesier, C. Sioris, J. Skupin, C. v. Savigny, M. W. Wuttke, and J. P. Burrows, SCIAMACHY in-flight instrument performance, Proceedings of the Envisat Calibration Review (SP-520), ESA Publications Division, 2002.
16. **[Bovensmann et al., 2002b]** Bovensmann, H., M. Buchwitz, S. Noël, K. U. Eichmann, V. Rozanov, J.P. Burrows, J. M. Flaud, G. Bergametti, J. Orphal, P. S. Monks, G. K. Corlett, A.P. Goede, T. von Clarmann, F. Friedl-Valon, T. Steck, H. Fischer, Sensing of Air Quality from Geostationary Orbit, Proc. of the 2002 EUMETSAT Meteorological Satellite Conference, Dublin, 2.-6.9.2002, EUMETSAT, Darmstadt, Germany, ISBN 92-9119-049, p. 89 - 96, 2002.
17. **[Bovensmann et al., 2002c]** Bovensmann, H., S. Noël,, P. Monks, A.P.H. Goede, J. P. Burrows, The Geostationary Scanning Imaging Absorption Spectrometer (GEOSCIA) Mission: Requirements and capabilities, accepted for publication in Adv. Space Res., 1849 - 1859, 2002.
18. . **[Bovensmann et al., 2004]** Bovensmann, H. K. U. Eichmann, S. Noël, J. M. Flaud, J. Orphal, P. S. Monks, G. K. Corlett, A. P. Goede, T. von Clarmann, T. Steck, V. Rozanov, J. P. Burrows, The Geostationary Scanning Imaging Absorption Spectrometer (GeoSCIA) as part of the Geostationary Tropospheric Pollution Explorer (GeoTROPE) mission: Requirements, concepts and capabilities, Adv. Space Res., 34, 694-699, 2004
19. **[Bovensmann et al., 1999]** Bovensmann, H., J. P. Burrows, M. Buchwitz, J. Frerick, S. Noël, V. V. Rozanov, K. V. Chance, and A. H. P. Goede, SCIAMACHY - Mission objectives and measurement modes, J. Atmos. Sci., 56, (2), 127-150, 1999.
20. **[Bracher et al., 2002]** Bracher A., M. Weber, K. Bramstedt, M. v. König, A. Richter, A. Rozanov, C. Savigny, and J. P. Burrows, Validation of ENVISAT trace gas data products by comparison with GOME/ERS-2 and other satellite sensors, ENVISAT Validation Workshop, ESA/ESRIN, Frascati,Italy, 9-13 December 2002, to be published by ESA Publications Division as Special Publication SP-531 (on CD-ROM), 2002.
21. **[Bramstedt et al., 2002a]** Bramstedt, K., K.-U. Eichmann, M. Weber, V. Rozanov, and J. P. Burrows, GOME ozone profiles: A global validation with HALOE measurements, Adv. Space Res. 29, 1637-1642, 2002.
22. **[Bramstedt et al., 2002b]** Bramstedt, K., M. Buchwitz, U. Blum, T. Blumenstock, C. Frankenberg, P. von der Gathen, R. Koelemeijer, M. de Maziere, A. Richter, C. von Savigny, H. Schrijver, A. Schulz, W. Steinbrecht, Comparison of scientific SCIAMACHY products with ground-based measurements, ENVISAT Validation Workshop, ESA/ESRIN, Frascati, Italy, 9-13 December 2002, to be published by ESA Publications Division as Special Publication SP-531 (on CD-ROM), 2002.
23. **[Bramstedt et al., 2002c]** Bramstedt, K., J. Gleason, D. Loyola, W. Thomas, A. Bracher, M. Weber, and J. P. Burrows, Comparison of total ozone from the satellite instruments GOME and TOMS with measurements from the Dobson network 1996-2000, Atmos. Chem. Phys. Discuss. 2, 1131-1157, 2002.
24. **[Buchwitz, 2000]** Buchwitz, M., Strahlungstransport- und Inversions-Algorithmen zur Ableitung atmosphärischer Spurengasinformationen aus Erdfernerkundungsmessungen in Nadirgeometrie im ultravioletten bis nahinfraroten

Spektralbereich am Beispiel SCIAMACHY, Ph. D. thesis (in German), University of Bremen, Logos Verlag Berlin (http://www.logos-verlag.de), ISBN 3-89722-469-0, ISSN 1615-6862, May 2000.

25. **[Buchwitz et al., 2000a]** Buchwitz, M., V.V. Rozanov, and J.P. Burrows, A near-infrared optimized DOAS method for the fast global retrieval of atmospheric CH_4, CO, CO_2, H_2O, and N_2O total column amounts from SCIAMACHY Envisat-1 nadir radiances, J. Geophys. Res. 105, 15,231-15,245, 2000.

26. **[Buchwitz et al., 2000b**] Buchwitz, M., V.V. Rozanov, and J.P. Burrows, A correlated-*k* distribution scheme for overlapping gases suitable for retrieval of atmospheric constituents from moderate resolution radiance measurements in the visible/near-infrared spectral region, J. Geophys. Res. 105, 15,247-15,261, 2000.

27. **[Buchwitz et al., 2000c**] Buchwitz, M., V.V. Rozanov, K.-U. Eichmann, R. de Beek, and J.P. Burrows, SCIATRAN - a new atmospheric radiative transfer model for the ultraviolet, visible, and near-infrared spectral regions, IRS 2000: Current problems in atmospheric radiation, Proceedings of the International Radiation Symposium, Smith and Timofeyev (Eds.), 365-368, St. Petersburg, Russia, 24-29 July 2000.

28. **[Buchwitz et al., 2002a**] Buchwitz, M., S. Noël, H. Bovensmann, and J. P. Burrows, Verification of SCIAMACHY Level 1 and 2 near-IR nadir data products by WFM-DOAS analysis, ENVISAT Validation Workshop, ESA/ESRIN, Frascati, Italy, 9-13 December 2002, to be published by ESA Publications Division as Special Publication SP-531 (on CD-ROM), 2002.

29. **[Buchwitz et al., 2002b**] Buchwitz, M., K. Bramstedt, S. Noël, H. Bovensmann, and J. P. Burrows, SCIAMACHY on ENVISAT: Trace gas vertical column retrieval using channel 8 nadir measurements: First preliminary results, ENVISAT Calibration Review, ESA/ESTEC, Noordwijk, The Netherlands, 9-13 September 2002, ESA Publications Division, Special Publication SP-520 (on CD-ROM), 2002.

30. **[Buchwitz et al., 2004a]** Buchwitz, M., S. Noël, K. Bramstedt, V. V. Rozanov, H. Bovensmann, S. Tsvetkova, and J. P. Burrows, Retrieval of trace gas vertical columns from SCIAMACHY/ENVISAT near-infrared nadir spectra: First preliminary results, Adv. Space Res., 2004.

31. **[Buchwitz and Burrows, 2004]** Buchwitz, M., and John P. Burrows, Retrieval of CH_4, CO, and CO_2 total column amounts from SCIAMACHY near-infrared nadir spectra: Retrieval algorithm and first results, SPIE 10th International Symposium "Remote Sensing", 8-12 September 2003, Barcelona, Spain, Conference 5235 "Remote Sensing of Clouds and the Atmosphere VIII", Editors K. P. Schäfer, A. Coméron, M. R. Carleer, R. H. Picard, Proceedings of SPIE Volume 5235, 375-388, 2004.

32. **[Buchwitz et al., 2004b]** Buchwitz, M., R. de Beek, K. Bramstedt, S. Noel, H. Bovensmann, and J. P. Burrows, Global carbon monoxide as retrieved from SCIAMACHY by WFM-DOAS, Atmos. Chem. Phys., 4, 1945-1960, 2004.

33. **[Buchwitz et al., 2004c]** Buchwitz, M., R. de Beek, J. P. Burrows, H. Bovensmann, T. Warneke, J. Notholt, J. F. Meirink, A. P. H. Goede, P. Bergamaschi, S. Körner, M. Heimann, J.-F. Muller, and A. Schulz, Atmospheric methane and carbon dioxide from SCIAMACHY satellite data: Initial comparison with chemistry and transport models, Atmos. Chem. Phys. Discuss. (accepted), 2004c.

34. **[Buchwitz et al., 2004d]** Buchwitz, M., R. de Beek, S. Noel, H. Bovensmann, and J. P. Burrows, Retrieval of CO, H_2O, CH_4, CO_2, and N_2O columns from SCIAMACHY/ENVISAT by WFM-DOAS: Current status, Proceedings of ENVISAT

Symposium 2004, 6.-10.9.2004, Salzburg, Austria, Special publication SP-572 (CD-ROM) from ESA publications division, 2004d.

35. **[Bühler et al., 2004]** S. A. Bühler, C. L. Verdes, S. Tsujimaru, A. Kleinboehl, H. Bremer, M. Sinnhuber, and P. Eriksson, The Expected Performance of the SMILES Submillimeter-Wave Limb Sounder Compared to Aircraft Data, submitted to Radio Science, 2004.

36. **[Burrows et al., 1999a]** Burrows, J.P., M. Weber, M. Buchwitz, V.V. Rozanov, A. LadstÃ¤dter-Weissenmayer, A. Richter, R. de Beek, R. Hoogen, K. Bramstedt, K.-U. Eichmann, M. Eisinger und D. Perner, The Global Ozone Monitoring Experiment (GOME): Mission Concept and First Scientific Results, J. Atm. Sciences, 56, 151-175, 1999.

37. **[Burrows et al., 1999b]** Burrows, J.P. , A. Richter, A. Dehn, B. Deters, S. Himmelmann, S. Voigt, and J. Orphal: "Atmospheric Remote-Sensing Reference Data from GOME: 2. Temperature-Dependent Absorption Cross Sections of O3 in the 231-794 nm Range", J. Quant. Spectrosc. Rad. Transfer 61, 509-517, 1999.

38. **[Camy-Peyret et al., 2004]** Camy-Peyret, C., et al. Atmospheric Chemistry Validation of ENVISAT (ACVE-2) workshop, ESA/ESRIN, Frascati, Italy, 3-7 May 2004 (http://envisat.esa.int/workshops/acve2/, ACVE-2_MIP18-CH4-CCP.pdf), 2004.

39. **[Chazette et al, 1998]** Chazette, P., C. Clerbaux, G. Megie, Direct estimate of the methan radiative forcing using nadir spectral radiances, Applied Optics, 37, 3113-3120, 1998.

40. **[Chedin et al., 2002**] Chedin, A., A. Hollingsworth, N. A. Scott, S. Serrar, C. Crevoisier, R. Armante, Annual and seasonal variations of atmospheric CO2, N2O and CO concentrations retrieved from NOAA/TOVS satellite observations, Geophys. Res. Let., 29 (8), 2002.

41. **[Chedin et al., 2003a**] Chedin, A., S. Serrar, N. A. Scott, C. Crevoisier, R. Armante, First global measurement of midtropospheric CO_2 from NOAA polar satellites: Tropical zone, J. Geophys. Res., 108 (D18), 4581, 2003.

42. **[Chedin et al., 2003b**] Chedin, A., R. Saunders, A. Hollingsworth, N. Scott, M. Matricardi, J. Etcheto, C. Clerbaux, R. Armante, C. Crevoisier, The feasibility of monitoring CO_2 from high-resolution infrared sounders, J. Geophys. Res., 108 (D2), 4964, 2003.

43. **[Christi et al., 2003]** Christi, M. J., and G. L. Stephens, Retrieving profiles of atmospheric CO_2 in clear sky and in the presence of thin cirrus clouds using spectroscopy from the near and thermal infrared: A preliminary study, Geophys. Res. Let., submitted, 2003.

44. **[Cira's AMSU Website]** http://amsu.cira.colostate.edu/

45. **[Clerbaux et al., 1998]** Clerbaux, C., P. Chazette, J. Hadji-Lazaro, G. Megie, J.-F. Müller, S. A. Clough, Remote sensing of CO, CH4, and O3 using a spaceborne nadir-viewing interferometer, J. Geophys. Res., 103 (D15), 18999-19013, 1998.

46. **[Clerbaux et al., 2003]** Clerbaux, C., J. Hadji-Lazaro, S. Turquety, G. Megie, P.-F. Coheur, Trace gas measurements from infrared satellite for chemistry and climate applications, Atmos. Chem. Phys., 3, 1495-1508, 2003.

47. **[Clough et al., 1995]** Clough, S. A., C. P. Rinsland, P. D. Brown, Retrieval of tropospheric ozone from simulations of nadir spectral radiances as observed from space, J. Geophys. Res., 100 (D8), 16579-16593, 1995.

48. **[CNES IASI web page**] http://smsc.cnes.fr/IASI/

49. **[Coldewey-Egbers et al., 2003]** Coldewey-Egbers, M., M. Weber, M. Buchwitz, and J.P. Burrows, Application of a modified DOAS method for total ozone retrieval from GOME data at high polar latitudes, Adv. Space Res., accepted 2003.
50. **[Connor et al., 2003]** Connor, B., CO_2 column smoothing errors for OCO, SCIAMACHY and AIRS, poster presented at AGU Fall Meeting, 2003.
51. **[Crisp et al., 2004]** D. Crisp, R. M. Atlas, F.-M. Breon, L. R. Brown, J. P. Burrows, P. Ciais, B. J. Connor, S. C. Doney, I. Y. Fung, D. J. Jacob, C. E. Miller, D. O'Brian, S. Pawson, J. T. Randerson, P. Rayner, R. S. Salawitch, S. P. Sander, B. Sen, G. L. Stephens, P. P.Tans, G. C. Toon, P. O. Wennberg, S. C. Wofsy, Y. L. Yung, Z. Kuang, B. Chudasama, G. Sprague, P. Weiss, R. Pollock, D. Kenyon, S. Schroll, Adv. Space Res., 34, 700-709, 2004.
52. **[Crisp et al., 2004b]** D. Crisp, et al., The Orbiting Carbon Observatory (OCO). 1. XCO2 science measurement requirements, draft paper version 3 October 2004, 2004.
53. **[Deblonde and English, 2002]** Godelieve Deblonde and Stephen English, Stand-alone 1d-var scheme for the ssmis, ssm/i and amsu instruments, ITSC-12, Lorne, 27 Feb-March 5, 2002. (http://cimss.ssec.wisc.edu/itwg/itsc/itsc12/posters/Deblonde_1DVar_poster.ppt).
54. **[Deblonde and English, 2003]** Godelieve Deblonde and Stephen English, One-dimensional variational retrieval from SSMIS-simulated observations, Journal of Applied Meteorology, Vol. 42, No. 10, pp. 1406-1420, 2003.
55. **[Deeter et al., SPIE]** Deeter, M. N., J. Wang, J. C. Gille, P. L. Bailey, Retrieval of tropospheric methane from MOPITT measurements: algorithm description and simulations, http://www.atmosp.physics.utoronto.ca/MOPITT/NCAR_SPIE_paper2.pdf
56. **[de Beek et al., 2004a]** de Beek, R., M. Buchwitz, V. V. Rozanov, and J. P. Burrows, Trace gas column retrieval from IR nadir spectra - a model study for SCIAMACHY, Adv. Space Res., Vol. 34, pp. 734-738, 2004.
57. **[de Beek et al., 2004b]** de Beek, R., M. Weber, A. Rozanov, A. Richter, and J. P. Burrows, Trace gas column retrieval - an error study for GOME-2, Adv. Space Res., Vol. 34, pp. 727-733, 2004.
58. **[de Beek et al., 1998]** de Beek, R., Bestimmung von Ozonvertikalprofilen aus Messungen des Satelliteninstruments GOME im ultravioletten und sichtbaren Spektralbereich, Ph.D. Thesis, U. Bremen, 1998.
59. **[de Laat and Aben, 2003]** Problems regarding the tropospheric O_3 residual method and its interpretation in Fishman et al. (2003) de Laat, A. T. J., I. Aben, Atmos. Chem. Phys. Discuss., 3, 5777-5802, 2003
60. **[de Maziere et al., 2002]** de Maziere, M., T. Coosemans, B. Barret, T. Blumenstock, P. Demoulin, H. Fast, D. Griffith, N. Jones, E. Mathieu, J. Mellqvist, R. Mittermeier, J. Notholt, C. Rinsland, A. Schulz, D. Smale, A. Strandberg, R. Sussmann, S. Wood, M. Buchwitz, Validation of ENVISAT-1 Level-2 products related to lower atmosphere O3 and NOy chemistry by an FTIR quasi-global network, ENVISAT Validation Workshop, ESA/ESRIN, Frascati, Italy, 9-13 December 2002, to be published by ESA Publications Division as Special Publication SP-531 (on CD-ROM), 2002.
61. **[de Maziere et al., 2004]** de Maziere, M., Barret, B., Blumenstock, T., Buchwitz, M., De Beek, R., Demoulin, P., Fast, H., Gloudemans, A., Griesfeller, A., Griffith, D., Ionov, D., Janssens, K., Jones, N., Mahieu, E., Melleqvist, J., Mittermeier, R. L., Notholt, J., Rinsland, C., Schrijver, H., Schultz, A., Smale, D., Strandberg, A., Strong, K., Sussmann, R., Warneke, T., Wood, S., Comparison between

SCIAMACHY scientific products and ground-based FTIR data for total columns of CO, CH_4, and N_2O, in Proceedings of Second Workshop on the Atmospheric Chemistry Validation of ENVISAT (ACVE-2; http://envisat.esa.int/workshops/acve2/), ESA/ESRIN, Frascati, Italy, 3--7 May 2004, 2004.

62. **[Diak et al., 1992]** George R. Diak, Dongsoo Kim, Mark S. Whipple, and Xiaohua Wu, Preparing for the AMSU, Bulletin American Meteorological Sociaty, Vol. 73, No. 12, pp. 1971-1984, 1992.

63. **[Diebel et al., 1995**] Diebel, D., et al., Trace gas study – Detailed analysis of the retrieval algorithms selected for the Level 1-2 processing of GOME data, ESA study, Contract 10728/94/NL/CN, 1995.

64. **[Diebel et al., 1996]** Diebel, D., F. Cayla, T. Phulpin, P. Courier, M. Langevin, IASI: Mission rationale and requirements, IASI-SM-0000-10-CNE/EUM, pp. 1-36, CNES/EUMETSAT, Darmstadt, 1996.

65. **[DMSP Homepage]** http://dmsp.ngdc.noaa.gov

66. **[Drouin et al., 2003]** A. Drouin and F. Karcher,Systematic errors of total ozone retrievals using the 9.7-micron channel Earth radiance, J. Geophys. Res., 108, D13, 4397, doi:10.1029/2001JD001501, 2003

67. **[Dufour et al., 2003]** Dufour, E., and F.-M. Breon, Spaceborn estimate of atmospheric CO_2 column by use of the differential absorption method: error analysis, Applied Optics, Vol. 42, No. 18, 3595-3609, 2003.

68. **[Eichmann et al., 2002]** Eichmann, K.-U. , M. Weber, K. Bramstedt, and J.P. Burrows, Ozone depletion in the NH winter/spring 1999/2000 as measured by GOME-ERS2, J. Geophys. Res. 107, 8280, doi:10.1029/2001JD001148, 2002.

69. **[Engelen et al., 2001]** Engelen, R. J., A. S. Denning, K. R. Gurney, G. L. Stephens, Global observations of the carbon budget 1. Expected satellite capabilities for emission spectroscopy in the EOS and NPOESS eras, J. Geophys. Res., 106 (D17), 20055-20068, 2001.

70. **[Engelen and Stephens, 2004]** Engelen, R. J., G. L. Stephens, Information content of infrared satellite sounding measurements with respect to CO_2, Journal of Applied Meteorology, 43, 373-378, 2004.

71. **[English, 2002]** Stephen English, Remote sensing of the atmosphere using microwave radiometry, URSI conference, 2002.

72. **[EOS-MLS-ATBD]** http://mls.jpl.nasa.gov/joe/eos_mls.html

73. **[EOS MLS Science Objectives]** http://mls.jpl.nasa.gov/joe/Short_EOS_MLS_Science_Objectives_V1.0.doc

74. **[EUMETSAT web page**] http://www.eumetsat.de/en/index.html

75. **[Eyre et al., 2002]** Eyre J., J.-N. Thepaut, J. Joiner, L. P. Riishojgaard, F. Gerard, Position paper: Requirements for observations for global NWP, AEG/NWP, EUMETSAT, Darmstadt, 25 pp., 2002.

76. **[Fetzer et al., 2003]** Eric Fetzer, Larry M. McMillin, David Tobin, Hartmut H. Aumann, Michael R. Gunson, W. Wallace McMillan, Denise E. Hagan, Mark D. Hofstadter, James Yoe, David N. Whiteman, John E. Barnes, Ralf Bennartz, Holger Vömel, Von Walden, Michael Newchurch, Peter J. Minnett, Robert Atlas, Francis Schmidlin, Edward T. Olsen, Mitchell D. Goldberg, Sisong Zhou, HanJung Ding, William L. Smith, and Hank Revercomb, AIRS/AMSU/HSB Validation,IEEE Transactions on Geoscience and Remote Sensing, Vol. 41, No. 2, Feb. 2003.

77. **[Fetzer et al., 2003b]** Eric J. Fetzer, Edward T. Olsen, Luke L. Chen, Denise E. Hagan and Evan Fishbein (Jet Propulsion Laboratory), Larry McMillin and Jiang

Zhou (NOAA / NESDIS), The Validation of AIRS Retrievals, ITSC- 13, Ste- Adèle, Canada, October 31, 2003.

78. **[Fetzer et al., 2003c]** E. Fetzer, H. H. Aumann, Frederick Chen, Luke Chen, Steve Gaiser, Denise Hagan, Thomas Hearty, Frederick W. Irion, Sung-Yung Lee Larry McMillin, Edward Olsen, Hank Revercomb, Phil Rosenkranz, David Staelin, Larrabee Strow, Joel Susskind, David Tobin, and Jiang VALIDATION OF AIRS/AMSU/HSB CORE PRODUCTS for Data Release Version 3.0, AIRS/AMSU/HSB Validation Report for Version 3.0 Data Release, Version 1.0 (JPL D-26538), August 2003.

79. **[Fishman et al., 2003]** Global distribution of tropospheric ozone from satellite measurements using empirically corrected tropospheric ozone residual technique: Identification of the regional aspects of air pollution, Atmos. Chem. Phys., 3, 893-907, 2003.

80. **[Fussen et al., 2004]** Fussen, D., et al., GOMOS Validation Summary, presentation given at the second ENVISAT atmospheric chemistry instruments validation workshop (ACVE-2), ESRIN, Frascati, Italy, 3-7 May 2004 (http://envisat.esa.int/workshops/acve2/)

81. **[GDP3ESA, 2002**] ERS-2 GOME GDP 3.0 Implementation and Delta Validation Report, http://earth.esrin.esa.it/pub/ESA_DOC/GOME/gd3/gdp3.htm

82. **[Glackin et al., 2003]** David L. Glackin, John D. Cunningham, and Craig S. Nelson, Earth remote sensing with NPOESS: instruments and environmental data products, Proceedings of SPIE, Vol. 5234, pp. 123-131, 2003.

83. **[Goldberg, 1999]** Goldberg, M. D., Generation of retrieval products from AMSU-A: Methodology and validation. 10th Int. ATOVS Study Conf., Boulder, CO, 219–229, 1999.

84. **[Goldberg, 2002]** Goldberg, M. D., Introduction to AMSU and ATMS. Second Workshop for Earth Science Satellite Remote Sensing, October 15 - 22, 2002.

85. **[Goldberg and Cheng, 2002]** Goldberg, M. D., and Z. Cheng, Ensuring consistency between AMSU-A climate temperature retrieval products from NOAA-15 and NOAA-16, ITSC 2002.

86. **[Goldberg, 2003]** M. D. Goldberg, Y. Qu, L. M. McMillin, W. Wolf, L. Zhou, and M. Divakarla, AIRS near-real-time products and algorithms in support of numerical weather prediction, IEEE Trans. Geosci. Remote Sensing, Vol. 41, pp. 379-389, Feb. 2003.

87. **[Goodrum et al., 2000]** Geoffrey Goodrum, Katherine B. Kidwell, and Wayne Winston (Editors), NOAA KLM user's guide, 2000.

88. **[Goutail et al., 2004**] Goutail, F., et al., GOMOS High Resolution Temperature, presentation given at the second ENVISAT atmospheric chemistry instruments validation workshop (ACVE-2), ESRIN, Frascati, Italy, 3-7 May 2004 (http://envisat.esa.int/workshops/acve2/)

89. **[Grody, 1993]** Norman C. Grody, Remote sensing of the atmosphere fromsatellites using microwave radiometry, in Atmospheric remote sensing by microwave radiometry, Editor: Michael A. Janssen, Wiley, 1993.

90. **[Hadji-Lazaro et al., 2003]** Hadji-Lazaro, J., S. Turquety, C. Clerbaux, G. Megie, Operational retrieval of trace gases concentrations from IASI spectra, presentation given at ASSFTS 11 workshop (Atmospheric Science from Space using Fourier Transform Spectroscopy) (http://www-imk.fzk.de/asf/ame/assfts/), Bad Wildbad, Germany, 8-10 October 2003.

91. **[Hoogen et al., 1999]** Hoogen, R., V.V. Rozanov and J.P. Burrows, Ozone profiles from GOME satellite data: Algorithm description and first validation, J. Geophys. Res. 104, 8263-8280, 1999.
92. **[Hoogen, 1998]** Hoogen, R., University of Bremen, Ph.D. thesis, 1998.
93. **[IASI web page]** http://www-airs.jpl.nasa.gov/
94. **[Kaiser et al., 2001a]** Kaiser, J. W., V. V. Rozanov, and J. P. Burrows, Theoretical precisions for SCIAMACHY limb retrieval, Adv. Space Res., Vol. 29, no 11, pp. 1837-1842, 2001.
95. **[Kaiser et al., 2001b]** Kaiser, J. W., K.-U. Eichmann, V. V. Rozanov, and J. P. Burrows, Precision estimates for SCIAMACHY limb retrievals, Proc. IGARSS 2001, 2001.
96. **[Kelder et al., 2004]** Kelder H., et al., SCIAMACHY Validation Summary, presentation given at the second ENVISAT atmospheric chemistry instruments validation workshop (ACVE-2), ESRIN, Frascati, Italy, 3-7 May 2004 (http://envisat.esa.int/workshops/acve2/)
97. **[Kidder et al., 2000]** Kidder, S.Q., Mitchell D. Goldberg, Raymond M. Zehr, Mark DeMaria, James F. W. Purdom, Christopher S. Velden, Norman C. Grody, and Sheldon J. Kusselson, Satellite analysis of tropical cyclones using the Advanced Microwave Sounding Unit (AMSU), Bull. Amer. Meteor. Soc., 81, 1241-1259, 2000 (see http://ams.allenpress.com/amsonline).
98. **[Kobayashi et al., 1999]** Kobayashi, H., A. Shimota, C. Yoshigahara, I. Yoshida, Y. Uehara, K. Kondo, Satellite-borne high-resolution FTIR for lower atmosphere sounding and its evaluation, IEEE Transactions on Geoscience and Remote Sensing, Vol. 37, No. 3, 1496-1507, 1999.
99. **[Kuang et al., 2002]** Kuang, K., J. S. Margolis, G. C. Toon, D. Crisp, and Y. Yung, Spaceborn measurements of atmospheric CO2 by high-resolution NIR spectrometry of reflected sunlight: An introductory study, Geophys. Res. Let. **29** (10.1029/2001GL014298), 2002.
100. **[Kunkee et al., 2002a]** David B. Kunkee, Narinder S. Chauhan, and James J. Jewell, Phase one development of the NPOESS conical-scanning microwave imager/sounder (CMIS), IGARSS 2002.
101. **[Kunkee et al., 2002b]** David B. Kunkee, Narinder S. Chauhan, and James J. Jewell, Spectrum management for the NPOESS conical-scanning microwave imager/sounder (CMIS), IGARSS 2002.
102. **[Kurosu et al., 1997]** Kurosu, T., and V. V. Rozanov and J. P. Burrows, Parameterization schemes for terrestrial water clouds in the radiative transfer model GOMETRAN, J. Geophys. Res., 102 (D18), 21809-21823, 1997.**[Kuze et al., 2000]** Kuze, A., H. Nakajima, J. Tanii, Y. Sasano, Conceptual design of solar occultation FTS for Inclined-Orbit Satellite (SOFIS) on GCOM-A1, Proc. SPIE Vol. 4131, 305-314, 2000.**[Lambert et al., 2003]** BIRA-IASB web page: http://www.oma.be/GOME/GOMEVal/GDP_O3tot.htm
105. **[Livesey et al., 2003]** N. J. Livesey, W. G. Read, L. Froidevaux, J. W. Waters, M. L. Santee, H. C. Pumphrey, D. L. Wu, Z. Shippony, and R. F. Jarnot, The UARS microwave limb sounder version 5 data set: theory, characterization, and validation, Journal of Geophysical Research, Vol. 108, No. D13, pp. 4378-4398, 2003.
106. **[Lubrano et al., 2003]** Lubrano, A. M., G. Masiello, M. Matricardi, C. Serio, V. Cuomo, Retrieving N_2O from nadir viewing infrared spectrometers, Tellus B (submitted), 2003.

107. **[Luo et al., 2002]** Luo, M., R. Beer, D. J. Jacob, J. A. Logan, C. D. Rodgers, Simulated observation of tropospheric ozone and CO with the Tropospheric Emission Spectrometer (TES) satellite instrument, J. Geophys. Res., 107 (D15), 2002.
108. **[McCormick et al., 2002]** SAGE III algorithm theoretical basis document: Solar and lunar algorithm, LaRC 475-00-108, Version 2.1, 2002.
109. **[Meyer, 2004]** Meyer, Jerome, Solar occultation measurements with SCIAMACHY in the UV-Visible-IR wavelength region, PhD thesis, University of Bremen, IUP/IFE, 2004.
110. **[Müller et al., 2002]** Müller, M. D., A. Kaifel, M. Weber, J.P. Burrows, A new method for retrieving total ozone from GOME data, Appl. Opt. 41, 5051-5058, 2002.
111. **[Munro et al., 1998]** Munro, R., R. Siddans, W. J. Reburn, and B. J. Kerridge, 1998: *Direct Measurements of Tropospheric Ozone from Space, Nature, 392,* pp.168-171.
112. **[NOAA Website]** http://www.aoc.noaa.gov/article_SSMIS_Underflight_Studies.htm
113. **[Noël et al., 2002]** Noël, S., H. Bovensmann, M. W. Wuttke, J. P. Burrows, M. Gottwald, E. Krieg, A. P. H. Goede, and C. Muller, Nadir, limb, and occultation measurements with SCIAMACHY, Adv. Space Res., 29, (11), 1819-1824, 2002.
114. **[NPOESS-CMIS-ATBD]** Algorithm Theoretical Basis Document (ATBD) for the Conical-Scanning Microwave Imager/Sounder (CMIS) Environmental Data Records (EDRs), 15 March 2001, http://www.npoess.noaa.gov/Library/ATBD_index.html
115. **[NPOESS TRD]** NPOESS Technical Requirements Document, App. D, 1997.
116. **[O'Brian, 2002]** O' Brian, D. M., Surface pressure from geostationary satellite observations in the O2 A-band, EUMETSAT, Darmstadt, 91 pp., 2002.
117. **[Ogawa et al., 2004]** Ogawa, T., T. Igarashi, M. Suzuki, Greenhouse gas observation with the GOSAT satellite, Abstract submitted for COSPAR 2004, http://www.cosis.net/abstracts/COSPAR04/01265/COSPAR04-A-01265.pdf
118. **[OMI/AURA web page]** http://eos-aura.gsfc.nasa.gov/instruments/omi/introduction.html
119. **[Pan et al., 1998]** Pan, L., J. C. Gille, D. P. Edwards, P. L. Bailey, Retrieval of tropospheric carbon monoxide for the MOPITT experiment, J. Geophys. Res, 103 (D24), 32277-32290, 1998.
120. **[Pitts et al**.] Pitts, M. C., L. W. Thomason, W. P. Chu, Satellite remote sensing of temperature and pressure by the stratospheric aerosol and gas experiment III, http://www-sage3.larc.nasa.gov/library/media/ams_satellite.pdf
121. [POAM III validation web page] http://wvms.nrl.navy.mil/solve/valid/valid.html
122. [Reburn et al., 1999] W.J. Reburn, R. Siddans, B.J. Kerridge, S. Bühler, A. von Engeln, K. Künzi, J. Urban, J. Wohlgemuth, D. Feist, N. Kämpfer, and H. Czekala, Study on upper troposphere / lower stratosphere sounding, ESA Contract No. 12053/97/NL/CN, Final Report, 1999.
123. [Rodgers, 1976] Rodgers, C. D., Retrieval of Atmospheric Temperature and Composition From Remote Measurements of Thermal Radiation, *Rev. Geophys. and Space Phys.*, **14**, p609-624, 1976.
124. [Rodgers, 2000] Rodgers, C. D., Inverse methods for atmospheric sounding: theory and practice, World Scientific Publishing Co., Singapur, 2000, ISBN 981-02-2740-X.
125. **[Rothman et al., 2003],** L. S. Rothman, L. S., A. Barbe, D. Chris Benner, L. R. Brown, C. Camy-Peyret, M. R. Carleer, K. Chance, C. Clerbaux, V. Dana, V. M. Devi, A. Fayt, J. M. Flaud, R. R. Gamache, A. Goldman, D. Jacquemart, K. W. Jucks, W. J. Lafferty, J. Y. Mandin, S. T. Massie, V. Nemtchinov, D. A. Newnham, A. Perrin, C. P.

Rinsland, J. Schroeder, K. M. Smith, M. A. H. Smith, K. Tang, R. A. Toth, J. Vander Auwera, P. Varanasi, and and K. Yoshino}, The HITRAN molecular spectroscopic database: edition of 2000 including updates through 2001, J. Quant. Spectrosc. Radiat. Transfer, 5-44, 82, 2003.

126. **[Rozanov et al., 2002]** Rozanov, V.V., M. Buchwitz, K.-U. Eichmann, R. de Beek, and J.P. Burrows, SCIATRAN - a new radiative transfer model for geophysical applications in the 240-2400 nm spectral region: The pseudo-spherical version, presented at COSPAR 2000, Adv. Space Res., Vol. 29, No. 11, 1831-1835, 2002.

127. **[Rozanov et al., 2001]** Rozanov, A., V. Rozanov, and J. P. Burrows, A numerical radiative transfer model for a spherical planetary atmosphere: Combined differential--integral approach involving the Picard iterative approximation, J. Quant. Spectrosc. Radiat. Transfer, 69, 491-512, 2001.

128. **[Rozanov et al., 1999]** Rozanov A., V. V. Rozanov, and J. P. Burrows, Combined differential-integral approach for the radiation filed computation in a spherical shell atmosphere: Non-limb geometry, J. Geophys. Res., 1999

129. **[Rozanov et al., 1998]** Rozanov, V.V., T. Kurosu, and J.P. Burrows, Retrieval of atmospheric constituents in the UV-visible: A new quasi-analytical approach for the calculation of weighting functions, J. Quant. Spectrosc. Radiat. Transfer 60, 277-299, 1998.

130. **[Rozanov et al., 1997]** Rozanov, V.V., D. Diebel, R. J. D. Spurr and J. P. Burrows, GOMETRAN: A radiative transfer model for the satellite project GOME - the plane-parallel version, J. Geophys. Res., 102 (D14), 16683-16695, 1997.

131. **[Russel et al., 1993]** Russel, J. M., et al., The Halogen Occultation Experiment, J. Geophys. Res., 98(D6), 10777-10797, 1993.

132. **[SAGE3-Val-Summary, 2003**] NASA, Stratospheric Aerosol and Gas Experiment (SAGE) III, Validation summary, October 15, 2001, http://eospso.gsfc.nasa.gov/ftp_docs/validation/Val_Summary_SAGE.pdf

133. **[Schrijver et al., 1998]** Schrijver, H., A.P.H. Goede, M.R. Dobber, M. Buchwitz, Retrieval of carbon monoxide, methane and nitrous oxide from SCIAMACHY measurements, Optical Remote Sensing of the Atmosphere and Clouds, edited by J. Wang, B. Wu, T. Ogawa, Z. Guan, Vol. 3501, 215-224, Beijing, China, 14-17 Sept 1998.

134. **[Shimoda, 2003**] Shimoda, H., GOSAT and its core sensor, presetation given on 2003/10/8, http://www-imk.fzk.de/asf/ame/assfts/O_P_4_Shimoda_H.pdf

135. **[Siddans et al., 1997]** Siddans, R., W. Reburn, B. J. Kerridge, Height-resolved ozone retrievals in the troposphere and lower stratosphere from GOME, Proc. 3rd ERS Symp., Florence, Italy, March 1997, ESA SP-414 Vol II, 615-620, 1997

136. **[Siddans et al., 1998]** Siddans, R., B. J. Kerridge, W. J. Reburn, R. Munro, Height-resolved ozone retrievals in the troposphere and lower stratosphere from GOME, ESA EOQ, 1998, http://esapub.esrin.esa.it/eoq/eoq58/eoq58-siddans.pdf

137. **[Skupin et al., 2002]** Skupin, J., S. Noël, M. W. Wuttke, H. Bovensmann, and J. P. Burrows, Calibration of SCIAMACHY in-flight measured irradiances and radiances - first results of level 1 validation, Proceedings of the Envisat Validation Workshop (SP-531), ESA Publications Division, 2002.

138. [SPARC web page]
http://www.aero.jussieu.fr/~sparc/SPARCReport1/1.05_SBUV/1.05_SBUV.html

139. [Susskind et al., 2003] Joel Susskind, Christopher D. Barnet, and John M. Blaisdell, Retrieval of atmospheric and surface parameters from AIRS/AMSU/HSB data in the presence of clouds, IEEE Transactions on Geoscience and Remote Sensing, Vol. 41, No. 2, pp. 390-409, Feb. 2003.

140. [Tellmann et al., 2003] Tellmann, S., V.V. Rozanov, M. Weber, and J.P. Burrows, Improvements in the tropical ozone profile retrieval from GOME UV/vis nadir spectra, Adv. Space Res., accepted, 2003.
141. **[TES web page]** http://aura.gsfc.nasa.gov/instruments/tes/introduction.html
142. **[TES ATBD V 1.1]** TES LEVEL 2 ALGORITHM THEORETICAL BASIS DOCUMENT, Version 1.1 Jet Propulsion Laboratory, California Institute of Technology Pasadena, California, JPL D-16474, 1999
143. **[TOMS V7 web page**],
http://daac.gsfc.nasa.gov/CAMPAIGN_DOCS/FTP_SITE/INT_DIS/readmes/toms.html#201
144. **[TOMS EP (Earth Probe) web page]**
http://toms.gsfc.nasa.gov/eptoms/dataqual/nominal.html
145. **[Turquety et al., 2002]** Turquety, S., J. Hadji-Lazaro, and C. Clerbaux, First satellite ozone distributions retrieved from nadir high-resolution infrared spectra, Geophys. Res. Lett., 29, 10.1029/2002GL016431, 2002.
146. **[Verdes et al., 2000]** C. Verdes, S. Bühler, A. von Engeln, P. Eriksson, T. Kuhn, K. Künzi, J. Urban, and D. Lamarre, The retrieval of data from sub-millimetre limb sounding CCN 2, ESTEC Contract No. 11979/97/NL/CN, Final Report, Sep. 2000.
147. **[Verdes et al., 2002]** C. Verdes, S. Bühler, A. von Engeln, T. Kuhn, K. Künzi, P. Eriksson, and B.-M. Sinnhuber, Pointing and temperature retrieval from millimeter-submillimeter limb soundings, Journal of geophysical research, Vol. 107, No. D16, 2002.
148. **[von Savigny et al., 2004]** von Savigny, C., A. Rozanov, H. Bovensmann, K.-U. Eichmann, J. W. Kaiser, S. Noël, V. V. Rozanov, B.-M. Sinnhuber, M. Weber, and J. P. Burrows, The Ozone hole break-up in September 2002 as seen by SCIAMACHY on ENVISAT, J. Atmosph. Sci. (in press), 2004.
149. **[Vountas et al., 1998]** Vountas, M., V.V. Rozanov and J.P. Burrows, Ring Effect: Impact of Rotational Raman Scattering on Radiative Transfer in Earth's Atmosphere, J. Quant. Spectrosc. Radiat. Transfer 60, 943-961, 1998.
150. **[Warneke et al., 2004]** Shipborn solar absorption measurements of CO_2, CH_4, N_2O and CO and comparison with SCIAMACHY WFM-DOAS retrievals, ACP (submitted), 2004.
151. **[Weber et al., 2002]** Weber, M., K.-U. Eichmann, F. Wittrock, K. Bramstedt, L. Hild, A. Richter, J.P. Burrows, and R. Müller, The cold Arctic winter 1995/96 as observed by the Global Ozone Monitoring experiment GOME and HALOE: Tropospheric wave activity and chemical ozone loss, Q. J. Roy. Meteor. Soc. 128, 1293-1319, 2002.
152. **[Weber et al., 2003]** Weber, M., S. Dhomse, F. Wittrock, A. Richter, B.-M. Sinnhuber, and J.P. Burrows, Dynamical Control of NH and SH Winter/Spring Total Ozone from GOME Observations in 1995-2002, Geophys. Res. Lett., 30, 1853, doi:10.1029/2002GL016799, 2003.
153. **[Weber et al., 2004a**] Weber, M., M. Coldewey-Egbers, L. N. Lamsal, R. de Beek, M. Buchwitz, and J. P. Burrows, Novel total ozone algorithm for backscatter UV satellite instruments, Proceedings of the Quadrennial Ozone Symposium 2004, extended abstract (submitted), 2004.
154. **[Weber et al., 2004b**] Weber, M., L. N. Lamsal, M. Coldewey-Egbers, K. Bramstedt, and K. Vanicek, Validation of GOME total ozone retrieved using WF-DOAS, Proceedings of the Quadrennial Ozone Symposium 2004, extended abstract (submitted), 2004.
155. **[Worden et al., 2004]** J. Worden, S. S. Kulawik, M. W. Shephard, S. A. Clough, H. Worden, K. Bowman, and A. Goldman, Predicted errors of tropospheric

emission spectrometer nadir retrievals from spectral window selection, J. Geophys. Res., 109, D09308, doi:10.1029/2004JD004522, 2004.
156. **[Yang et al., 2002]** Yang et al., Atmospheric CO_2 retrieved from ground-based near IR solar spectra, Geophys. Res. Let., Vol. 29, No. 9, 10.1029/2001GL014537, 2002.

14 List of Acronyms and Abbreviations

ABS	Advanced Baseline Sounder
ACVE	(ENVISAT) Atmospheric Chemistry Validation (Workshop)
AIRS	Atmospheric InfraRed Sounder
AMF	Air Mass Factor
AMSU-A	Advanced Microwave Sounding Unit-A
ATBD	Algorithm Theoretical Baseline Document
ATMS	Advanced Technology Microwave Sounder
BUV	Backscatter Ultra Violet
CMIS	Conical scanning Microwave Imager/Sounder
CrIS	Crosstrack Infrared Sounder
DMSP	Defense Meteorological Satellite Program
DOAS	Differential Optical Absorption Spectroscopy
EP	Earth Proble
ERBS	Earth Radiation Budget Satellite
ERBS	Earth Radiation Budget Satellite
ESA	European Space Agency
ESTEC	European Space TEchnology Center
EVERGREEN	EnVisat for Environmental Regulation of GREENhouse gases
FOV	Field Of View
FTIR	Fourier Transform InfraRed
FTS	Fourier Transform Spectrometer
FWHM	Full Width at Half Maximum
GCOS	Global Change Observation Satellite
GIFTS	Geosynchronous Imaging Fourier Transform Spectrometer
GOME	Global Ozone Monitoring Experiment
GOMOS	Global Ozone Monitoring by Occultation of Stars
GOSAT	Greenhouse gas Observing SATtelite
HALOE	HALogen Occultation Experiment
HES	Hyperspectral Environmental Suite
HIRS	High resolution Infrared Radiation Sounder
IASI	Infrared Atmospheric Sounding Interferometer
IFOV	Instantaneous Field Of View
IMG	Interferometric Monitor for Greenhouse gases
IR	InfraRed
IUP/IFE	Institute of Environmental Physics (IUP) / Institute of Remote Sensing (IFE) of the University of Bremen, Germany
JPL	Jet Propulsion Laboratory
LEO	Low Earth Orbit
LOS	Line Of Sight
LUT	Look Up Table
MASTER	Millimetre-wave Acquisitions for Stratosphere-Troposphere Exchange Research
MLS	Microwave Limb Sounder

MOPITT	Measurement Of air Pollution In The Troposphere
MSG	Meteosat Second Generation
MTG	Meteosat Third Generation
MW	MicroWave
NA	Not Assessed
NASA	National Aeronautic and Space Administration
NIR	Near Infra Red
NPOESS	National Polar-orbiting Operational Environmental Satellite System
NPP	NPOESS Preparatory Project
NWP	Numerical Weather Prediction
OCO	Orbiting Carbon Observatory
SBUV	Solar Backscatter Ultra Violet
SCIAMACHY	SCanning Imaging Absorption spectroMeter for Atmospheric CHartographY
SOFIS	Solar Occultation FTS for Inclined-orbit Satellite
SOPRANO	Sub-Millimetre Observation of Processes in the Atmosphere noteworthy for Ozone
SPARC	Stratospheric Processes And their Role in Climate
SSM/T	Special Sensor Microwave/Temperature
SSMIS	Special Sensor Microwave Imager/Sounder
SWIR	ShortWave InfraRed
TBC	To Be Confirmed
TBD	To Be Defined
TES	Tropospheric Emission Spectrometer
TIR	Thermal InfraRed
TOMS	Total Ozone Mapping Spectrometer
UARS	Upper Atmosphere Research Satellite
UV	Ultra Violet
WFM-DOAS	Weighting Function Modified DOAS